



ADVANCED MASTERS IN STRUCTURAL ANALYSIS OF MONUMENTS AND HISTORICAL CONSTRUCTIONS

# Master's Thesis

Vivek Namdev

**A new laboratory test to assess the resistance of porous materials to salt crystallization: Assessment of natural stone painted with limewashes**



University of Minho

**Czech Republic** | 2022



**CZECH TECHNICAL UNIVERSITY IN PRAGUE**  
**Faculty of Civil Engineering**  
Thákurova 7, 166 29 Prague 6, Czech Republic


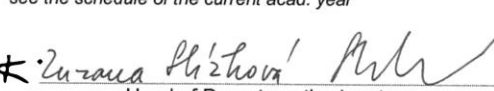


## DIPLOMA THESIS ASSIGNMENT FORM

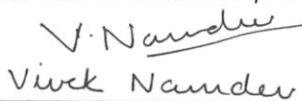
### I. PERSONAL AND STUDY DATA

Surname: Namdev	Name: Vivek	Personal number: +351 927 408 373
Assigning Department: Department of Mechanics		
Study programme: Civil Engineering		
Study branch/spec.: Advanced Masters in Structural Analysis of Monuments and Historical Constructions		

### II. DIPLOMA THESIS DATA

Diploma Thesis (DT) title: A new laboratory test to assess the resistance of porous materials to salt crystallization: assessment of natural stone painted with limewashes	
Diploma Thesis title in English: A new laboratory test to assess the resistance of porous materials to salt crystallization: assessment of natural stone painted with limewashes	
Instructions for writing the thesis: The main goal of the thesis is the evaluation of the test recently developed by the RILEM ASC Technical Committee in natural stone treated with two types of limewashes. Limewashes are inorganic paints composed of an aqueous suspension of calcium hydroxide. The main advantages of using limewashes as surface coatings are with its eco-friendly, anti-septic, breathability, and good thermal performance. However, this type of paint becomes easily friable when exposed to weathering agents and it is usually necessary to re-apply a new coat yearly. The addition of linseed oil to the limewash has been recently studied and showed promising results to overcome some of the pure limewash drawbacks. The second goal of the thesis is to evaluate the performance of the stone treated with pure limewash and limewash with linseed oil towards the resistance to salt crystallisation.	
List of recommended literature: - Lubelli B, Cnudde V, Diaz-Goncalves T, Franzoni E, Van Hees RP, Ioannou I, Menendez B, Nunes C, Siedel H, Stefanidou M, Verges-Belmin V, Viles H (2018) Towards a more effective and reliable salt crystallisation test for porous building materials: state of the art. Mater Struct 51 (2). <a href="http://dx.doi.org/10.1617/s11527-018-1180-5">http://dx.doi.org/10.1617/s11527-018-1180-5</a> . - Nunes C, Mlsnová K, Válek J, Limewashes with linseed oil: effect on the moisture transport of natural stone. In Proc. 14th Int. Congress on the deterioration and conservation of stone. Halle: Mitteldeutscher Verlag, 2020 - (Siegesmund, S.; Middendorf, B.), s. 591-596. ISBN 978-3-96311-172-3. - ICOMOS-ISCS (2008) Illustrated glossary on stone deterioration patterns. Ateliers 30 Impression, Champigny/Marne.	
Name of Diploma Thesis Supervisor: Ass. Prof. Zuzana Slížková Ph.D. and Mgr. Cristiana Nunes, Ph.D.	
DT assignment date: 5.4.2022	DT submission date in IS KOS: 6.7.2022 <i>see the schedule of the current acad. year</i>
 DT Supervisor's signature	 Head of Department's signature

### III. ASSIGNMENT RECEIPT

<i>I declare that I am obliged to write the Diploma Thesis on my own, without anyone's assistance, except for provided consultations. The list of references, other sources and consultants' names must be stated in the Diploma Thesis and in referencing I must abide by the CTU methodological manual "How to Write University Final Theses" and the CTU methodological instruction "On the Observation of Ethical Principles in the Preparation of University Final Theses".</i>	
13.04.2022 Assignment receipt date	 Vivek Namdev Student's name

## DECLARATION

Name: Vivek Namdev  
Email: viveknamdev12@gmail.com  
Title of the Msc Dissertation: A new laboratory test to assess the resistance of porous materials to salt crystallization: assessment of natural stone painted with limewashes  
Supervisor(s): Mgr. Cristiana Nunes, Ph.D.  
Doc. Ing. Zuzana Slížková, Ph.D.  
Year: 2022

I hereby declare that all information in this document has been obtained and presented in accordance with academic rules and ethical conduct. I also declare that, as required by these rules and conduct, I have fully cited and referenced all material and results that are not original to this work.

I hereby declare that the MSc Consortium responsible for the Advanced Masters in Structural Analysis of Monuments and Historical Constructions is allowed to store and make available electronically the present MSc Dissertation.

University: Czech Technical University in Prague

Date: July 6, 2022

Signature:



V. Namdev

This page is left blank on purpose

## ACKNOWLEDGEMENTS

The present research work would have been incomplete without the continuous support and contribution of people mentioned below who have guided and motivated me towards the completing of my master's degree. First of all I would like to extend my gratitude to my supervisor Mgr. Cristiana Nunes, Ph.D and co-supervisor Ass. Prof. Zuzana Slížková Ph.D., who introduced me to interesting concepts of material science and helped me to organize this research during my time spent at the Institute of Theoretical and Applied Mechanics of the Czech Academy of Sciences (ITAM) in Prague. I acknowledge their time, patience and expertise in answering my queries on the subject and extending their full technical support whenever I needed regardless of their prior commitments.

I would like to acknowledge the contribution of remarkable people I met at ITAM who kept me motivated and extended their support throughout my research. To the RILEM committee, for letting me contribute to their ongoing research and giving me opportunity to present this research work in front of the committee. I would like to thank Mgr. Dita Frankeová. for her time to explain and assist me to operate the lab equipment whenever I requested. To Ing. Michaela Vondráčková Ph.D for giving me insight about laboratory procedures, cutting and preparing of specimens whenever I requested her. I thank Mr. Marek Eisler for teaching me how to operate and test specimens using ultrasonic device. I thank Ms. Pavla Bauerova for helping me understand SEM analysis and Mr. Radek Sevcik from Telc for performing IC analysis on numerous samples. I would also like to thank researchers from ITAM who might be not directly connected to this research but they have given me an insight about the importance of research work and how to conduct it which I found fascinating while reading numerous research proposals displayed in the corridors of ITAM building. Furthermore I would like to thank security personals near ITAM reception who have always welcomed me with a smile and tried communicating instead of language barrier.

I would like to acknowledge support from SAHC Consortium for the generous financial aid they provided that helped me towards completion of the degree program successfully. I am thankful to consortium coordinator Prof. Paulo B. Lourenco at UMinho Guimaraes, Portugal for the initial course work and making his administration available for addressing all the queries before and during the master's program. I would like to extend my gratitude to all the professors from the consortium universities (UMinho, CTU, UPC and Unipd) for stitching this unique program and making themselves approachable while sharing their wisdom about the heritage conservation from various parts of the European Union. I would also like to acknowledge the efforts of Prof. Petr Kabele for making every resource and help available while carrying out this dissertation work at his home institution CTU Prague in Czech Republic.

I would like to thank all the SAHC students from different parts of the world who attended this master's program with me and extended their support both inside and outside the class and made the journey comfortable and memorable, without their friendship the journey would have been less exciting.

Lastly but most importantly, I was able to complete my master's degree with continuous support from my family and friends back in India, I will be always grateful for your belief in me. THANK YOU !!

This page is left blank on purpose

## **ABSTRACT**

Soluble salts represent one of the most important causes of building materials' degradation. Currently, in the practice of construction and conservation, the durability of materials with respect to salt crystallization is mostly determined by accelerated aging tests carried out in the laboratory. However, the existing (standard) crystallization test procedures do not often reproduce realistically the transport and crystallization processes, resulting in degradation patterns that are different from those observed in natural conditions. To tackle this problem, in 2016, the RILEM Technical Committee ASC-271 "Accelerated laboratory test for the assessment of the durability of materials with respect to salt crystallisation" was launched to develop an effective laboratory weathering test. The test should reliably assess the durability of porous building materials against salt crystallisation within a reasonable period, accelerating the deterioration process without significantly altering its mechanism.

The main goal of the thesis is the evaluation of the test recently developed by the RILEM ASC Technical Committee in natural stone treated with one type of limewash. Limewashes are inorganic paints composed of an aqueous suspension of calcium hydroxide. The main advantages of using limewashes as surface coatings are with its eco-friendly, anti-septic, breathability, and good thermal performance. However, this type of paint becomes easily friable when exposed to weathering agents and it is usually necessary to re-apply a new coat yearly. The addition of linseed oil to the limewash has been recently studied and showed promising results to overcome some of the pure limewash drawbacks. The second goal of the thesis is to evaluate the performance of the stone treated with pure limewash towards the resistance to salt crystallisation. Different techniques (e.g. salt distribution by ultrasonic pulse velocity, scanning electron microscopy, ion chromatography) were used to assess the degradation process.

*Keywords:* Salt Crystallization, Accelerated Aging, Natural Stone, Limewash



This page is left blank on purpose.

## ABSTRAKT

### **Nový laboratorní test k posouzení odolnosti porézních materiálů vůči krystalizaci solí - posouzení přírodního kamene s povrchovou úpravou vápennými nátěry**

Vodorozpuštěné soli jsou velmi často příčinou degradace stavebních materiálů. V současné době je životnost stavebních materiálů s ohledem na krystalizaci solí většinou zjišťována zkouškami zrychleného stárnutí prováděnými v laboratoři. Stávající (standardní) zkušební postupy však často nereprodukuje realisticky transportní a krystalizační procesy solí ve stavebních materiálech, což vede k jiným projevům poškození než jaké jsou pozorované v přírodních podmínkách. K vyřešení tohoto problému byl v roce 2016 ustanoven technický výbor RILEM ASC-271 s názvem „Zrychlený laboratorní test pro posouzení odolnosti materiálů s ohledem na krystalizaci solí“ s cílem vytvořit nový, účinný laboratorní test. Zkouška by měla spolehlivě posoudit odolnost porézních stavebních materiálů proti krystalizaci solí v přiměřené době, s využitím stejného mechanismu degradace, jaký probíhá obvykle v přírodě.

Hlavním cílem diplomové práce je využití zkušebního postupu nedávno vyvinutého technickým výborem RILEM ASC pro vyhodnocení odolnosti přírodního pískovce ošetřeného vápenným nátěrem. Vápenný nátěr je anorganický prostředek obsahující vodnou suspenzi hydroxidu vápenatého. Hlavními výhodami použití vodné suspenze hydroxidu vápenatého – vápenného nátěru - jsou jejich ekologické a antiseptické vlastnosti, prodyšnost a dobré tepelné vlastnosti. Tento typ nátěru však při vystavení povětrnostním vlivům snadno degraduje a obvykle je nutné jej každý rok obnovovat. Slibné výsledky k překonání některých nedostatků čistě vápenného nátěru mají laboratorní zkoušky chování vápenného nátěru s přidáním lněného oleje. Druhým cílem práce je zhodnotit životnost kamene ošetřeného čistě vápenným nátěrem a vápenným nátěrem se lněným olejem vůči krystalizaci solí. K posouzení degradačního procesu byla použita řada analytických metod (např. mikroskopie, měření rychlosti šíření ultrazvukového signálu, chemické analýzy).

**Klíčová slova:** krystalizace solí, zrychlené stárnutí, přírodní kámen, vápenný nátěr

This page is left blank on purpose.

## TABLE OF CONTENTS

Declaration.....	i
Acknowledgements.....	iii
Abstract.....	v
Abstrakt.....	vii
Table of Contents .....	ix
List of Figures.....	xi
List of Graphs.....	xii
List of Tables.....	xii
1. Introduction	
1.1 Motiavtion	
1.2 Aims and Objectives	
1.3 Thesis Outline	
2. State of The Art	
2.1 Existing Accelerated Aging Tests on Salt Crystallization	
2.2 Sodium Sulphate and Porous Building materials	
2.3 Porous Building Materials and Salt Damage	
2.4 Limewash and Salt Crystallization of Porous Building materials	
3. Methodology	
3.1 Stone Characterization	
3.2 Salt Crystallization Aging Tests	
3.3 Methods of Analysis: Assessment of Damage and Salt Analysis	
3.3.1 Visual Observations	
3.3.2 Material Loss, Mass Evolutiona and Salt Efflorescence	
3.3.3 Ultrasonic Pulse Velocity (UPV)	
3.3.4 Analysis of Salt Distribution	
3.3.4.1 Ion Chromatography (IC)	
3.3.4.2 Scanning Electron Mircoscopy (SEM)	
4. Results and Discussions	
4.1 Comparison between RILEM and EN12370	

4.1.1 Salt Accumulation

4.1.2 Salt Absorption and Ion Chromatography (IC)

4.1.3 Scanning Electron Microscopy (SEM)

4.1.4 Drying Rate, Salt Efflorescence and Material Loss

4.1.5 Damage Assessment

4.1.6 Ultrasonic Pulse Velocity (UPV)

5. Conclusion and Recommendations

5.1 Durability of the Porous Materials

5.2 Aging Tests

5.3 Assessment Methods

5.4 Future Work

References

Appendix

## LIST OF FIGURES

Figure 1: Example of stone weathering and salt damage near Charles Bridge, Prague Czech Republic .....	19
Figure 2: Overview of the most common salt contamination procedures (a) repeated total immersion of the specimen (b) repeated partial immersion (c) continuous partial immersion[8] .....	20
Figure 3: Schematic representation of durability of a stone, subject to salt damage[8].....	20
Figure 4: Experimental setup used in the contamination experiments: (a) capillary absorption followed by drying (b) continuous capillary absorption .....	21
Figure 5: Phase diagram for sodium sulfate. ....	24
Figure 6: (a) Example of specimens used during the EN and RILEM test, (b) Mšené and Opuka stones during reference capillary test .....	26
Figure 7: Example of measurements of geometrical characteristics of specimens (a) Height (b) Diameter, (c)Weight .....	28
Figure 8: Top: Example of complete immersion of EN specimens (a) Before test (b) After immersion Bottom: Contamination for 2h (c) Opuka (d) Mšené .....	29
Figure 9: (a) Example of drying of EN specimens (b) Example of drying at room conditions .....	30
Figure 10: Examples of RILEM Samples (a) With Parafilm (b) With 5mm parafilm on top (c) Bottom sealed after salt contamination/rewetting.....	31
Figure 11: Example of RILEM samples partial immersion before and after salt contamination (a) Mšené (b) Opuka.....	32
Figure 12: Example of RILEM samples during oven drying (a) Drying room conditions (b) Oven drying .....	32
Figure 13: Example of lime coated Mšené samples used during RILEM test procedure P2 (a) Lime Putty (b) Lime painted specimen (c) Salt contamination of limewash coated samples .....	33
Figure 14: (a) Example of debris collected during RILEM test (b) Example of materials loss calculated using filtration method .....	35
Figure 15: Example of ultrasonic tests performed on specimens (a) through diameter (b) through height).....	36
Figure 16: Determination of ultrasonic velocity by the direct transmission method (a) UPV in EN samples (b) UPV in RILEM samples along height (c) UPV in RILEM samples along diameter .....	37
Figure 17: Schematic representation of specimens used for destructive and non-destructive testing. ....	38
Figure 18: (a) Example of sample preparation (b) Example of prepared samples .....	38
Figure 19: (a) Example of samples marked equally at 1mm interval for salt with ion chromatography analysis at each layer from evaporative surface (b) SEM samples embedded in epoxy resin and prepared for microscopic analysis.....	39
Figure 20: (a) Visible salt layer formed after drying specimens during RILEM test accumulation phase (b) Grinding of specimen manually into fine powder for each 1mm layer for ion chromatography (IC) test .....	40
Figure 21: SEM investigation of salt laden samples (cross sections) showing granular structure (a) Mšené uncoated (b) Mšené lime coated (c) Opuka uncoated with 1-salt accumulation.....	44
Figure 22: SEM microphotographs of uncoated Mšené stone (MR4) with RILEM procedure P2 .....	47
Figure 23: SEM microphotographs of limewash coated Mšené stone (MRL4) with RILEM procedure P2 .....	48
Figure 24: SEM microphotographs of salt crystals created in pores of Mšené stone (MR4, uncoated).....	49
Figure 25: SEM microphotographs of salt crystals created in pores of Mšené stone (MRL4, limewash coated).....	49
Figure 26: SEM microphotographs of uncoated Opuka specimen (OPR4) with RILEM procedure P2 .....	50
Figure 27: SEM microphotographs of salt crystals created in pores of Opuka stone (OPR4, uncoated).....	51
Figure 28: Example of Mšené (a) and Opuka (b) specimen deterioration .....	61
Figure 29: Example of material loss during EN12370 tests (a) Material Loss during wetting stage (b) Sand disintegration in Mšené specimens (ME1-ME4) (c) Scalping of sedimentation layers from sides of Opuka specimens (OPE1-OPE4).....	61

Figure 30: Example of chromatic alteration and material deterioration of EN Mšené specimens (ME1-ME4) tested with procedure P1 during 15 cycles.....	62
Figure 31: Summary of macroscopic visual observations during RILEM tests (a) 1-Salt contamination cycle, uncoated Mšené specimens (MR5-MR7) tested with procedure P2 (b) 2-Salt contamination cycles, uncoated Mšené specimens (MR1-MR3) tested with procedure P3 .....	63
Figure 32: Example of debris (salt efflorescence and material loss) collected during RILEM tests (a) 1-Salt contamination cycle, uncoated Mšené specimens (MR5-MR7) tested with procedure P2 (b) 2-Salt contamination cycles, uncoated Mšené specimens (MR1-MR3) tested with procedure P3 .....	63
Figure 33: Summary of macroscopic visual observations during RILEM tests (a) 1-Salt contamination cycle, limewash coated Mšené specimens (MRL1-MRL4) tested with procedure P2 (b) 1-Salt contamination cycle, uncoated Opuka specimens (OPR1-OPR4) tested with procedure P2.....	64
Figure 34: Example of debris (salt efflorescence and material loss) collected during RILEM tests (a) 1-Salt contamination cycle, lime-coated Mšené specimens (MRL1-MRL4) tested with procedure P2 (b) 1-Salt contamination cycle, uncoated Opuka specimens (OPR1-OPR4) tested with procedure P2 ....	64
Figure 35: Example of material loss from (a) bottom surface and (b) top surface (Right) of EN Opuka specimen during wetting stage tested procedure P1 .....	65
Figure 36: (a) Example of salt brushed off from Opuka specimens after drying stage (b) Example of stone material loss from top part of the specimen .....	66
Figure 37: Example of chromatic alteration and material deterioration of EN Opuka specimens (OPE1-OPE4) tested with procedure P1 during 15 cycles.....	66

## LIST OF GRAPHS

Graph 1: Average salt absorbed amount (wt. %) during salt accumulation phase with RILEM procedure P2 and P3 (a) Comparison of Mšené and Opuka stones (b) Comparison of only Mšené stones .....	42
Graph 2: Average salt absorbed amount (wt. %) in each cycle (a) Mšené stone (ME1-ME4) (b) Opuka stone (OPE1-OPE4) with EN procedure P1 .....	42
Graph 3 Salt distribution upto 6mm depth from evaporative surface with procedure P2.....	43
Graph 4: Average residual moisture content after 16h of drying (a) Mšené (ME1-ME4) (b) Opuka (OPE1-OPE4) stones with EN procedure P1 .....	52
Graph 5 : Comparison between drying time (a) Mšené stone (uncoated MR5-MR7) (b) Opuka stone (uncoated OPR1-OPR4) with procedure P2 following RILEM standards .....	53
Graph 6 : Comparison between drying time (a) Mšené stone (uncoated MR5-MR7) with procedure P2 (b) Mšené stone (uncoated MR1-MR3) with procedure P3 following RILEM standards .....	53
Graph 7 : Comparison between drying time (a) Mšené stone (uncoated MR5-MR7) (b) Mšené stone (limewash coated MRL1-MRL4) with procedure P2 following RILEM standards .....	54
Graph 8: Average Debris brushed off from (a) Mšené stone (b) Opuka stone aged with procedure P1 .....	55
Graph 9: Debris collected from RILEM test specimens tested with procedure P2 and P3.....	55
Graph 10: Mass variation of (a) Mšené and (b) Opuka specimens with EN procedure P1 .....	56
Graph 11: Mass variation comparison of (a) uncoated Mšené and (b) uncoated Opuka specimens with procedure P2.....	58
Graph 12: Mass variation in (a) uncoated Mšené (2-Salt) with procedure P3 and (b) limewash coated Mšené specimens with procedure P2 .....	58
Graph 13 (a) Salt efflorescence and (b) material loss in RILEM specimens with procedures P2-P3...	59
Graph 14 Mass variation comparison between procedure P1 and P2 (a) Mšené (b) Opuka .....	59
Graph 15: UPV of specimens in sound state before starting (a) EN and (b) RILEM tests .....	67
Graph 16: Ultrasound Pulse Velocity (UPV) of (a) Opuka and (b) Mšené stone during 15 aging cycles of EN 12370 Test .....	68
Graph 17: Comparison of first 4 cycles ultrasound velocity (through height) for Opuka and Mšené samples with test procedure P1-P2-P3.....	69
Graph 18: UPV changes in Opuka and Mšené stone measured at first 2-4-6-8-10 mm and after 5mm regular intervals from the evaporative surface in test procedure P2-P3.....	71



## LIST OF TABLES

Table 1: Porosity and bulk density of the stones [37] .....	27
Table 2: Main pore size and solid Density Properties of samples - NAKI18 project [37].....	27
Table 3: Summary of testing procedures for accelerated aging tests.....	28
Table 4: Summary of salt solution used during the EN12370 test cycles .....	29
Table 5: Summary of test conditions used during the RILEM test cycles .....	31

## **1. INTRODUCTION**

### **1.1 Motivation**

Salt crystallization in porous materials constitutes one of the most frequent causes of decay of buildings in a wide range of environment [1]. Stones and masonry materials when exposed to the changing environment they are subjected to physical, chemical and biological weathering that can damage these materials over time. In many situations, this degradation is due to the action of various types of soluble salts entrapped in masonry from internal or external sources or a combination of both. Internal sources involve the dissolution or chemical transformation of the material itself or the use of salt-rich materials (e.g. dolomitic and cement-based mortars). External sources can be the vicinity of the sea, animal excrements, agriculture, deicing salts, microorganisms, conservation treatments (e.g. Na- and K- silicates waterglass), or capillary rise of ground water [2].

When doing prevention and conservation work on our architectural heritage, it is important to understand the durability of the stones depends both on their intrinsic properties and on the decay factors in the environment. When we talk about the durability of a material we are referring to its resistance to alteration or decay, and its capacity to maintain the same size, shape, properties and aesthetic appearance over time [3]. In order to assess the durability of building materials to salt weathering, accelerated laboratory tests are carried out. The existing EN12370 test standards produces unrealistic in-situ behavior of weathering of the porous building material and with the aim of developing more realistic accelerated test RILEM Technical committee TC 271-ASC focused developing a laboratory salt crystallization tests for porous building materials that represents deterioration mechanisms occurring onsite [4].

### **1.2 Aim and Objectives**

The objective of this research is to compare results from test procedure developed by RILEM 271-ASC Technical Committee and check reliability of the results with existing European standards EN12370 test for assessing durability of two different natural stones with respect to salt crystallization. Under scope of the research two natural stones types i.e. Mšené sandstone and Opuka marlstone (mainly used in historic building restoration works around Czech Republic) were tested in laboratory at Institute of Applied and Theoretical Mechanics, Prague under different test conditions. Under the scope of this thesis Mšené stone's durability was also analyzed to see effect of salt crystallization with application of limewash and check the effectiveness of the limewash as a protective and aesthetic surface treatment of the natural stones.

### **1.3 Thesis Outline**

This thesis is divided into five parts:

Part 1: The first section of thesis outlines the objectives of the thesis.

Part 2: The second section encompasses a comprehensive review of the literature on the topic to understand the background of the salt crystallization and application of limewash to desalinate the stone under the effect of salt crystallization.

Part 3: The third section highlights detailed methodology and experiments performed at laboratory for the assessment of stone under the effect of salt crystallization. Under this section the two existing tests EN12370 and RILEM-ASC were performed on two stone types and their effectiveness was evaluated.

Part 4: The fourth section presents results obtained using non-destructive and destructing test.

Part 5: The final section of the thesis concludes the study and highlights the reliability of the two test standards which use different environmental conditions. This section also highlights outcomes from the analysis performed and recommends future studies.

## 2. STATE OF THE ART

The deterioration of natural stone may be caused in many different ways due to fluctuation in moisture contents. But in porous stone the most significant deterioration agents are the atmospheric pollution, salt crystallization and freezing [5]. The assessment of material's durability in historic buildings could be understood by performing accelerated weathering tests in laboratory that can provide reliable results and suggest methods to repair and reduce their decay without changing its mechanism within a reasonable period of time. Figure 1 shows an example of stone weathering and salt deposit on the sculptures and masonry work near Charles Bridge in city of Prague, Czech Republic.

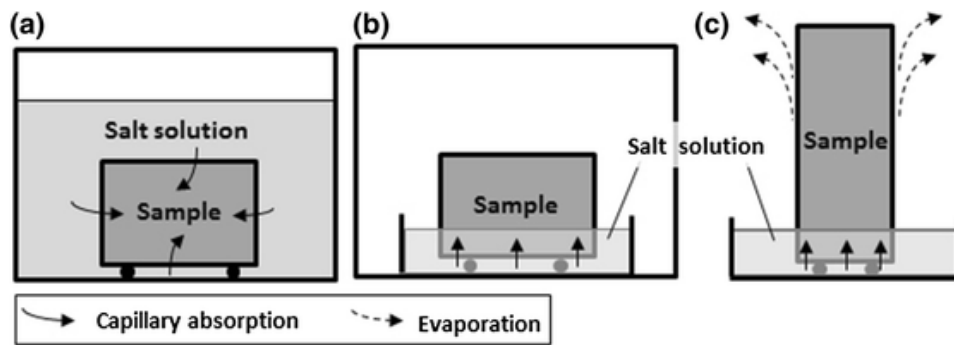


**Figure 1: Example of stone weathering and salt damage near Charles Bridge, Prague Czech Republic**

### 2.1 Existing Accelerated Aging Tests on Salt Crystallization

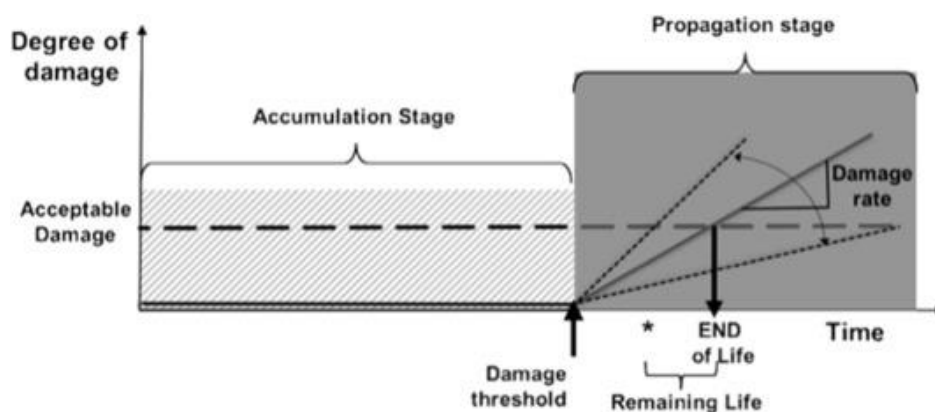
Accelerated aging cycles are lab tests where severe or extreme environments (e.g. heat, moisture, sunlight, pollution, etc.) can be replicated and applied to simulate decay, or to accelerate the regular processes of weathering[6]. The durability of porous building materials can be assessed with the help of accelerated aging tests over a longer period of time which can provide a way to assess decay of materials or methods to avoid salt crystallisation. Lubelli et al. have recently summarized the shortcoming of some salt crystallization tests and of the mathematical models based on the accepted salt crystallization theories[7]. Existing crystallization tests has few limitations as they are either extremely time consuming or fails to reproduce the salt transport or crystallization process which could result in unrealistic damage types. When comparing the results between the different existing accelerated crystallization tests the result could become less reliable as most of the existing standards do not prescribes an accurate, reliable and quantitative method or technique for monitoring damage development during the test.

The most widely used standard test, EN 12370, relies on cycles of impregnation by full immersion (Figure 2) of specimens in a sodium sulfate solution, followed by drying at 105 °C. This leads to damage during the re-wetting phase of a cycle and, because of the contamination procedure and the extreme salt load and drying temperature, is not expected to be representative for most situations found in practice, as for example capillary rise. Therefore, the issue of knowing how to obtain reliable results from accelerated testing remains open [2].



**Figure 2: Overview of the most common salt contamination procedures (a) repeated total immersion of the specimen (b) repeated partial immersion (c) continuous partial immersion[8]**

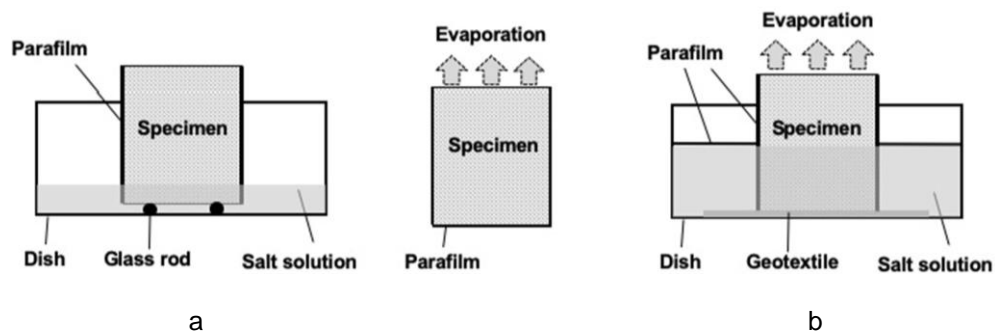
Compared to EN 12370 standard, the salt crystallization test developed by the RILEM TC 271-ASC proposes a new approach different from existing salt crystallization tests and derived from a common approach to the durability of natural stones. It starts from the consideration that it is necessary to accumulate a certain amount of salt, i.e., reach a certain degree of pore filling before damage initiates. Salt damage can thus be seen as a process developing in two stages: accumulation and propagation Figure 3.



**Figure 3: Schematic representation of durability of a stone, subject to salt damage[8]**

During the accumulation phase, salt should precipitate in a thin layer close to the evaporative surface to create a localized accumulation zone, as this is the most common situation found onsite.

Water transport properties, governed by the pore structure of the material, and crystallization kinetics will control the salt distribution in the accumulation phase [9-10]. In the propagation phase, also the mechanical properties of the material and the environmental conditions will play an important role in the eventual damage mechanism [8]. By clearly separating between a salt accumulation and a damage propagation phase, the test procedure distinguishes itself from existing salt weathering tests.



**Figure 4: Experimental setup used in the contamination experiments: (a) capillary absorption followed by drying (b) continuous capillary absorption**

The RILEM MS-A.1 also proposes the use of more realistic test conditions, i.e. contamination by capillary absorption (Figure 4) of 10 wt% sodium sulphate or sodium chloride solution followed by drying at 20 °C and 50% relative humidity (RH), but still has the important limitation of being very time consuming[22].

The effectiveness salt crystallization test procedures also depends on several factors like specimen type, shape, size and number of replicates; salt type and amount; salt contamination procedure; drying conditions; methods of assessment of damage and criteria of evolution of decay. As per (RILEM TC 127-MS,1998) the first recommendation is to use of specimens comprising a combination of materials. In fact, testing mortars or plasters as single materials could result in misleading or incomplete results, as the behaviour of these materials is strongly affected by the adjacent ones[11].

In laboratory tests, mainly single salts are used however in buildings salt mixtures are commonly found, rather than individual salts. The most common salt used in laboratory tests is sodium sulfate which is often prescribed in standards [11,12] and recommendations [11,13]. As alternatives, magnesium sulphate [11,14] or sodium chloride [13] are also considered. The main reason for using sodium sulphate is its aggressiveness, which is attributed to its several hydrated phases with different solubility degrees [11,15] and which has been widely experimentally confirmed by the scientific literature. Another important variable in salt contamination procedures is the concentration of the salt solution. The use of highly concentrated or saturated solutions of Na<sub>2</sub>SO<sub>4</sub> [12] and NaCl [11,16] is common in salt crystallisation tests. The concentration of the salt solution affects the location of salt accumulation and crystallization and thus damage type and severity. Given the same amount of salt in a specimen, damage is more likely to develop if salt accumulates in a thin layer of material rather than

if it is homogeneously distributed in the specimen, because pores become more completely filled, which leads to the development of a higher crystallization pressure [11,17].

Another important factor salt contamination method. The most common salt contamination procedures entail the repeated total or partial immersion of specimens in a salt solution, followed by a drying period (wet-dry cycles), or their continuous partial immersion (simultaneous absorption and drying) (Figure 2 and Figure 4). Generally, in partial immersion tests, contamination with salt solution is provided through the surface opposite to the evaporation surface (test surface). In those cases when total immersion or spraying techniques are used, the contamination and the evaporation surfaces coincide. Arizzi et al. [11,18] studied the effect of salt deposition (from the test surface) and capillary salt up-take on mortar specimens, and observed that salt capillary uptake produced more damage than salt deposition.

The drying and cooling conditions used in salt crystallization tests have a major influence on the nature, location and rate of salt crystallization, and thus the type of damage induced. Goncalves and Brito [11,19] provide a summary of the key theoretical stages of drying involved in porous building materials. Factors affecting drying rates are temperature, air movement and relative humidity within the experimental set-up. As the complete drying of specimens may require a very long time, particularly when they are salt-contaminated, drying is often accelerated by the use of high temperatures, low RH and high air speed. The way that high temperatures are obtained can also influence the results. Gomez Heras and Fort [11,20] investigated whether heating by radiation and convection caused different effects.

Different methods of assessment and monitoring as recommended in various tests which are as important as other testing factors. RILEM Tests No. V.1a, b (total immersion) [11,21] and EN 12370 [11] prescribe reporting the mass change or the number of cycles needed to completely destroy the samples (in case complete disintegration occurs in less than 15 cycles). A photographic record of the specimen condition is required only at the beginning and at the end of the test. RILEM Test No. V.2 (partial immersion) [11,21] requires a "visual (photographic) evaluation" only, and recording the mass change is stated to be "less suitable" in this case. Similarly, RILEM MS-A.1 [11,22] suggests recording the visual changes (by photographs and description) and the number of units that have failed after each cycle.

Some non-destructive techniques also focus on the observation of changes occurring on the surface of the material. Vazquez et al. [11,23] measured color changes in limestone samples after salt crystallization tests. As salt damage generally affects the surface of the material, laser [11,24, 25] and optical profilometers [26] have been used to characterize the surface decay and monitor its evolution. Other authors use a combination of digital camera, reflectography and fiber optic microscope images. Recently, more advanced techniques such as X-ray CT [11,23, 122], and neutron tomography have been successfully applied to study the development of damage in the bulk of the material. These 3D imaging techniques allow not only qualitative monitoring of the weathering process, but also

quantitative determination of the location of the accumulation of salt and the opening of fractures [11,27]. Synchrotron radiation energy-dispersive X-ray diffraction has also been used to monitor salt distribution in limestone samples [11,28]. In some studies, the difference in mechanical (flexural, tensile and/or compressive) strength of the material before and after the crystallization test is used as a measure of decay [11,29], sometimes in combination with NDT methods like ultrasonic pulse velocity test.

Among the destructive techniques for the study of the effect of salt crystallization on a material, mercury intrusion porosimetry (MIP) is one of the most commonly used. The measurement of changes in porosity and pore size distribution by MIP is considered to provide information on the location of salt deposition. One of the limitations of mechanical strength measurements is that the combined effect of salt accumulation in pores (increasing the material strength, moisture, and damage (decreasing the material strength), complicate the interpretation of the results. Microscopy techniques, including optical and (environmental) electron scanning microscopy, sometimes equipped with energy dispersive X-ray spectrometry, are also often used to study damage due to salt crystallization. Generally, microscopic observations are carried out at the end of the test, without prior desalination of the sample, to assess the presence and type of damage and relate this to the salt distribution in the specimen[11].

## **2.2 Sodium Sulphate and Porous Building Materials**

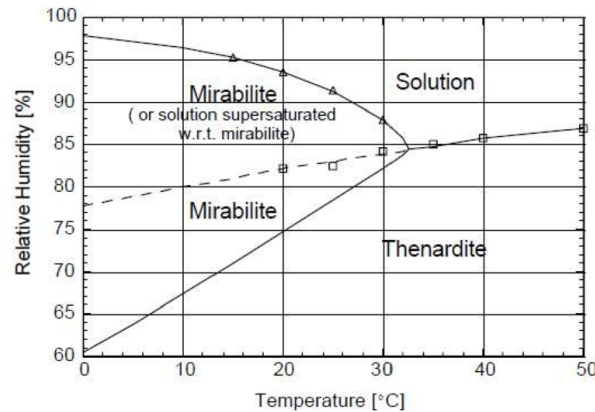
The deterioration induced by salt crystallization has been studied for over a century and points out relevant issues with regards to the most common salts present in monument and structures, such as the high damage inducing sodium sulfate, the ubiquitous sodium chloride, and the less damaging gypsum. Because sodium sulfate induces such fast and intense deterioration in materials, it has been the salt most used for crystallization tests to evaluate mechanical resistance (durability) of materials[7].

The oldest salt crystallization test uses a  $\text{Na}_2\text{SO}_4$  solution to impregnate the samples and then subject them to wet-drying cycles [7] since it can result in intense damage to the substrate. It was used to test durability and mechanical resistance. The deterioration of the substrate can be attributed to the crystal growth that may occur both during the drying as well as the wetting step [7] and that both thenardite, the anhydrous form, and mirabilite, the decahydrate, can crystallize simultaneously, one at the expense of the other, thus inducing repeated crystallization cycles [7,30].

Macroscopic and microscopic scale experiments using magnetic resonance imaging and phase contrast microscopy demonstrate that sodium sulfate that has both hydrated and anhydrous phases can lead to severe damage in sandstone during rewetting/drying cycles, but not during humidity cycling. During rewetting (a rapid process) in regions (pores) that are highly concentrated in salt, anhydrous microcrystals dissolve only partially, giving rise to a heterogeneous salt solution that is supersaturated with respect to the hydrated phase. The remaining anhydrous crystals then act as seeds for the formation of large amounts of hydrated crystals, creating grape-like structures that expand rapidly. These clusters can generate stresses larger than the tensile strength of the stone,



leading to damage. On the other hand, with humidification (a slow process) and after complete deliquescence of salt crystals, the homogeneous sodium sulfate solution can reach high concentrations during evaporation without any nucleation, favoring the formation of isolated anhydrous crystals (thenardite). The crystallization of the anhydrous salt generates only very small stresses compared to the hydrated clusters and therefore causes hardly any damage to the stone.



**Figure 5: Phase diagram for sodium sulfate.**

**Note: The continuous lines indicate the boundaries of the stable phases. Triangles and squares are experimental data for mirabilite and thenardite, respectively [35]. The discontinuous line corresponds to a solution in metastable equilibrium with respect to thenardite and supersaturated with respect to mirabilite**

Rodriguez Navarro et al. [7,31] showed that under normal conditions, i.e., non-equilibrium, 40% RH and 20°C and relative fast evaporation, the anhydrous thenardite will crystallize directly from solution (although it is below the 32.4°C thenardite-mirabilite transition point) inducing significant deterioration to the substrate and thereby also reflecting the importance of crystallization kinetics (Figure 5). Furthermore, no direct hydration of thenardite occurred, with mirabilite being produced only from the dissolution of thenardite and its reprecipitation [7]. For materials with a relatively homogeneous pore system, those with finer pores tend to suffer more deterioration from salt crystallization than those with larger pores. Further studies by Cultrone and Sebastián [7,32] confirmed the increase of smaller pores after salt crystallization tests is possibly caused by microfissures formation. Benavente et al. [7,33] characterized material parameters of several different rocks and applied a non-standard  $\text{Na}_2\text{SO}_4$  crystallization test to determine their resistance to it. Using a principal component analysis they correlated the resulting salt weathering to the pore structure of the stone, its water transport properties, as well as its mechanical strength finding that the latter was the most important parameter in resisting this particular salt weathering in agreement with previous tests carried out on bricks [7,34]. It would appear that this nonstandard crystallization test proved to be more useful than the accepted standard test.

### **2.3 Porous Building Material and Salt Damage**

Porous building materials such as stone, brick, mortar, and concrete have unique intrinsic characteristics that will impact the way salt crystallization-dissolution processes will affect their material integrity. [37] Soluble-salt crystallization inside porous materials generates crystallization and/or hydration pressures likely to exceed the elastic limit of the material, causing its failure. The hygric and mechanical behaviour of porous materials is significantly influenced by any moisture and contaminating agents they contain. When salts are dissolved in water that is absorbed by the material, they will crystallize as the material dries out. Crystallization inside the porous structure induces expansive forces in the material that can eventually lead to damage and cracking. It is possible to predict the behaviour of porous materials due to salt crystallization knowing pore volume, pore size distribution, tensile strength of these materials and the values of crystallization pressures of the different salts which appear[36].

### **2.4 Limewash and Salt Crystallization of Porous Building materials**

Preventing salt deterioration and treating salt problems include controlling the ingress of salts and water, removing of any damaging salts already present (desalination), modifying the environmental conditions to reduce damaging cycles from any remaining salts, and/or using materials known to be less vulnerable to salt attack[38]. Desalination and environmental control (to control temperature and relative humidity and thus reduce the likelihood of crystallisation and dissolution cycles) should be effective . Methods that are unlikely to prevent salt deterioration, and indeed are likely to enhance it, are the application of water repellents. Several recent studies have shown that such techniques encourage subflorescence rather than efflorescence of salts, thus increasing the likelihood of damage[38].

Limewash is an effective surface covering for a wide range of water-absorptive surfaces. The main advantages of using limewashes in the conservation of old buildings' facades are with its compatibility with the original porous materials thanks to its high water vapour permeability and water-shedding properties, antiseptic features that hinder biocolonization, and the preservation of the traditional aesthetical image of the building [39,40]. The main drawbacks related to the use of limewashes in exterior walls are its low durability towards rain, high soiling retention, and reduced washing resistance, thus demanding frequent maintenance, especially in polluted areas rich in sulphurous gases [40]. The success of limewash application is dependent upon the quality of the surface, or substrate, to which it is applied. There are 3 major factors associated with the substrate: 1) mechanical key, 2) absorbency, and 3) chemical compatibility. Limewash can beneficially consolidate damaged substrates as limewash is vapour-permeable, allowing a building to breathe from the inside to the outside. Carbonation of the surface over time, and encouraged during application by cycles of wetting and drying, increases the beauty and durability of the limewashed surface[41].

### 3. METHODOLOGY

#### 3.1 Stone Characterization

The EN12370 and RILEM test under this study were performed on two types of natural substrates: Mšené sandstone and Opuka marlstone. Both these stones used in tests are widely used as part of heritage/historic restoration interventions and building constructions around Czech Republic. Apart from their historic significance in building restoration and construction in Czech Republic, these two stone types were mainly selected based on their distinctive behaviour in terms of capillary action and water transport inside the stones which largely depends on the pore size distribution and their mechanical properties. The assessment of limewash and its effectiveness during the salt crystallization was only carried out on with RILEM Mšené (Prague sandstone) specimens as previous research showed that the limewash was not effective in the protection of Opuka stone due to low adhesion to this substrate[40]. As due to the presence of wider pore space in Mšené stone, the penetration of limewash coats becomes better in the superficial stone layer compared to Opuka stone as the Opuka stone itself restricts the penetration of limewash coats forming a layer that is less prone to lime coat absorption [40].

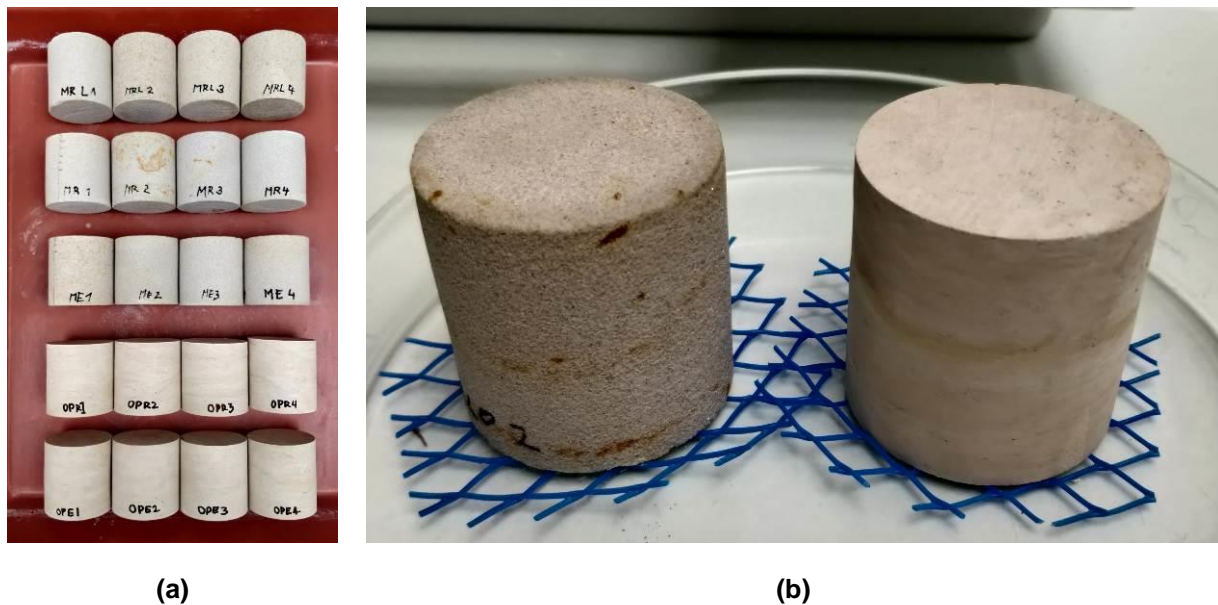


Figure 6: (a) Example of specimens used during the EN and RILEM test, (b) Mšené and Opuka stones during reference capillary test

#### Mšené

Mšené stone, commonly known internationally as Prague sandstone, is quarried nearby Mšené-lažně, a town about 40 km from Prague, and has been used in buildings and sculptures since the 14th century. Mšené is coarse-grained siliceous sandstone of grey colour with yellow-brown stains. The

features of this stone, namely its homogeneity, high porosity and unimodal pore size distribution, lead researchers to use it in salt crystallization research studies[40].

### **Opuka**

Opuka is a sandy marlstone quarried in the vicinity of Prague and was largely used in buildings and sculptures mostly from the 9th to the 14th century in the Bohemian region. In this study, the variety commonly known as Gold Opuka was used. It is a very fine-grained stone mainly composed of silica, calcite, and clay; it has yellow-beige colour and shows visible bedding planes [40].

The physical characteristics of the stones relevant to the present study are summarized in Table 1. The properties were determined in a previous work using specimens of the same stone blocks. Physical properties of Czech stones determined in the NAKI18 project the values are the average ( $\pm$ standard deviation) [37].

**Table 1: Porosity and bulk density of the stones [37]**

Stone type	Physical characteristics measured using RILEM Test No. II.2				
	Water absorption at atm. pressure 24h (wt. %)	Water absorption at atm. pressure 48 h (wt. %)	Bulk Density (kg.m <sup>3</sup> )	Open porosity, 48 h at vacuum (v. %)	Water Absorption, 48 h at vacuum (wt. %)
<b>Mšené</b>	12.0 $\pm$ 0.2	12.3 $\pm$ 0.2	1861.9 $\pm$ 12.2	29,7 $\pm$ 0,4	15,9 $\pm$ 0,3
<b>Opuka bedding layers in horizontal direction</b>	8.2 $\pm$ 0.1	9.4 $\pm$ 0.6	2045,0 $\pm$ 28,7	23,5 $\pm$ 0,8	11,5 $\pm$ 0,6

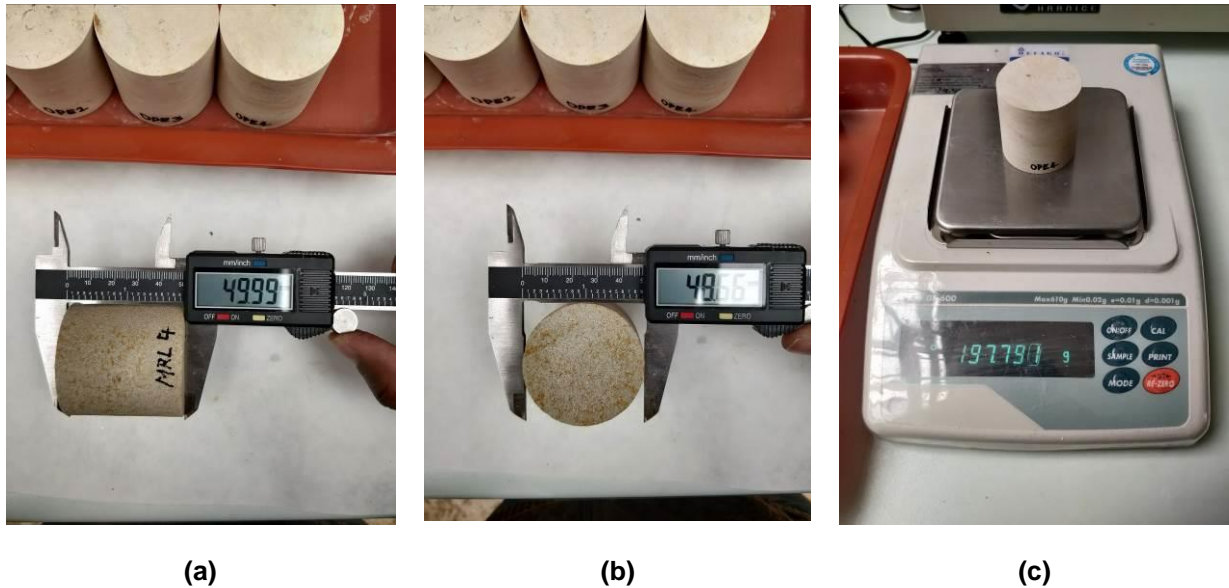
**Table 2: Main pore size and solid Density Properties of samples - NAKI18 project [37]**

Stone type	Main Pore Size <sup>2</sup> ( $\mu$ m)	Solid Density (kg/m <sup>3</sup> )
<b>Mšené</b>	27	2897
<b>Opuka</b>	0.2	2672

## **3.2 Salt Crystallization Aging Tests**

Before the tests, all the selected stone specimens (Mšené and Opuka) were visually inspected for any possible visible surface defects and were cleaned following the EN and RILEM test standards. All the specimens were kept at room condition inside a desiccator with silica gel for 24h to ensure that specimens were completely dry before initiating the test. The physical characteristics i.e. height, diameter and dry weight of each specimen were recorded in their initial undamaged state. The height and diameter were measured using digital vernier calipers with precision up to two decimal places and

the dry weight of each specimen were recorded on a digital balance with precision up to  $10^{-3}$  g and accuracy up to  $10^{-2}$  g. Before commencing the test, ultrasonic pulse velocity (UPV) test was also performed on each specimen in its undamaged state and the results were analyzed after each test cycle and compared to assess the damage propagation in specimens due to salt crystallization.



**Figure 7: Example of measurements of geometrical characteristics of specimens (a) Height (b) Diameter, (c)Weight**

**Table 3: Summary of testing procedures for accelerated aging tests**

TEST	Standard	No of cycles	No. of specimens	Sample ID
<b>P1</b> (uncoated)	EN 12370	15 Wet/Dry Cycles	Mšené: 4 Opuka: 4	ME1-ME4 OPE1-OPE4
<b>P2</b> (uncoated and limewash coated)	RILEM 271-ASC	1 Salt Accumulation Cycle 4 Salt Propagation Cycles	Mšené: 3 Opuka: 4 Mšené: 4	MR5-MR7 OPR1-OPR4 MRL1-MRL4
<b>P3</b> (uncoated)	RILEM 271-ASC	2 Salt Accumulation Cycle 4 Salt Propagation Cycles	Mšené: 4	MR1-MR4

For assessment of salt crystallization on durability of two natural stone types (Mšené and Opuka) as discussed in the previous section 3.1, three test procedures (P1-P3) were performed specimens following the norms of existing EN12370 and new RILEM Test for determining of resistance of natural stone towards salt crystallization. Test performed are summarized in Table 3.

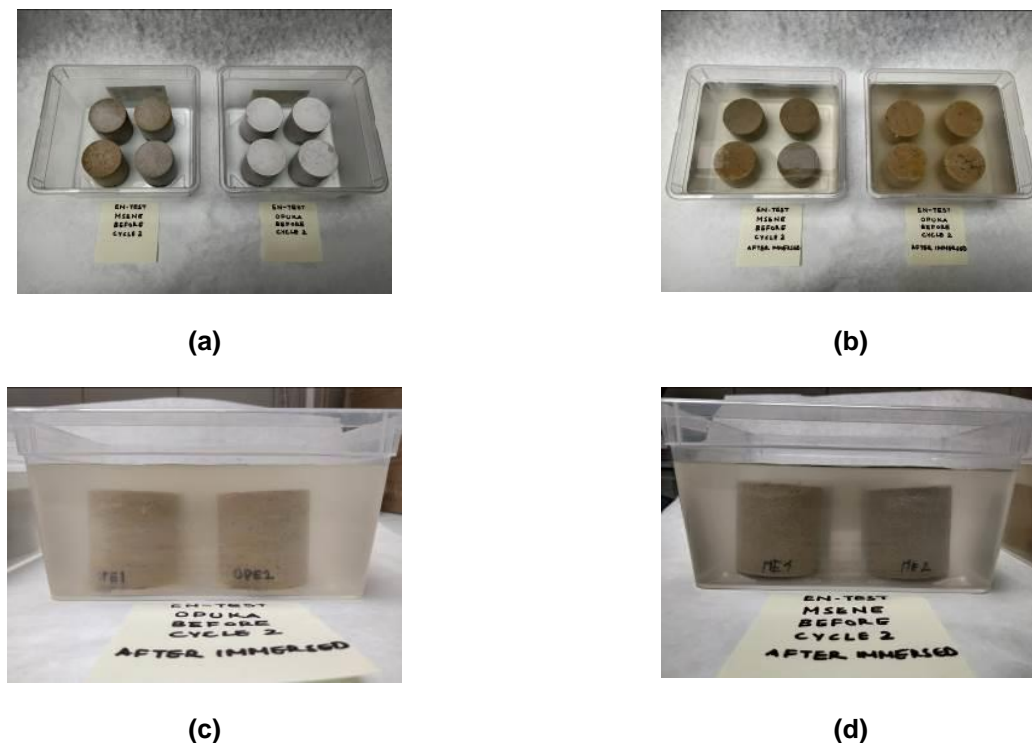
The Test Procedure P1 was performed according to EN 12370 test standards where baseline process was modified during the drying stage. The drying was two directional from the top and the side surface. Drying through the bottom surface was partially controlled by placing group of 4 stone specimens (Mšené and Opuka) together in a separate petri dish inside the oven. During the test

procedure P1, a total number of 15 wet-dry cycles were performed on the stone specimens by complete immersion in 14wt.% mirabilite ( $\text{Na}_2\text{SO}_4 \cdot 10\text{H}_2\text{O}$ ) salt solution. The Test Procedure P2 and P3 followed the RILEM test norms which simulated more realistic in-situ behaviour of the material being tested. The test cycles with procedure P2 and P3 were performed in two phases (accumulation and propagation) with partial immersion of stone specimens into 5wt.% thenardite ( $\text{Na}_2\text{SO}_4$ ) salt solution as per RILEM standards. Due to limited time available, the following study mainly compares results obtained from the first 4 cycles of the two test standards (EN and RILEM).

**Table 4: Summary of salt solution used during the EN12370 test cycles**

Cycle	Exposure Method	Concentration of Salt (w.t.%)	Rewetting	Drying Conditions
Cycle 1 -15	Full Immersion	14% $\text{Na}_2\text{SO}_4 \cdot 10\text{H}_2\text{O}$	All Cycles Salt Solution	Starts at 40 °C and increase to 105 °C

**Test Procedure P1 – EN12370:** Following the EN 12370 Test procedure, a 14% salt solution of sodium sulphate decahydrate ( $\text{Na}_2\text{SO}_4 \cdot 10\text{H}_2\text{O}$ ) was prepared for 1-15 test cycles and the specimens were completely immersed in the salt solution for 2hrs in a rectangular plastic container measuring 19.5 x 16.5 x 9.5 cm. A group of four specimens of each stone type were kept together in one single plastic container with a salt solution ca.10mm above the top of the specimens and the containers were covered with the plastic lid to prevent evaporation. The specimens were left to soak in the salt solution for 2h at  $20 \pm 0.5$  °C.



**Figure 8: Top: Example of complete immersion of EN specimens (a) Before test (b) After immersion**

**Bottom: Contamination for 2h (c) Opuka (d) Mšené**



(a)



(b)

**Figure 9: (a) Example of drying of EN specimens (b) Example of drying at room conditions**

**RILEM 271 ASC TESTS:** The RILEM test was conducted in two phases according to procedure developed by RILEM Technical Committee 271-ASC, in which accumulation phase aims at impregnating the specimens with specific salt solution by capillarity during the wetting stage followed by drying in oven at 40°C / 15±5%RH with low airflow until specimens are 80% dried of their initial water weight. The propagation phase aims at developing damage inside the porous structure of the substrates due to salt crystallization by repeated rewetting of the specimens with distilled water followed by initial drying of the specimens at room temperature for 24hrs and further drying in oven at 40°C / 15±5%RH with low airflow until they are 80% dried of their initial water weight during each cycle [41].

Before initiating the RILEM test and contaminating the specimens with salt solution, a single layer of parafilm was wrapped around circumference of core cut cylindrical stone specimens which was secured using a textile tape to ensure adequate sealing of the specimens during the wetting and drying phase. Additional layer of parafilm was also wrapped around the top of the specimens extending 5mm above the top surface to collect efflorescence or material debris during the RILEM test. After wrapping specimens with parafilm, the ultrasonic pulse velocity (UPV) test was performed on each RILEM test specimens in their initial dry (sound) state without any damage.

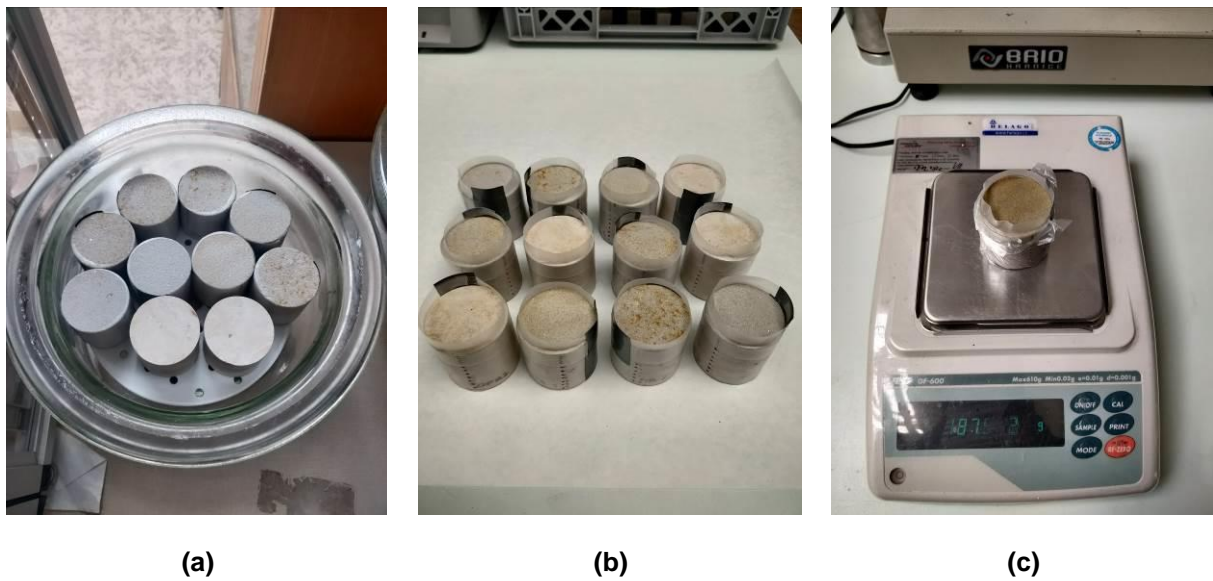


Figure 10: Examples of RILEM Samples (a) With Parafilm (b) With 5mm parafilm on top (c) Bottom sealed after salt contamination/rewetting

Table 5: Summary of test conditions used during the RILEM test cycles

Procedure	Exposure Method	Concentration of Salt (w.t.%)	Rewetting	Drying Conditions
P2 (uncoated and limewash coated)	Partial Immersion	5% Na <sub>2</sub> SO <sub>4</sub> (1 accumulation phase)	Distilled Water (propagation phase)	40 °C and 15±5% RH
P3 (uncoated)	Partial Immersion	5% Na <sub>2</sub> SO <sub>4</sub> (2 accumulation phase)	Distilled Water (propagation phase)	40 °C and 15±5% RH

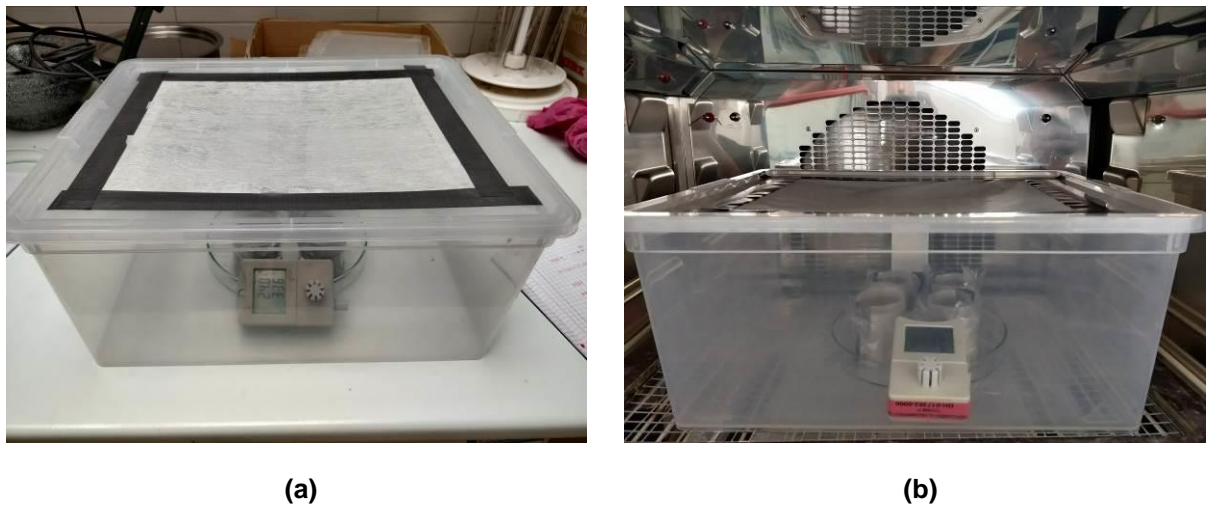
**Test Procedure P2 - RILEM uncoated 1 salt contamination:** During the accumulation phase, group of 4 specimens of each stone type (Mšené and Opuka) were separately placed inside a petri dish above a plastic mesh with salt solution 10(±3)mm to ensure that contamination with salt solution happens through the bottom of each specimens (MR1-MR7 and OPR1-OPR4) through capillary absorption as per norms of RILEM Test. The specimens were soaked until the top of the samples were wet (CMC) with salt solution during the accumulation phase. After contaminating specimens with 5% sodium sulphate (Na<sub>2</sub>SO<sub>4</sub>) salt solution (thenardite), the wet weight of each specimen was measured and the bottom of each specimen was sealed using a layer of thin plastic sheet. Each specimen's wet weight was also measured with bottom wrapped and the deductions were made accordingly to relate change in the wet-dry mass in each cycle during the accumulation phase. Specimens were then placed inside a plastic container and were covered with lid with Japanese textile



on top to maintain reduce air flow which resembles the in-situ conditions. Samples during the accumulation phase were dried at 40°C / 15±5% RH in oven by maintaining low air low.



**Figure 11: Example of RILEM samples partial immersion before and after salt contamination (a) Mšené (b) Opuka**

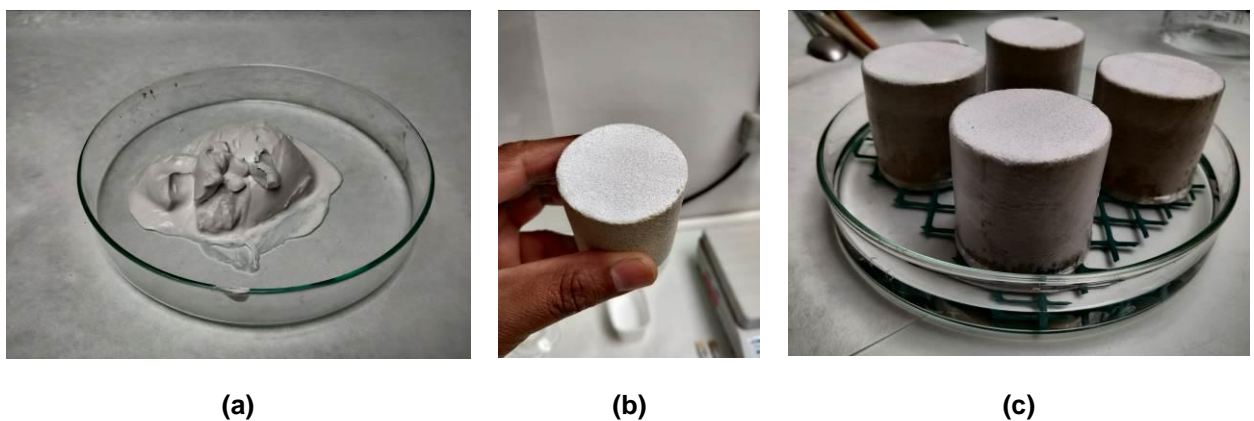


**Figure 12: Example of RILEM samples during oven drying (a) Drying room conditions (b) Oven drying**

During the propagation phase, the specimens were removed (at end of accumulation phase) from the oven when they were 80% dried of the initial water weight and were left for cooling at room condition ( $T=22^{\circ}\text{C}\pm 2$  at 45% RH  $\pm 15\%$ ) for 4hrs inside the plastic box after removing the plastic sheet from the bottom surface. After cooling, the specimens were rewetted with distilled water until the top of the samples were wet (CMC) with by partial immersion following capillarity from the bottom surface at room condition ( $T=22^{\circ}\text{C}\pm 2$  at 45% RH  $\pm 15\%$ ) and the bottom was sealed again with plastic sheet after rewetting. The wet weight of the specimens was recorded with and without sealing the specimen's

bottom before starting the drying process. Initially the specimens were dried at room conditions ( $T=22^{\circ}\text{C}\pm 2$  at  $45\% \text{ RH} \pm 15\%$ ) inside a plastic container for 24h followed by oven drying till specimens were dried 80% of the initial water weight. The weight was regularly monitored during the drying stage using a digital balance with precision up to  $10^{-3}\text{g}$  and accuracy of  $10^{-2}\text{g}$ . At the end of each cycle during the propagation phase, the material loss was also calculated by brushing the evaporative surface of specimens with a soft brush and collecting the loose debris (material and salt efflorescence). The weight of loose debris and specimens were measured on a digital balance with precision of  $10^{-4}\text{g}$  and accuracy of  $10^{-3}\text{g}$  before and after removing loose debris to quantify the material loss during each propagation cycle. During the drying stage in accumulation and propagation phase, temperature and the relative humidity were monitored using digital thermo controllers.

**RILEM with 1 salt contamination and limewash:** Before beginning the RILEM test, group of selected 4 Mšené stone specimens (MRL1-MRL4) were coated with limewash application over its evaporative surface to assess the antiseptic properties of limewash against the salt crystallization. A pure lime putty with mass of ca.  $50\pm 3$  wt.% of class CL90 was used on the specimen's evaporative surface which was prepared by storing air lime hydrate powder under water for 1 year following standards of EN459-1 [42]. Before applying the first coat of limewash, the specimen's top surface was wetted with distilled water using soft brush to ensure adequate penetration and adherence of the limewash inside the porous structure of the specimens and avoiding crazing of the limewash paint. A total number of 6 limewash coats were applied on each specimen's top surface at a regular interval of 24h in a crisscrossed manner and the weight of each specimen was recorded before and after application of limewash coats. The rest of the test procedure of sample preparation, accumulation phase and propagation phase was same as for uncoated Test Procedure P2.



**Figure 13: Example of lime coated Mšené samples used during RILEM test procedure P2 (a) Lime Putty (b) Lime painted specimen (c) Salt contamination of limewash coated samples**

**Test Procedure P3 - RILEM with 2 salt contamination:** As per the RILEM standards specimens are impregnated with only single salt contamination during its accumulation phase. Test Procedure P3 was performed on a group of three Mšené stone specimens (MR1-MR3) with variation introduced

during the salt accumulation phase of the test. The drying conditions were same as Test Procedure P2 in the accumulation phase. As a variation to existing RILEM standards, the Test Procedure P3 was performed with 5% sodium sulphate ( $\text{Na}_2\text{SO}_4$ ) salt solution (thernadite) with 2 salt accumulation cycles, which increased the salt concentration inside the specimen's porous structure inducing more crystallization pressure further resulting in more damage and salt efflorescence compared to Test Procedure P2. The rest of the test procedure of sample preparation and propagation was same as Test Procedure P2. The results from Test Procedure P3 were compared to Test Procedure P1 and P2 in section 4.

Also it was noticed initial layer of parafilm showed sign of hairline cracks due to temperature variation while drying during the accumulation phase. An additional layer of parafilm was again applied along the periphery of each specimen and the weight difference of new parafilm layer was calculated which was deducted from the initial dry weight of the specimens to compare the mass evolution during the test.

### **3.3 Methods of analysis: Assessment of damage and salt analysis**

The change in specimen's characteristics were regularly monitored during the EN and RILEM tests and detailed analytical tests (destructive and non-destructive) were performed on selected specimens to precisely understand the damage induced by salts.

#### **3.3.1 Visual Observations**

The alteration in physical visual appearance of each specimen was monitored photographically during the EN and RILEM test procedures. Photographs were taken at the end of each drying stage to understand salt efflorescence and damage severity type following the ICOMOS glossary [43] and MDCS atlas [44].

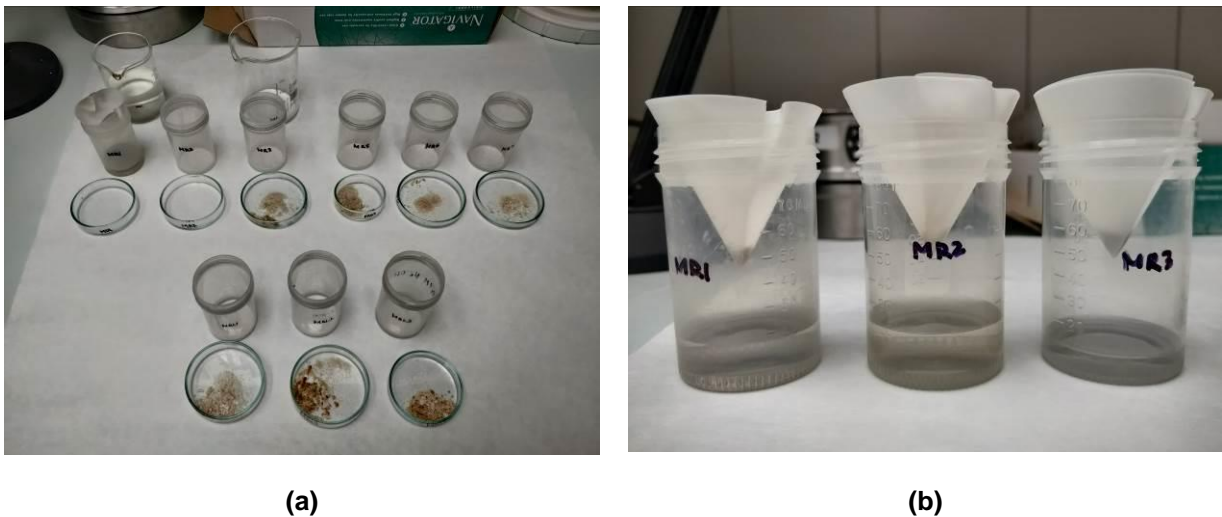
#### **3.3.2 Material Loss, Mass Evolution and Salt Efflorescence**

The specimens were carefully monitored for material loss and salt efflorescence during the experiment using digital weight balance with a resolution of  $10^{-3}$ g and accuracy of  $10^{-2}$ g. Each specimens initial sound weight was measured before beginning the EN and RILEM test procedures through which the damage propagation was tracked during the aging cycles.

During EN test, the wet weight of each specimen was monitored after every salt contamination during the 15 aging cycles. After drying, the specimen's new dry weight was calculated before and after brushing any salt efflorescence accumulated near the specimen's evaporative surface. Any large material loss observed during wetting, drying, handling or during salt efflorescence brushing were collected in a petri dish which were further dried and weighed to calculate the mass loss in each cycle. At the completion of 15 test cycles, the final dry weight of EN specimens were measured post desalination after achieving the constant dry mass. Although most of the material damage was

observed during the wetting stage, the material loss in EN specimens was calculated only through the dry mass achieved after the end of each test cycle.

During the RILEM test cycles, the weight of each specimen was recorded both before and after salt contamination and the amount of salt absorbed by the specimens was calculated during the accumulation phase which helped quantifying the salt efflorescence developed during each propagation cycle. As RILEM test was carried out in two phases: accumulation and propagation, during the drying stage of two phases the weight of each specimen was regularly monitored at an interval of ca.24h until 80% of the moisture had evaporated. At end of drying cycles during the propagation phase, the debris (salt efflorescence and material loss) were collected from specimen's evaporative surface using a soft brush and they were weighed on a digital balance with resolution of  $10^{-4}$ g and accuracy of  $10^{-3}$ g. At the completion of RILEM test, the debris collected were diluted in distilled water and were filtered with the help of filter paper to quantify the material loss and calculate the salt efflorescence developed in each propagation cycle (Figure 14). The filtration of the debris was only carried out for the RILEM specimens [8].



**Figure 14: (a) Example of debris collected during RILEM test (b) Example of materials loss calculated using filtration method**

### 3.3.3 Ultrasonic Pulse Velocity (UPV)

The deterioration and damage progression in stone specimens was regularly monitored using non-destructive ultrasonic pulse velocity (UPV) testing method at the end of each cycle(drying stage). One of the advantage of this method is that the compactness of stone specimens could be easily measured after salt weathering and the same specimens can be further used for destructive testing like scanning electron microscopy (SEM) and ion chromatography (IC) which makes results comparable between destructive and non-destructive methods. As the velocity inside the porous materials

depends on the percentage pores, the volume and the type of fissures, the mineralogical composition, the density and the moisture. The way the waves propagate inside the stone depends on the direction and the orientation and this provides a picture of the degree of anisotropy, which varies depending on the orientation of the components (grains, pores, etc), the rock fabric and its structure. The presence and distribution of anisotropies will affect, at least partially, the durability of the stones [45].

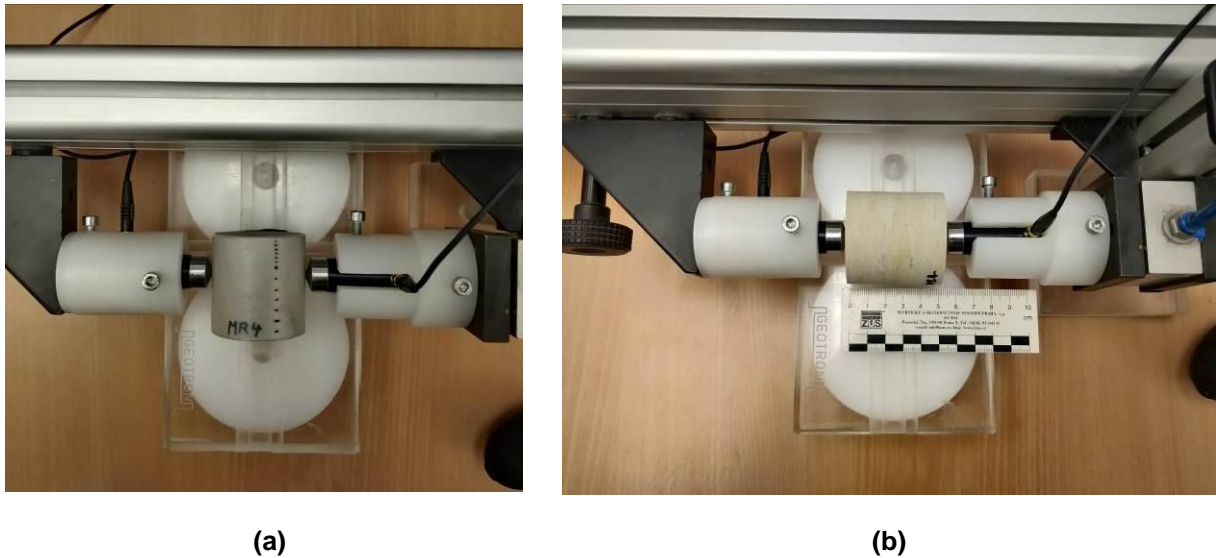
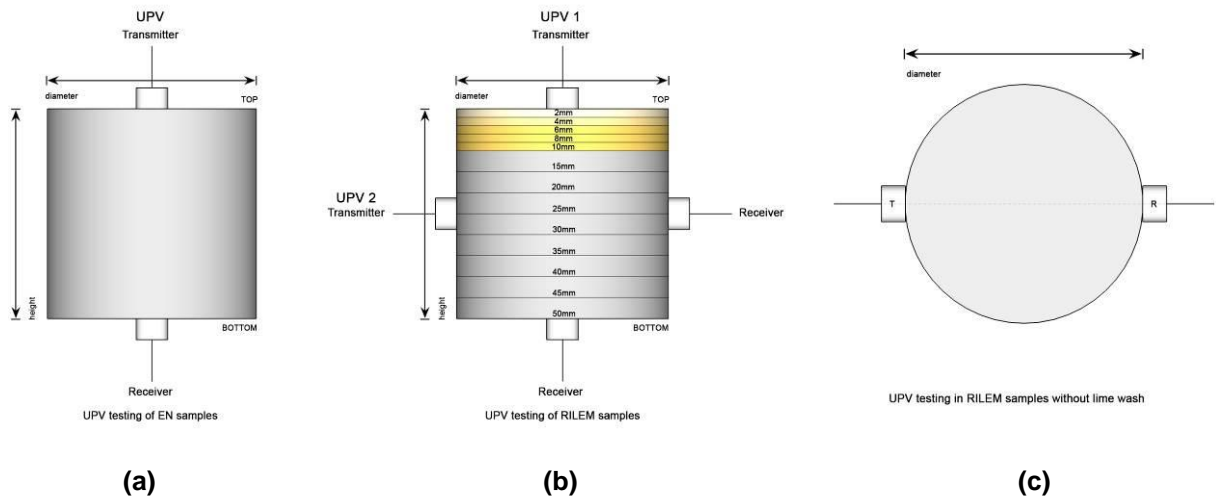


Figure 15: **Example of ultrasonic tests performed on specimens (a) through diameter (b) through height)**

UPV measurements were performed to assess the salt distribution non-destructively, using a portable instrument (USG 40 Krompholz Geotron Elektronik (DE) with pointy-ended transducers with a contact section of  $\varnothing$  2 mm. Only one measurement on EN specimens was taken through the height as compared to RILEM specimens. UPV test in RILEM specimens was performed through the height at the center of specimen and through the diameter along the height of the specimens. Along the height, first 10mm was marked at interval of 2mm where the salt concentration was expected to be higher and then followed by marking specimens at interval of 5mm each till the bottom of the RILEM test specimens show in Figure 16. Initial UPV test was also performed on EN and RILEM test specimens in their sound state. During the test UPV was performed after cooling the specimens at the end of each test cycle.



**Figure 16: Determination of ultrasonic velocity by the direct transmission method (a) UPV in EN samples (b) UPV in RILEM samples along height (c) UPV in RILEM samples along diameter**

### 3.3.4 Analysis of the salt distribution

The sodium sulphate (5wt.%  $\text{Na}_2\text{SO}_4$ ) salt concentration and distribution was only analyzed for the selected stone specimens tested with RILEM procedure using two destructive testing methods: ion chromatography (IC) and scanning electron microscopy (SEM). The Mšené (uncoated and limewash coated) and Opuka (uncoated) specimens analysed with IC and SEM were only contaminated once with salt solution during the accumulation phase. At the end of single salt accumulation phase, the stone specimens MR4, OPR4 and MRL4 were split into two equal halves (along the height) using a hammer and a chisel after they were completely dried (Figure 18). Before splitting the selected stone specimens, the non-destructive UPV test was also conducted as per methodology discussed in previous section to compare the results from the destructive and non-destructive test and check the reliability of the two testing methods for salt distribution and damage propagation assessment. Figure 17 below summarizes the type of specimens selected for IC and SEM analysis for assessment of salt distribution

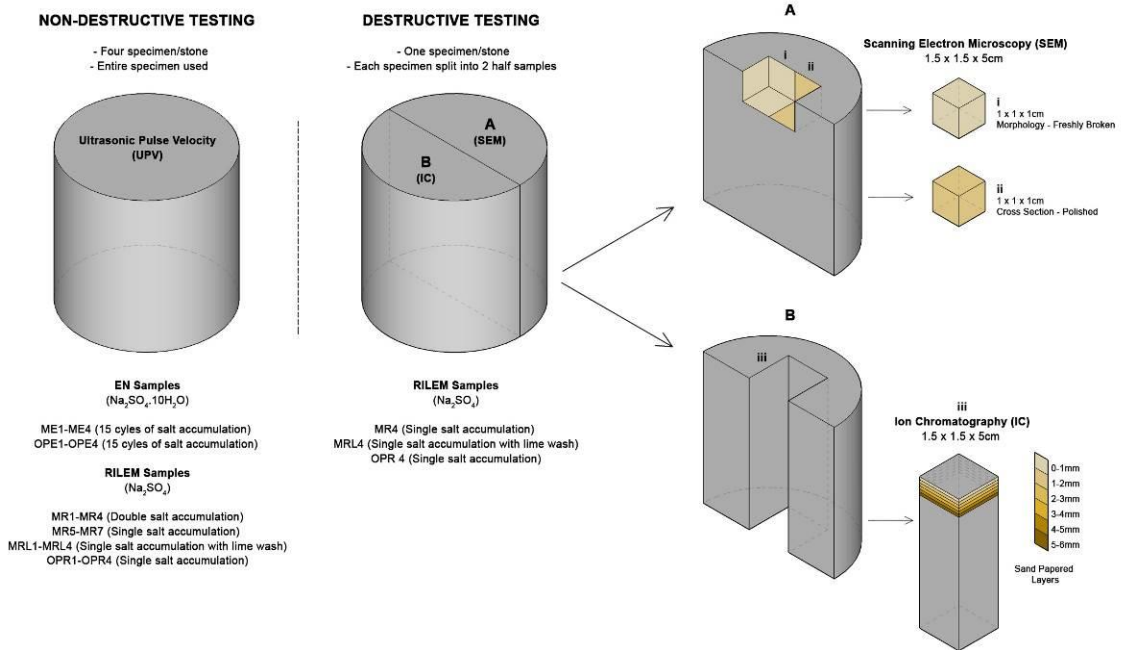


Figure 17: Schematic representation of specimens used for destructive and non-destructive testing

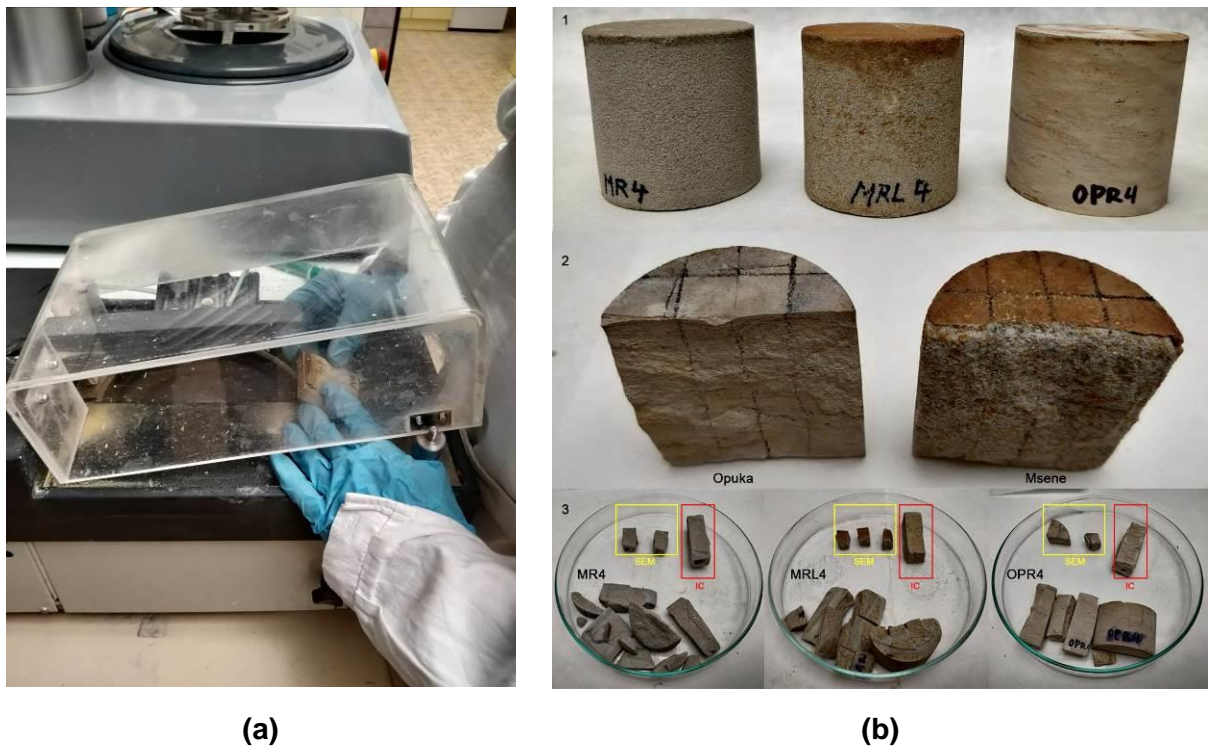


Figure 18: (a) Example of sample preparation (b) Example of prepared samples

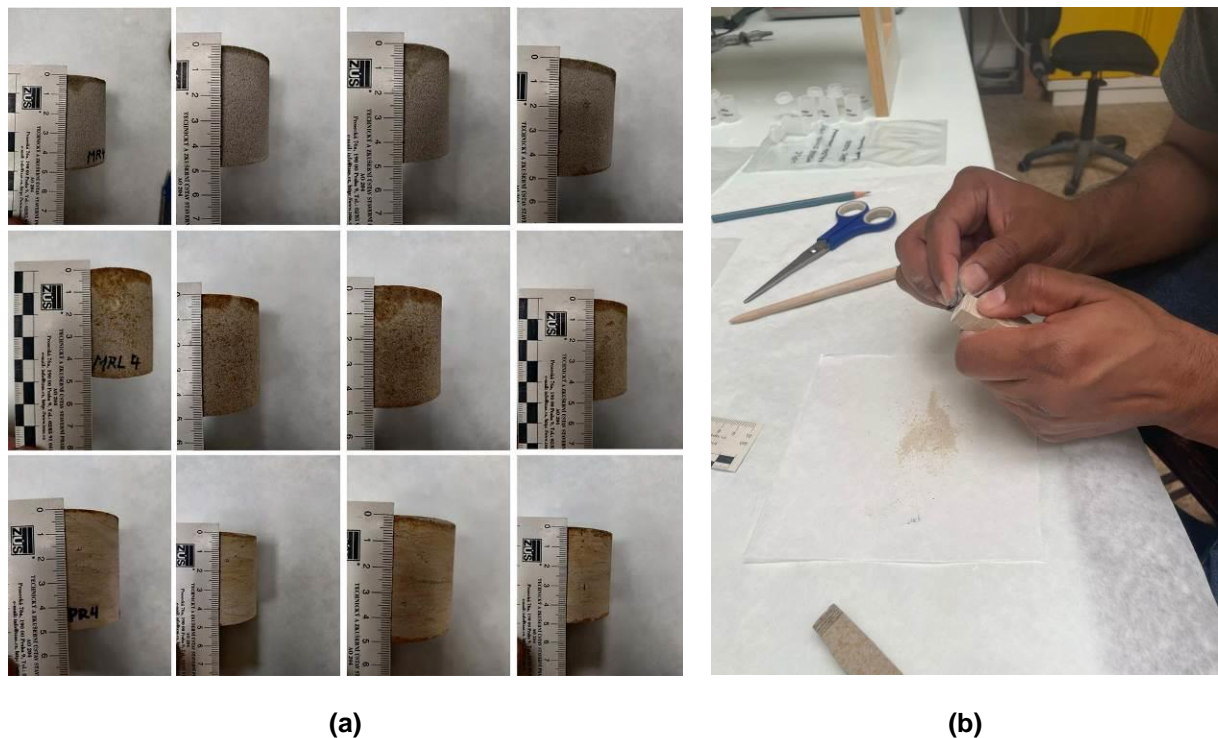


**Figure 19: (a) Example of samples marked equally at 1mm interval for salt with ion chromatography analysis at each layer from evaporative surface (b) SEM samples embedded in epoxy resin and prepared for microscopic analysis**

### 3.3.4.1 Ion Chromatography (IC)

The salt concentration near the evaporative surface was only analysed for the RILEM lime coated (MRL4) and uncoated Mšené (MR4) and Opuka (OPR4) stone specimens through means of ion chromatography using Dionex ISC-5000. A rectangular cross-section sample measuring 1.5 x 1.5 x 5 cm was cut through the first half part of the RILEM stone specimens using a mechanical saw cutter using isopropanol to avoiding any salt dissolution [Figure 18(a)]. Using a pencil, reference lines were marked on the cross-section obtained at an interval of 0-1, 1-2, 2-3, 3-4, 4-5 and 5-6mm starting from the top of evaporative surface up to the depth of 6mm Figure 19(a). Each 1mm layer of the cross-section was manually hand grinded [Figure 20(b)] into a fine powder using a fine grade sand paper to get the precise information about the salt distribution in the first salt-rich outer layers [Figure 20(a)]. The weight of the grinded salt and stone powder was kept within the same range to acquire more precise results. Anions ( $\text{SO}_4^{2-}$ ) and cations ( $\text{Na}^+$ ) were analysed by ion chromatography (IC) for each layer and the results in parts per million (ppm-mg/L) were converted to wt.% (relative to the dry sample weight) and the sum of the equimolar contents of  $\text{Na}^+$  and  $\text{SO}_4^{2-}$  was estimated. The salt amount present in each layer was calculated as the percentage of the total salt content present in the sample during accumulation phase. The average amount of each ion (in wt.%) in each group of three specimens contaminated with each procedure was calculated in relation to the respective total weight of each group of samples.





**Figure 20: (a) Visible salt layer formed after drying specimens during RILEM test accumulation phase (b) Grinding of specimen manually into fine power for each 1mm layer for ion chromatography (IC) test**

### 3.3.4.2 Scanning Electron Microscopy (SEM)

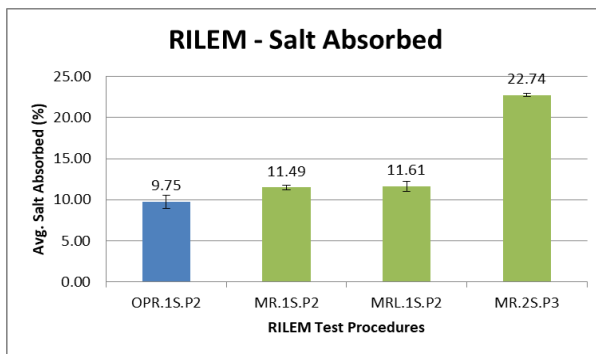
The morphology and distribution of sodium sulphate ( $\text{Na}_2\text{SO}_4$ ) salt within the stone's porous structure was analysed with the help of SEM microphotographs on the selected specimens (MR4-MRL4-OPR4) tested with RILEM test procedure P2. Microanalysis was conducted on freshly fractured stone cross section of size ca. 1 x 1 x 1 cm along with polished cross sections ca. 1 x 1 x 1 cm embedded in low viscosity epoxy resin (EPO-TEK) under vacuum. The polished stone specimens were dried for 24h of polymerization and were then grinded with SiC paper (STRUERS) at 500, 1000, 2400 and 300 rpm for 5min (each step) using isopropanol as coolant (to avoid salt dissolution) with final polishing with water-free diamond polishing suspensions (9,3 and 1mm). Before starting the SEM analysis, the surface of each resin embedded polished sample were coated with a 15nm carbon layer in BALTEK SCD 050 Sputter Coater after which the samples were observed for SEM with an MIRA II LMU (Tescan) microscope equipped with energy dispersive X-ray detector (EDX) from Bruker AXS at high vacuum and 15kV voltage and a working distance of 15 nm using secondary electron detector and backscatter electron (BSE) imaging. The morphology of the stone's exterior surface and interior matrix was mapped upto 2mm depth from the evaporative surface as the results from the ion chromatography

(IC) confirmed the high salt concentration is in the first 2mm beneath the specimen's evaporative surface. Multiple SEM microphotographs were acquired in constant conditions with different magnifications to see the salt penetration and salt crystals location. As the microphotographs from the freshly broken cross-section did not provide the relevant data due to the unevenness of the surface, results acquired from polished cross sections. SEM microphotographs were considered for the further analysis of salt distribution in specimens as discussed in section 4.

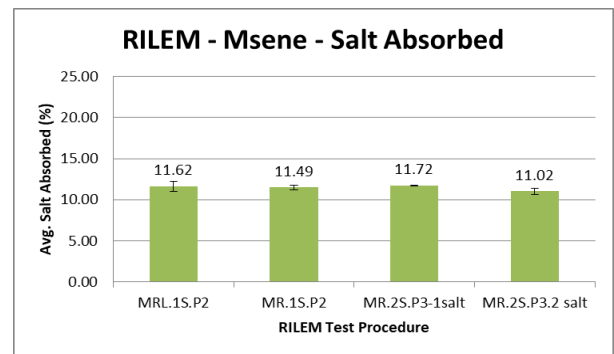
## 4. RESULTS AND DISCUSSIONS

### 4.1 Comparison between RILEM and EN12370

#### 4.1.1 Salt Accumulation

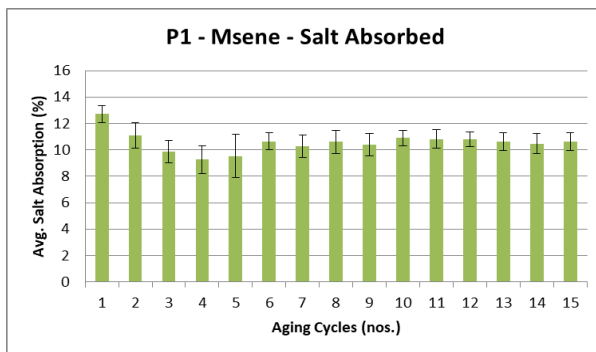


(a)

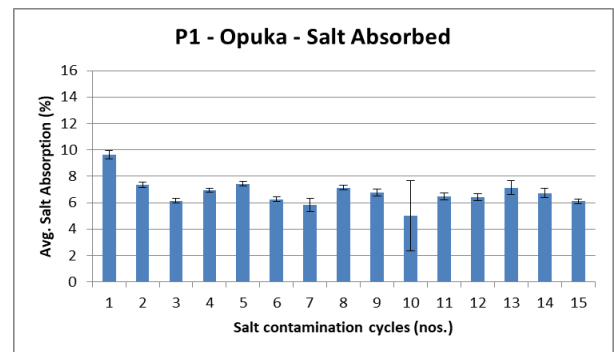


(b)

**Graph 1: Average salt absorbed amount (wt. %) during salt accumulation phase with RILEM procedure P2 and P3 (a) Comparison of Mšené and Opuka stones (b) Comparison of only Mšené stones**



(a)



(b)

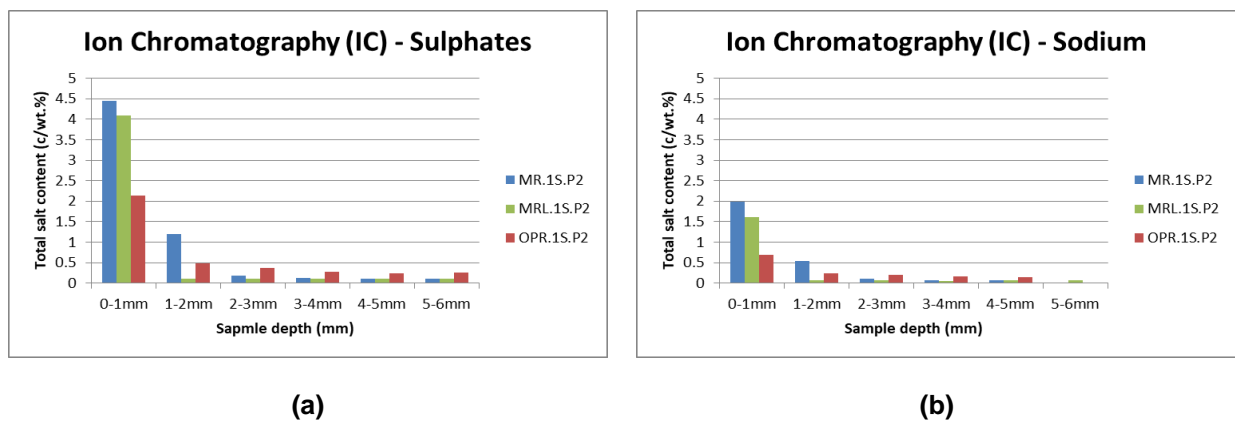
**Graph 2: Average salt absorbed amount (wt. %) in each cycle (a) Mšené stone (ME1-ME4) (b) Opuka stone (OPE1-OPE4) with EN procedure P1**

From the Graph 1 it is seen that the average salt quantity absorbed by the two substrates (Mšené and Opuka) tested with RILEM procedures (P2 and P3) were in a close range even due to their distinctive porous structure which draws attention towards the salt contamination method of partial immersion adopted during the salt accumulation phase. Both the substrates as mentioned before were contaminated until the substrates critical moisture content (CMC) was achieved which resulted in comparable salt absorption amount. Graph 1(a) compares the average salt amount absorbed by the

two substrates during salt accumulation cycle with RILEM procedures P2 and P3. The average salt quantity absorbed by the Opuka stone (OPR1-OPR4) tested with RILEM test standard was 9.75% which was comparatively higher than the average salt amount absorbed by Opuka stone tested with EN12370 standard which is shown in Graph 2(b). The average salt quantity absorbed by the EN Opuka specimens (OPE1-OPE4) which was 7%. Graph 1(b) compares average salt amount absorbed between Mšené stone (uncoated and limewash coated) with one and two salt accumulation cycle. The two salt accumulation cycles were only performed on uncoated Mšené stones following procedure P3. The overall average salt amount absorbed by Mšené stone (uncoated and limewash coated) during salt accumulation cycles was 11.4% (with procedure P2 and P3) which was close to average salt amount absorbed by the Mšené stone tested with EN procedure P1 [Graph 2(a)]. The average salt amount absorbed during each cycle by Mšené stone tested with EN standards was 10.5%.

#### 4.1.2 Salt Absorption and Ion Chromatography (IC)

Assessment of salt distribution and its concentration inside the aged specimens was only studied on specimen tested with RILEM standards using destructive testing through ion chromatography. One sample of uncoated Mšené (MR4), limewash coated Mšené (MRL4) and uncoated Opuka (OPR4) was selected from group of four samples aged with test procedure P2 (1-Salt accumulation). The salt distribution depth analyzed with IC provided useful information about the salt crystallization damage near the evaporative surface of specimens. The higher salt concentration near the evaporative surface in RILEM specimens implies risk of potential damage due to increased crystallization pressure.

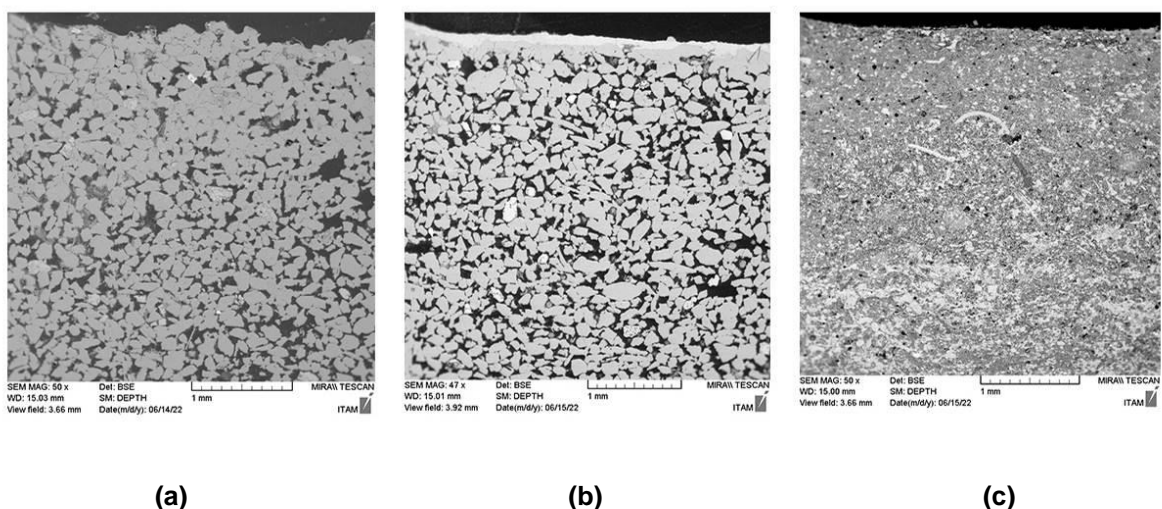


**Graph 3 Salt distribution upto 6mm depth from evaporative surface with procedure P2**

The three selected RILEM specimens (MR4-MRL4-OPR4) for the ion chromatography showed different accumulation of salt in the first 6 mm depth beneath the evaporative surface as shown in Graph 3 (a)(b). When comparison was made between the uncoated and limewash coated Mšené specimens the former specimens showed higher salt concentration near the evaporative surface. Most of the salt in uncoated Mšené specimens was concentrated in the first 2mm depth beneath the

evaporative surface compared to the limewash coated specimens where the high amount of salt was concentrated in 1mm depth beneath evaporative surface. Due to the large pore network of Mšené specimens more salt was transported during the drying stage in accumulation phase resulting in increased salt concentration towards the top evaporative surface and leaving less salt inside the pores of the specimens and producing less damage. From the Graph 3(a)(b) it is seen the concentration of salt the beneath the evaporative surface in uncoated Opuka specimen was half of that of Mšené (coated and uncoated) specimens. The results from the salt absorption [Graph 1(a)] shows the almost similar salt amount was absorbed during the accumulation phase for both Mšené (uncoated and limewash coated) and Opuka (uncoated) specimen (as the specimens were soaked until the top of the specimens became wet) but due to fine pores of Opuka specimens the movement of salt was restricted towards the evaporative surface during drying which resulted in presence of more residual salt within the subsurface of the Opuka which is also confirmed from the mass evolution (Graph 14) where the Opuka specimens showed increased mass variation when compared with the initial sound weight even after completion of 4 propagation cycles. It was seen that in Opuka specimens the salt concentration is higher than Mšené below the 2mm depth of the evaporative surface but even with the presence of salt inside the fine pores of Opuka no damage was observed on surface during the propagation cycles due to higher mechanical strength of Opuka overcoming the damage due to salt crystallization. It is seen that the concentration of salt after 2mm depth beneath the evaporative surface becomes half in Mšené stones compared to that of Opuka specimens. More rewetting cycles for the Opuka specimens during propagation phase could result in drawing more salt towards the evaporative surface and more damage could be observed.

### 4.1.3 Scanning Electron Microscopy (SEM)



**Figure 21: SEM investigation of salt laden samples (cross sections) showing granular structure (a) Mšené uncoated (b) Mšené lime coated (c) Opuka uncoated with 1-salt accumulation**

The scanning electron microscopy (SEM) analysis was performed only on the RILEM specimens with 1 salt accumulation tested with procedure P2 (uncoated and limewash coated) which was able to give microscopic evaluation of  $\text{Na}_2\text{SO}_4$  concentration in specimens near the evaporative surface. SEM analysis gave more precise assessment of the thickness of the salt layer including information about the salt distribution in pores, location of the salt, salt crystallization form and salt crystallization habit. Salt concentration in Mšené (MR4-uncoated and MRL4-lime coated) specimens was higher near the evaporative surface as compared to Opuka (OPR4-uncoated) specimen but was mainly present as a very thin layer concentrated in the first two millimetres of the subsurface in all the three stone specimens analysed with SEM.

**Mšené (lime-coated and uncoated):** Uncoated Mšené specimen (MR4) contaminated according to procedure P2 with 5wt.%  $\text{Na}_2\text{SO}_4$  showed uneven salt distribution mainly concentrated between the first 2mm layer below the evaporative surface (Figure 22) compared to lime-coated Mšené specimen (MRL4) tested with the similar procedure P2 where a thin uniform layer of salt was found concentrated only in the first 1mm layer towards the evaporative surface (Figure 23).

Although both the Mšené specimens (lime coated and uncoated) had identical pore network and identical salt uptake mechanism, the two specimens displayed different drying behaviour during the accumulation phase resulting in completely different salt distribution inside the pores of specimens. It could be seen from Figure 22 and Figure 23 that both uncoated and limewash coated Mšené specimens showed development of salt crust near the evaporative surface but the salt distribution in limewash coated specimen beneath 1mm of evaporative surface was comparatively less and more uniform than uncoated specimen, the same was also confirmed through ion chromatography analysis. It is believed that the salt transport mechanism was altered in limewash coated specimen drawing more sodium sulphate closer towards the evaporative surface and leaving less salt inside the pores compared to uncoated specimen. The limewash penetrated into the subsurface filled the pores beneath the evaporative surface hence resulted in more salt efflorescence in the initial propagation cycles. At the end of final propagation cycle with the application of limewash ca.40% salt (in comparison to salt absorbed) was able to come out as salt efflorescence desalinating the Mšené specimen much faster and protecting the aesthetics of the evaporative surface compared to uncoated specimens.

The salt crystals in the Mšené uncoated and limewash coated specimens were found with the help of the SEM microphotographs and elemental mapping and few crystals were located near the evaporative surface. Due to the limitation of magnification and sensitivity of the electron beam it was hard to distinguish between the quartz and the salts even through elemental mapping. But it was seen in the uncoated Mšené specimens the salt crystals formed a thin sensitive lattice of salt (Figure 22-bottom row) which could have been also altered while preparing the samples for SEM analysis. Close up SEM microphotographs of salt crystals analysed 2mm beneath the evaporative surface for uncoated Mšené

specimens are presented in Figure 24. It could be seen different salt crystals were formed around the pores of stone but is inconclusive about the behaviour of salt crystals.

The salt crystals in the Mšené limewash coated specimens were hard to distinguish because of the layer of the lime penetrated beneath the evaporative surface, but with few point imaging the salt crystals were located but it is inconclusive to say the found crystals were salts as elemental mapping was ineffective for such greater magnification due to sensitivity of electron beam.

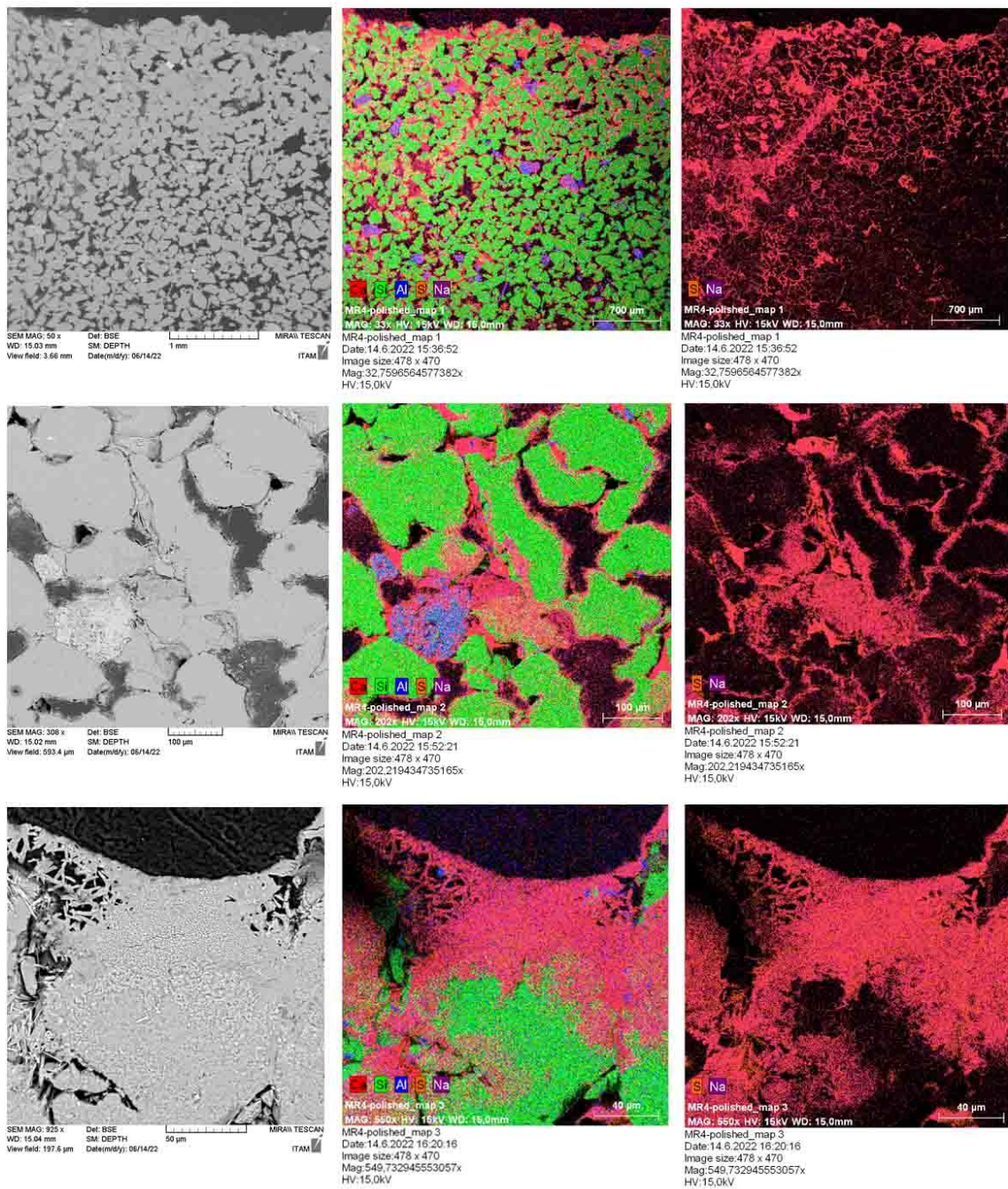


Figure 22: SEM microphotographs of uncoated Mšené stone (MR4) with RILEM procedure P2



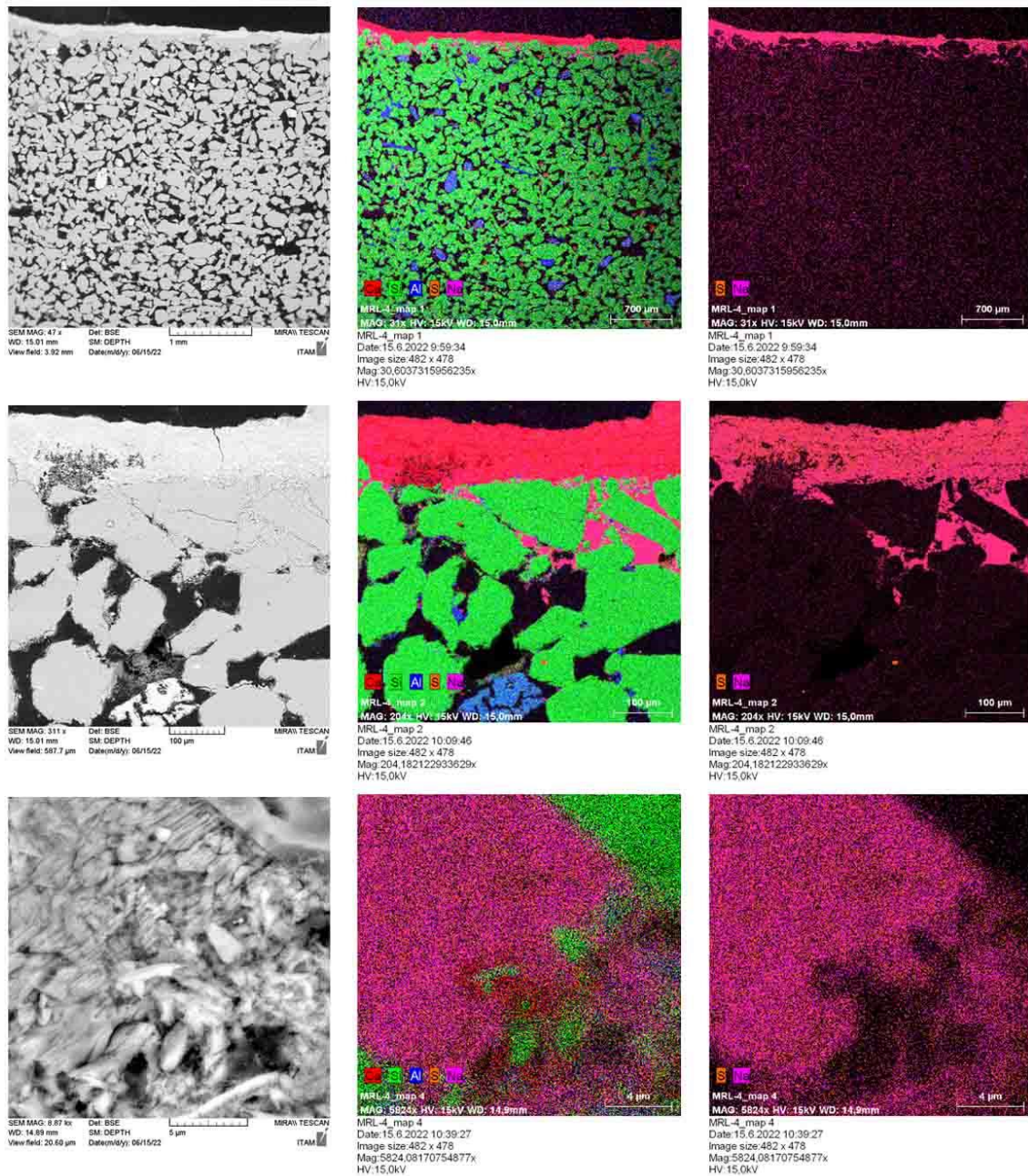
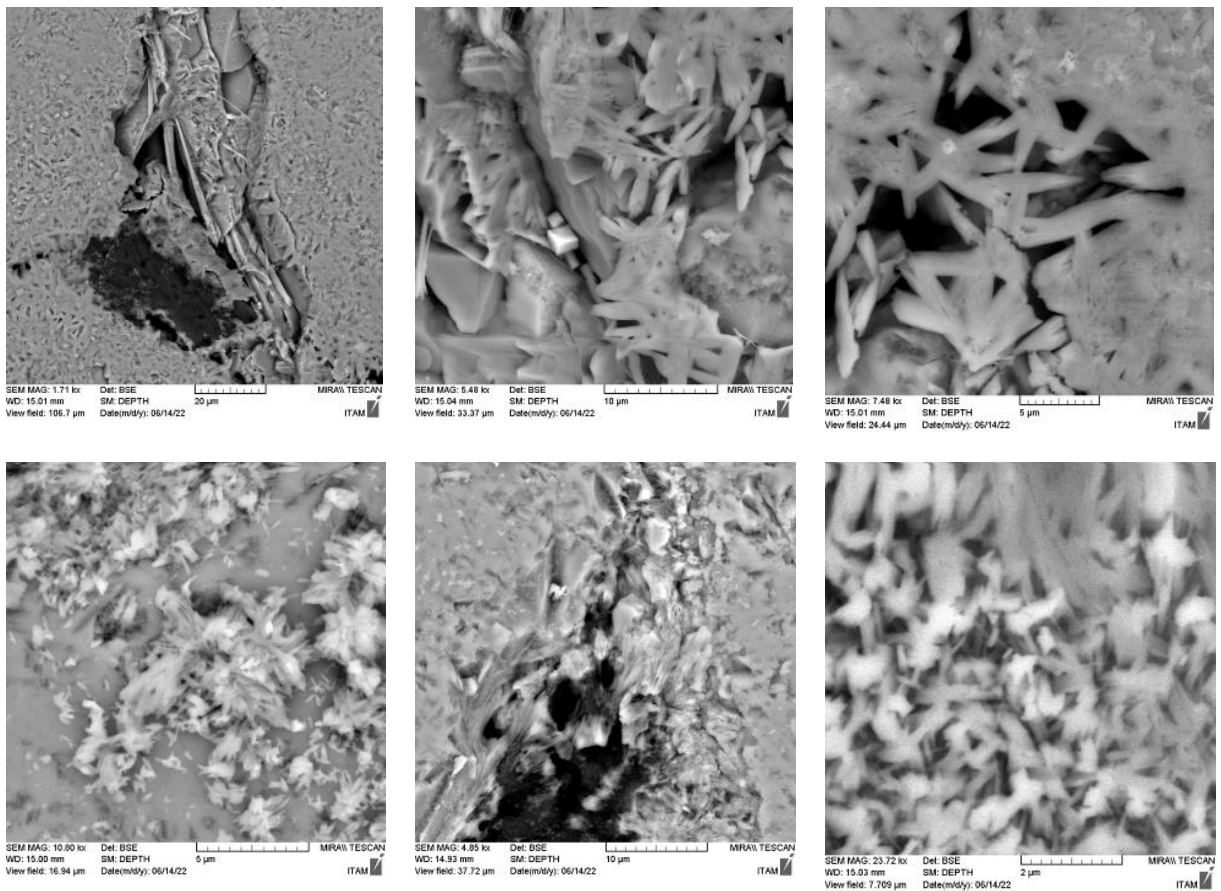
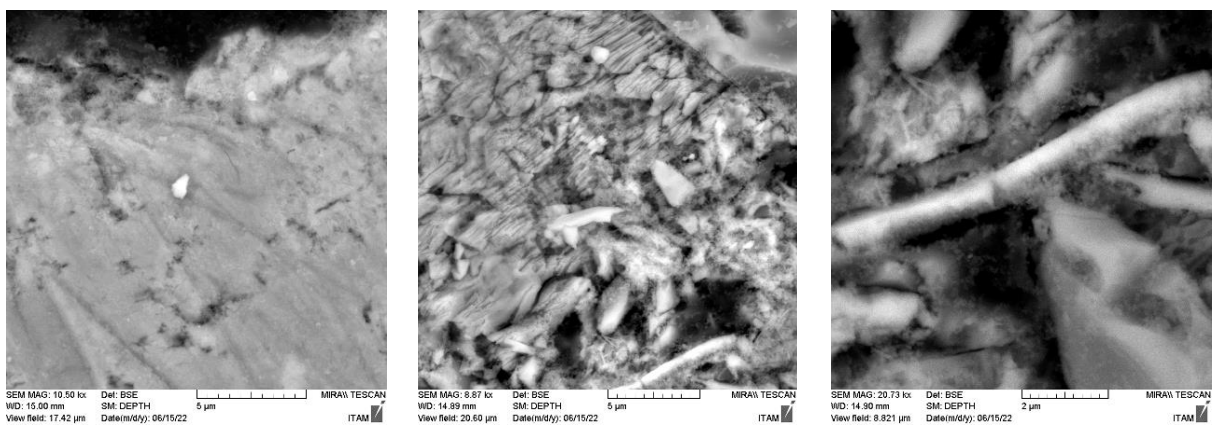


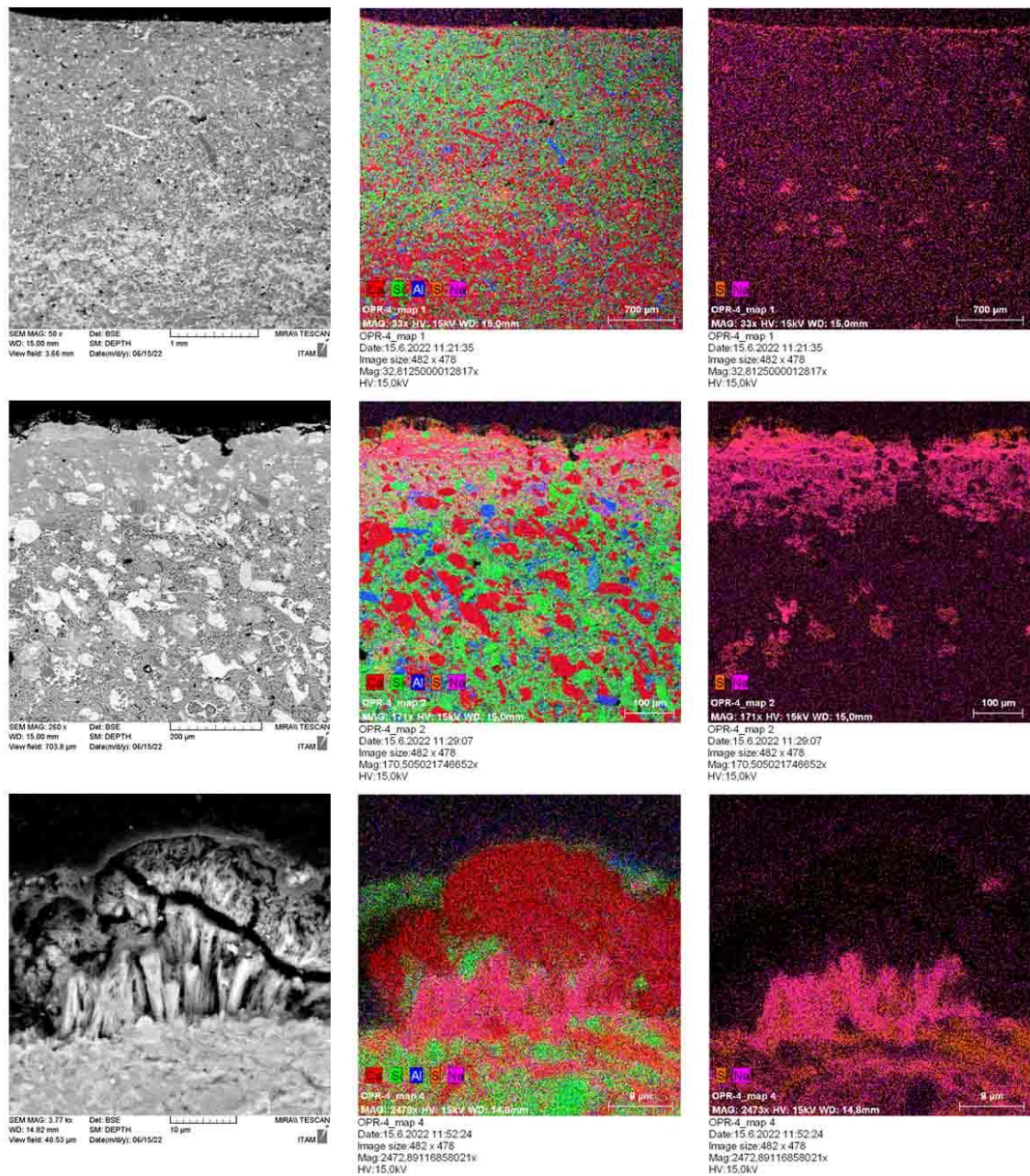
Figure 23: SEM microphotographs of limewash coated Mšené stone (MRL4) with RILEM procedure P2



**Figure 24: SEM microphotographs of salt crystals created in pores of Mšené stone (MR4, uncoated)**



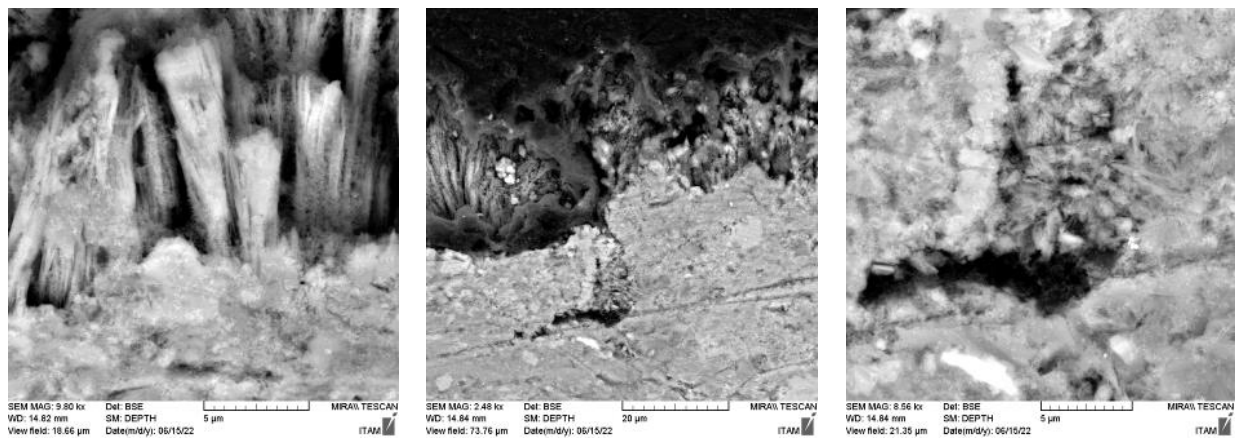
**Figure 25: SEM microphotographs of salt crystals created in pores of Mšené stone (MRL4, limewash coated)**



**Figure 26: SEM microphotographs of uncoated Opuka specimen (OPR4) with RILEM procedure P2**

**Opuka Stone (uncoated):** The SEM analysis on uncoated Opuka specimens also found the salt was near the evaporative surface but the concentration of the salt was not as prominent when compared to the Mšené specimens. It was seen from the ion chromatography test that salt concentration near the evaporative surface was half compared to uncoated and limewash coated Mšené specimens and even it was seen through ultrasonic pulse velocity (discussed in section) although the average velocity was higher near the evaporative surface but it was below the average sound state velocity which implies the salt was uniformly distributed inside the fine pores of opuka and did not migrate towards the

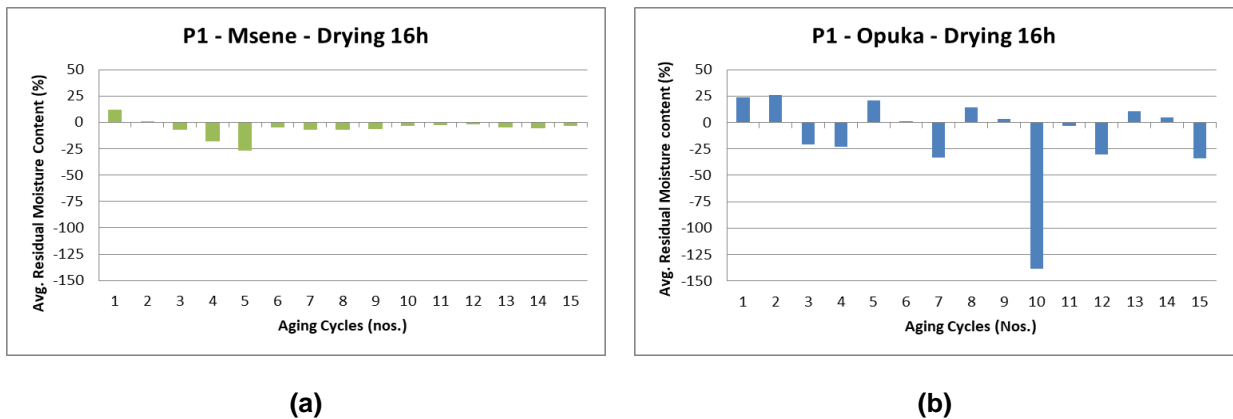
evaporative surface as it was in the case of Mšené. As the SEM analysis was only done for the first 2mm beneath the evaporative depth it did not give the fair conclusion about the concentration of sodium sulphate near the evaporative surface. Due to the small pore size of Opuka compared to Mšené it could be estimated even the salt migrated towards the evaporative surface but they were confined in the fine pores which was hard to detect even through elemental mapping. There were very rare locations where few salt crystals were detected near the evaporative surface which are presented in Figure 26 (mid and bottom row). The salt crystals formed were hard to see through the element mapping again due to limitation of the magnification but few salt crystals formed near the evaporative surface as shown in Figure 27. More SEM analysis along the depth could give much better understanding of the salt distribution inside the pores of Opuka stone.



**Figure 27: SEM microphotographs of salt crystals created in pores of Opuka stone (OPR4, uncoated)**

#### **4.1.4 Drying Rate, Salt Efflorescence and Material Loss**

**Drying Rate:** The drying speed of Mšené and Opuka stones were tested both at high temperature-high relative humidity with EN test (procedure P1) and also at comparatively low temperature-low relative humidity with RILEM test (procedure P2 and P3) using different salt concentrations recommended in the two standards. Following EN12370 standards both the substrates (Mšené and Opuka) were contaminated using complete immersion with high concentration (14wt.%) of sodium sulphate salt solution. On an average 7% of salt solution was absorbed by Opuka specimens (OPE1-OPE4) compared to Mšené specimens (ME1-ME4) which absorbed average 10.5% of salt solution during each cycle as shown in Graph 2 (a) and (b). Since the drying of Mšené and Opuka stones with procedure P1 started at high relative humidity at 40°C with increasing the temperature to 60°C, 80°C and to 105°C (every hour) and overnight drying at 105°C for 16h, induced more damage on specimens due to high salt concentration and high drying conditions as compared to specimens tested with RILEM test procedures (P2 and P3).



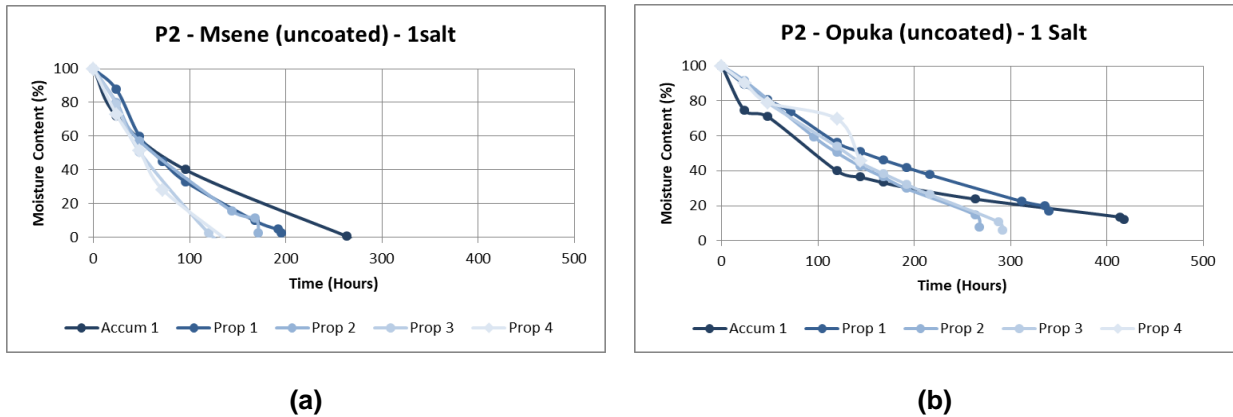
**Graph 4: Average residual moisture content after 16h of drying (a) Mšené (ME1-ME4) (b) Opuka (OPE1-OPE4) stones with EN procedure P1**

With procedure P1 Mšené specimens (ME1-ME4) lost 100% moisture in the first 16h of drying compared to Opuka specimen (OPE1-OPE4) which lost average of between 90-100% moisture after 16h of drying as shown in Graph 4 (a) and (b). Between the two substrates, Mšené exhibited trend of negative residual moisture content during each cycle except during the initial first cycle whereas Opuka showed negative trend due to material loss and positive trend residual moisture content due to salt uptake during few intermediate aging cycles. Drying with procedure P1 limited the capillary transport of salt towards the evaporative surface of the two substrates as the high temperature and high humidity altered the kinetics of evaporative drying inducing more damage at the outer surface of the specimens. It could be also established with test procedure P1 both the substrates lost more than 80% moisture during the first 16h drying period which is an unrealistic in-situ behavior of the materials regardless of their different distinctive nature.

Drying of two substrates with procedure P1 (EN12370) was highly accelerated compared to drying with procedure P2 and P3 (RILEM). The two RILEM test procedures performed during the study produced more realistic environmental conditions of slower uniform drying at 40°C / 15±5%RH with low airflow which enabled the capillary transport during longer drying time favoring transportation of salt towards the evaporative surface without altering the kinetics of evaporative drying. The data presented in the graphs (5-6-7) below compares the drying speed amongst the two different RILEM test procedures P2 and P3 between two substrates.

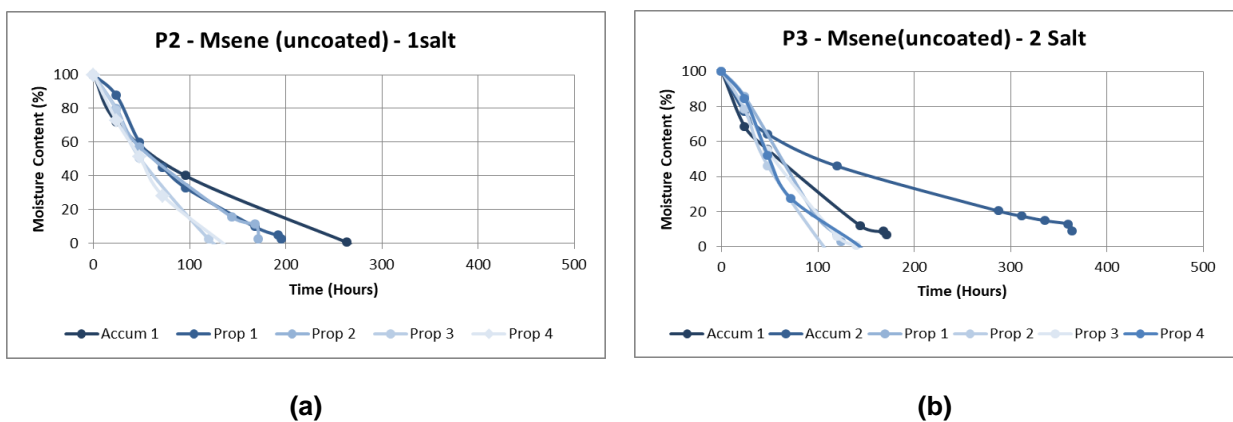
The drying of the two substrates with different test procedures performed depended on the drying conditions (temperature and relative humidity), salt absorbed and porosity of the substrates. During the salt accumulation phase, the substrates tested with RILEM test procedures were contaminated until the top of the samples were wet (CMC) and not with 80% of the amount of water introduced during the accumulation phase. Graph 1 shows the average salt absorbed by Mšené and Opuka substrates during the salt accumulation wetting stage with RILEM test procedures P2 and P3. For RILEM specimens the drying phase was monitored and stopped until 80% of the water had

evaporated, this varied along the cycles (reduced) probably due to the development of salt efflorescence in various specimens used during the test.



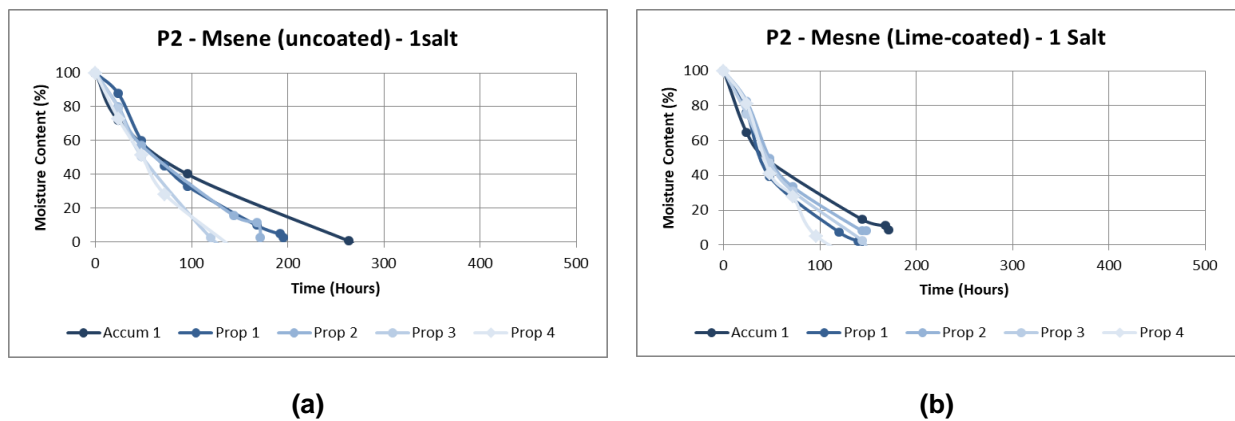
**Graph 5 : Comparison between drying time (a) Mšené stone (uncoated MR5-MR7) (b) Opuka stone (uncoated OPR1-OPR4) with procedure P2 following RILEM standards**

The Graph 5 clearly shows with RILEM procedure P2 (1 Salt) drying rate of uncoated Opuka specimens (OPR1-OPR4) was slower when compared to that of uncoated Mšené specimens (MR5-MR7) during the both accumulation and propagation phase of the test which was mainly due to the different pore network and salt movement across pores. Uncoated Opuka specimens took average 13 days compared to uncoated Mšené specimens, which took 8 days to dry until 80% water during the salt accumulation phase with procedure P2 (1 Salt). During the last cycle (cycle 4) of the propagation phase the drying of uncoated Mšené specimens was accelerated up to an average of 6 days compared to Opuka which took average 10 days with procedure P2 (1 salt).



**Graph 6 : Comparison between drying time (a) Mšené stone (uncoated MR5-MR7) with procedure P2 (b) Mšené stone (uncoated MR1-MR3) with procedure P3 following RILEM standards**

The Graph 6 shows the comparison between the two RILEM procedure performed on the uncoated Mšené specimens with one Salt (P2) and two Salt (P3) accumulation cycles. It was observed the initial drying of the with procedure P2 was fast during the accumulation phase compared to procedure P3 due to high amount of salt uptake during two Salt accumulation cycles performed according to procedure P3. Drying of the Mšené specimens with both the procedure P2 and P3 was accelerated with the same range close to 5 days at the end of last propagation cycle.



**Graph 7 : Comparison between drying time (a) Mšené stone (uncoated MR5-MR7) (b) Mšené stone (limewash coated MRL1-MRL4) with procedure P2 following RILEM standards**

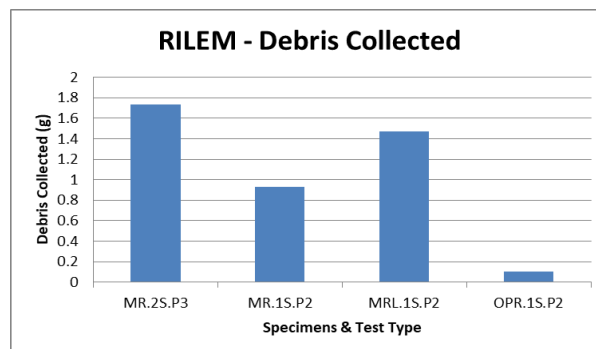
The Graph 7 shows the comparison between the drying rate of uncoated and limewash coated Mšené specimens tested following the RILEM standards. It could be seen that with procedure P2 the drying rate was incremented with the application of limewash during both accumulation and propagation phase compared to uncoated Mšené substrate. With the application of limewash the effective evaporative surface was increased drawing more salts towards the evaporative surface resulting in quick accelerated drying of less than 7 days at end of the final propagation cycle.

**Salt Efflorescence:** When comparing the salt efflorescence developed by the two substrates tested with different test procedures (P1-P2-P3) it was observed RILEM Mšené specimens showed highest degree of salt efflorescence developed near the evaporative surface as seen in the general observation section. Although both the substrates tested with EN procedure (P1) had more severe material loss during the aging cycles compared to RILEM procedures (P2 and P3) the amount of salt efflorescence was negligible in EN specimens at the end of each test cycle and hence was not quantified with the filtration method but the material loss during the each cycle was calculated by comparing the dry mass at the end of each subsequent cycles. The debris that were brushed off at the end of the EN test drying cycles was not an appropriate indicator about the amount salt migrated as salt afflorescence towards the evaporative surface for both the substrates. Average debris collected after drying of EN specimens indicated the more salt was brushed off from Opuka specimens contrary to Mšené

specimens which shows the salt did not get absorbed throughly into the interior matrix of the Opuka specimens with procedure P1 and was mostly accumulated near the outer surface during the short 2h of contamination by complete immerison as shown in Graph 8. The salt was more abosred inside the EN Mšené specimens and it crystallized inside the pores upon drying the specimens at higher drying conditions. It was observed that the average salt absorbed by each EN Mšené specimen during each aging cycle was 2.45g and avergae debris collected from each specimens were 0.07g compared to each EN Opuka specimens which absorbed an average 1.89g of salt in each cycle and and average of 0.11g debris (mostly dried salt) were collected from each specimen in each test cycle. The higher debris collected in Opuka specimens compared to the Mšené specimens with procedue P1 was a result of salt accumulating on surface of Opuka during contamination as discussed before which was also responsible for the white chromatic alteration.



**Graph 8: Average Debris brushed off from (a) Mšené stone (b) Opuka stone aged with procedure P1**



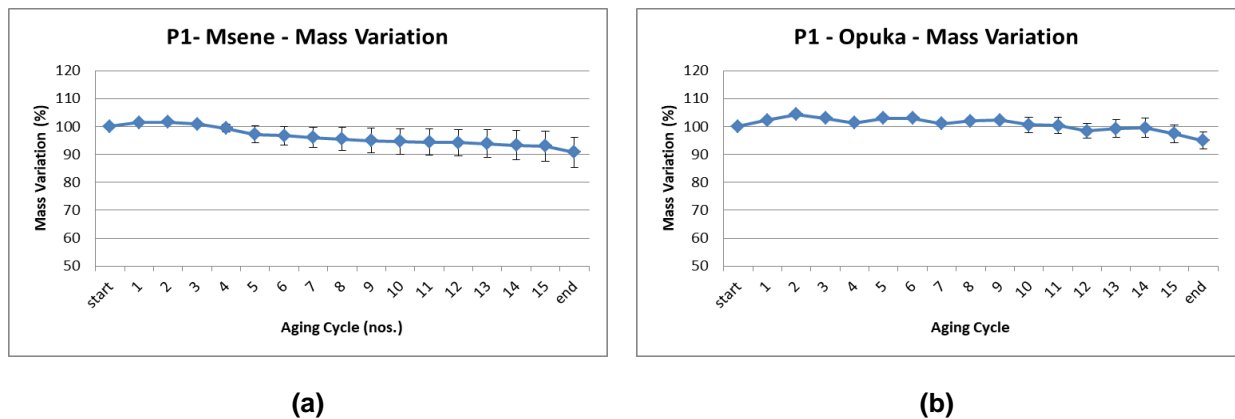
**Graph 9: Debris collected from RILEM test specimens tested with procedure P2 and P3**

The debris collected from the evaporative surface of Mšené and Opuka substrates tested with RILEM test procedures P2 showed different pattern compared to EN test procedure P1. RILEM Mšené specimens showed more salt efflorescence developed during the propagation cycles as discussed in



general observation section and RILEM Opuka specimens hardly showed any salt efflorescence over the evaporative surface. The Graph 9 shows the average debris brushed off from the two uncoated substrates contaminated with procedure P2, limewash coated Mšené specimens tested and uncoated Mšené specimens tested with procedure P3 with procedure P2. It could be seen from the graph that the debris collected from the Opuka specimens tested with procedure P2 were the least compared to other RILEM specimens.

**Mass Variation and Material Loss:** The mass variation and materials loss during the 15 aging cycles with test procedure P1 was noticeable in both Mšené and Opuka samples although Mšené specimens (ME1-ME4) showed more mass loss and damage during the wetting cycles compared to the Opuka specimens (OPE1-OPE4). In EN Mšené specimens sand disintegration was observed from the surface during the wetting stage in each aging cycle. At the completion of each test cycle there was some minute dislodging of sand particles due to handling of specimens but it was neglected while quantifying the material loss. EN Opuka specimens showed white dusty fine salt powdery layer after completion of each drying stage of the cycle which would also detach during handling and hence was also neglected while quantifying the material loss.



**Graph 10: Mass variation of (a) Mšené and (b) Opuka specimens with EN procedure P1**

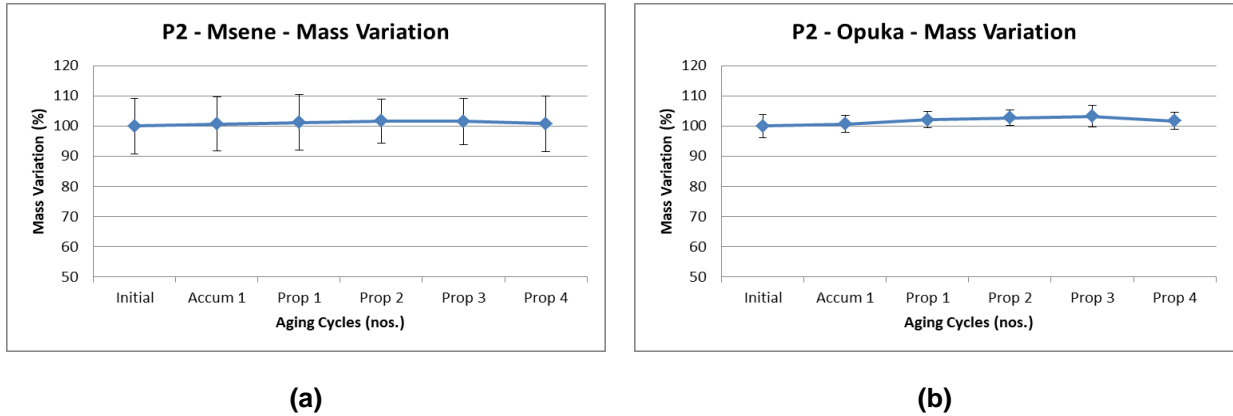
EN Mšené specimens (ME1-ME4) tested with procedure P1 showed increase in mass during the first three cycles of the test due to the salt uptake and then followed continuous decreasing trend of mass variation from the 4<sup>th</sup> cycle onwards up till the end of the test. The decrease in the mass after the 3<sup>rd</sup> cycle indicated that from 3<sup>rd</sup> cycle the salt uptake became more saturated as seen from Graph 2 and more and more material loss was observed after each cycle. As the salt uptake is saturated a trend of increasing standard deviation is also seen during each cycle as material loss increased which can be seen from the Graph 10(a). As discussed in the general observation section the top and bottom of the EN Mšené specimens were rounded off during the continuous aging cycles, the rounding of the edges was the result of increase salt concentration around the edges during the drying stage of the cycles. During the wetting stage, the super saturation was reached quickly around the edges making the

corners more vulnerable thus inducing more damage near edges. Material loss in EN Mšené specimens became more prominent towards the end of the EN test and it could be seen that standard deviation of mass loss was the highest at the end of the test. Overall an average of ca.10% material loss was observed after the end of the test in the EN Mšené specimens. When comparing the mass loss of EN Mšené specimens with the EN Opuka specimens (OPE1-OPE4), repeated arching trend is observed in the Opuka specimens and the standard deviation during the aging cycles was comparatively very less compared to EN Mšené specimens as seen from the Graph 10(b). There was a small or negligible standard deviation observed in the first 9 cycles of the test (P1) which reflected the homogeneous behavior of the Opuka substrate and the standard deviation increased more after 10<sup>th</sup> cycles due to significant material loss from few specimens used during the test. The repeated arching of mass loss observed in EN Opuka specimens was mainly due increase in the salt uptake and decrease was due to material loss. Overall an average of ca.6% material loss was observed after the end of the test in the EN Opuka Specimens.

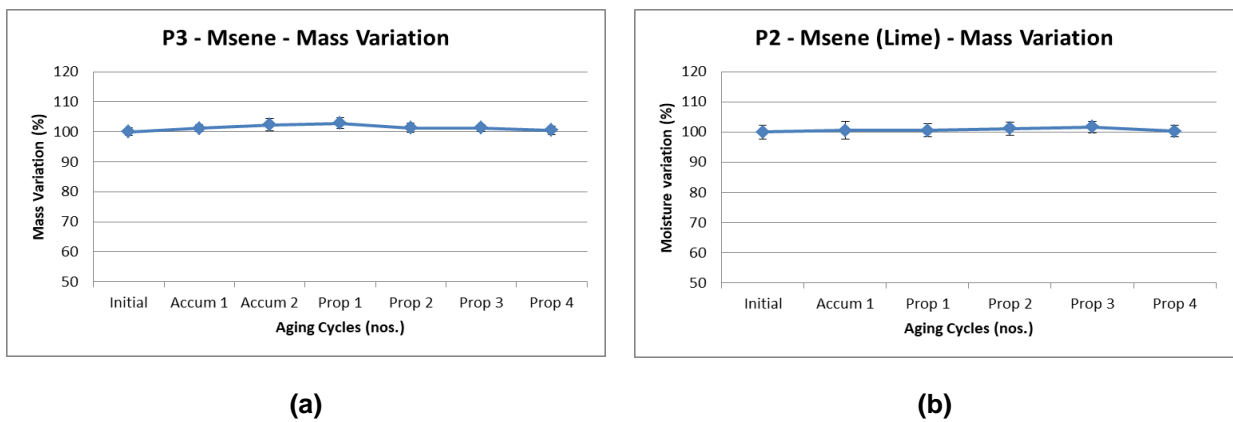
Material loss in RILEM specimens tested with procedure P2 and P3 was negligible compared EN specimens for first 5-6 aging cycles. As the two phased (accumulation and propagation) RILEM test is governed by the kinetics of evaporative drying, the salt is transported towards the surface of evaporation and thus the higher salt concentration and damage develops in the outer layer of the stone which is a common phenomenon found on building sites. Lower temperature in RILEM tests means slower drying rate which enables the capillary transport of salts during the drying for a longer time. The mass loss data discussed here clearly shows the during the RILEM accumulation phase a trend of increase in mass is seen because of the salt uptake but as the rewetting with water continues during the propagation phase the more salt is transported towards the evaporative surface slowly as salt efflorescence bringing back the mass variation of the specimens close to their sound state weight at the end of 4th propagation cycle during the RILEM test.

It was observed after rewetting specimens with water during the propagation phase and with slower drying there was very minute damaged observed in the fabric of the two substrates tested with RILEM procedure P2 (1-Salt) except development of salt efflorescence and small amount of sand disintegration was noticed in uncoated Mšené specimens (MR5-MR7). The uncoated Opuka specimens (OPR1-OPR4) tested with procedure P2 (1-Salt) showed only slight chromatic alteration near the evaporative surface but no salt efflorescence or material loss was observed during the four propagations cycles indicating development of subsflorescence resulting in pore clogging and hence effecting the drying. The higher standard deviation observed in mass variation in uncoated Mšené specimens as seen from the Graph 11(a) was a result of choice of the specimens selected for the test as one of the specimens amongst the group of three had a less initial average mass compared to the other two specimens but the overall standard deviation in mass variation of individual specimens was very small and comparable to each other even having physical geometrical difference. As the test concluded (after propagation cycle 4) the maximum mass variation in both uncoated Mšené and uncoated Opuka specimens tested with procedure P2 was ca.1% which was very close to each other

but higher than their initial sound state weight which indicates presence of some residual salt inside the pores of the two substrates after the end of the test. The material loss was only quantified for the uncoated Mšené specimens (MR5-MR7) tested with procedure P2 as there was very less to no material loss observed for the Opuka specimens (OPR1-OPR4) during the first 4 propagation cycles as shown in Graph 9.



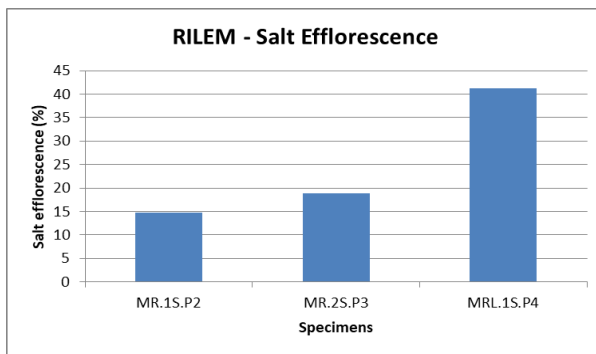
**Graph 11: Mass variation comparison of (a) uncoated Mšené and (b) uncoated Opuka specimens with procedure P2**



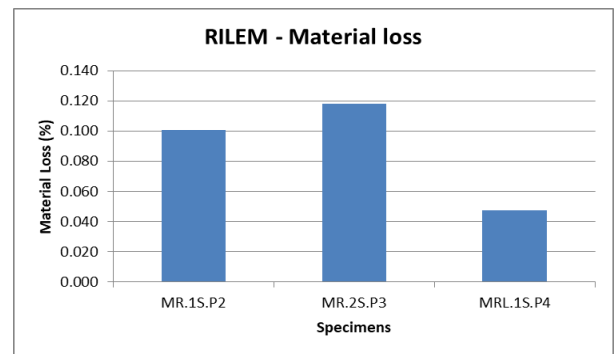
**Graph 12: Mass variation in (a) uncoated Mšené (2-Salt) with procedure P3 and (b) limewash coated Mšené specimens with procedure P2**

The similar trend is noticed in uncoated Mšené substrates (MR1-MR3) tested with procedure P3 (2-Salt) and limewash coated Mšené specimens (MRL1-MLR3) tested with procedure P2 (1-Salt). Initial mass was increased in specimens after the salt accumulation phase during the testing with procedure P2 and P3. With the procedure P3 which was performed with two salt accumulation cycles the mass increased upto ca.2% more than its initial sound state weight after the completion of 1st propagation cycle which was the highest mass variation increase observed within the two different RILEM test procedures (P2 and P3). In the limewash coated Mšené specimens the mass variation was increased

to ca.1% of their initial sound weight during the 3rd propagation cycle. Standard deviation in mass variation during the test procedure P3 was very less as seen from the Graph 12(a). The effectiveness of limewash in Mšené specimens tested with procedure P2 was evident in drawing salt towards the evaaporative surface hence it was observed the highest salt efflorescence seen from Graph 13(a) and lowest material loss seen from Graph 13(b) was observed in the Mšené specimens coated with limewash when compared with the other uncoated Mšené specimens tested with procedure P2 and P3. The comparison of mass evolution within the RILEM procedures P2 and P3 could be made as the salt reduced during the propagaition cycles reaching closer to their sound state weight. The low salt concentration (5wt.% Na<sub>2</sub>SO<sub>4</sub>) used in RILEM test procedures resulted in the lesser degree of damage in the specimens as the salt did not reach to a point where it could induce damage in the substrates.

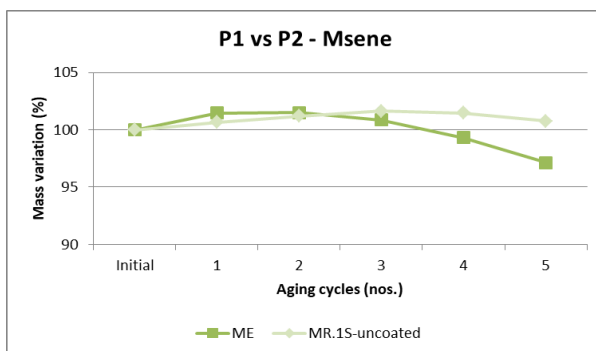


(a)

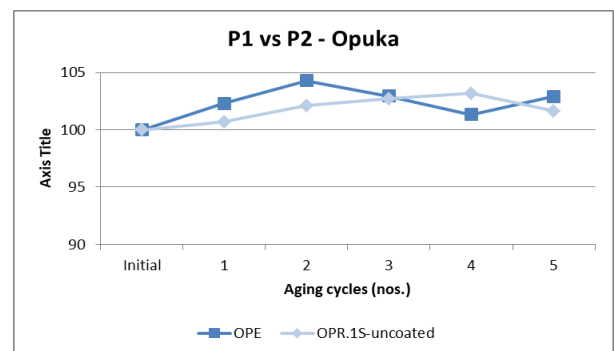


(b)

Graph 13 (a) Salt efflorescence and (b) material loss in RILEM specimens with procedures P2-P3



(a)



(b)

Graph 14 Mass variation comparison between procedure P1 and P2 (a) Mšené (b) Opuka

When mass variation and material loss is compared for the two substrates (Mšené and Opuka) tested procedure P1 (EN12370) and P2 (RILEM) the difference in the mass variation and material loss could

be mainly attributed to the drying conditions, different salt concentrations used during the two test procedures and salt contamination method (complete and partial immersion). Comparison between first 5 cycles of the two test procedure P1 and P2 is shown in the Graph 14.

The Mšené specimens (ME1-ME4) tested with EN procedure P1 showed mass loss of ca.3% from its initial sound weight by the end of 5th aging cycle compared to uncoated Mšené specimen (MR5-MR7) tested with procedure P2 where an increase of ca.1% mass was observed from the initial sound weight by the end of 5th aging cycle. As discussed before the arching trend in mass variation was seen in EN Opuka specimens (OPE1-OPE4) tested with procedure P1. EN Opuka specimens showed an increased ca.3% mass by the end of 5th aging cycle followed by its previous cycle where the mass was ca.1.5% less due to increased material loss. The RILEM uncoated Opuka specimens (OPR1-OPR4) tested with procedure P2 also displayed arching trend where the highest mass increase of ca.3% (from initial sound weight) was observed during the end of 4th cycle followed by decreasing trend to ca.1% mass above the initial sound state weight of the specimens. Although the two substrates tested with procedures P1 and P2 were subjected to different testing conditions the results from the initial 5 cycles are quite comparable in terms of salt uptake. At the later cycles the results become very distinctive as the testing conditions of procedure P1 become more unrealistic in terms of regular salt contamination and drying at high temperature along with salt concentration used impacting the degradation degree of the two substrates.

#### **4.1.5 Damage Assessment**

**Visual Change:** The changes in visual appearance of Mšené and Opuka stones used in the experimental tests were monitored while performing the EN12370 and RILEM test procedures P1-P2-P3 discussed in the previous section. Both the stone specimens exhibited different degradation patterns mainly due to their distinctive nature, mechanical properties, testing conditions, salt concentration and contamination method used following the two test standards. Specimens tested in accordance with EN 12370 standards by completed immersion (test procedure P1) showed more damage during the 15 aging cycles [Figure 28 (a)(b)] as compared to the RILEM standard where only one or two salt accumulation cycles were performed along with the total of 4 propagation cycles with the partial immersion (test procedure P2 and P3). The observations of visual damage and deterioration in stone specimens with two test standards are as follows.

##### **Mšené**

The degradation pattern observed in Mšené EN stone specimens (ME1-ME4) tested with procedure P1 was mainly sand disintegration [Figure 29 (a)(b)] during the wetting stage of the test contaminated with 14% sodium sulphate decahydrate ( $\text{Na}_2\text{SO}_4 \cdot 10\text{H}_2\text{O}$ ) salt solution. As the aging cycles continued (with procedure P1) surface erosion was observed with rounding of edges near the top and bottom portion of the cylindrical stone specimens. Among the group of four EN specimens, ME1 showed heterogeneous deterioration as compared to other specimens (ME2-ME4) which showed more

homogeneous deterioration but the overall deterioration pattern was more or less similar for the four Mšené EN specimens. The top and bottom edges exhibited higher dislodging of sandy particles due to the strong evaporative flux around edges during the wetting stage of the test cycle. After few drying cycles white fine sized particles were observed on the top and around the periphery of the Mšené specimens (ME1-ME4) which was due to the quick drying of specimens at higher temperature after a short 2h wetting period with complete immersion. The Mšené specimens (ME1-ME4) barely showed any hard surface salt efflorescence which could have induced any surface damage and moreover some small crystals were observed attached to the surface which were easily brushed off after each drying stage of the test cycle. Chromatic alteration of EN Mšené specimen is shown in Figure 30.

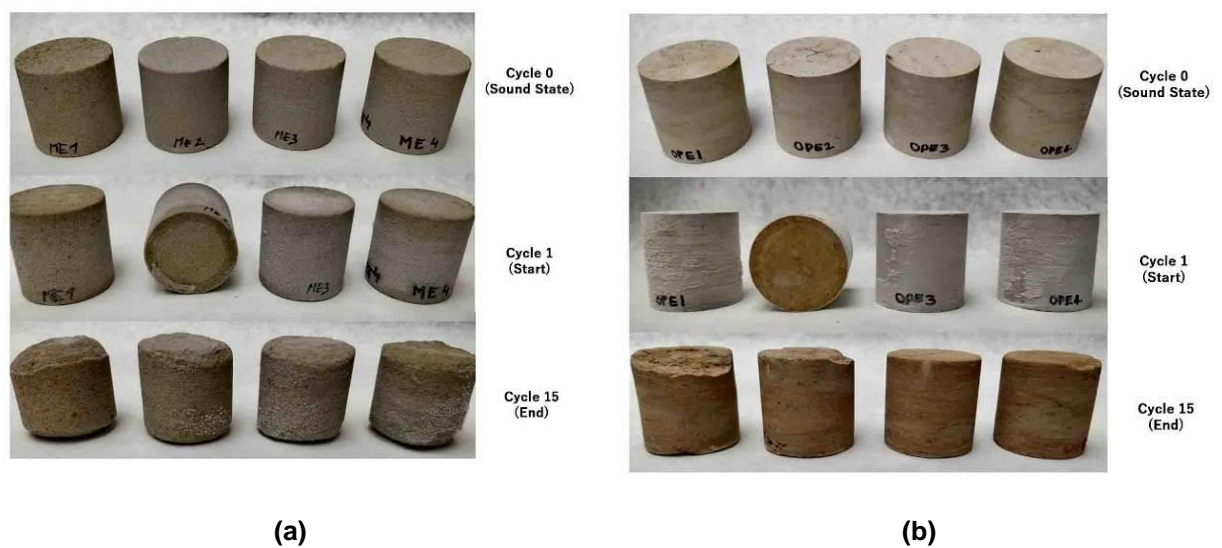


Figure 28: Example of Mšené (a) and Opuka (b) specimen deterioration

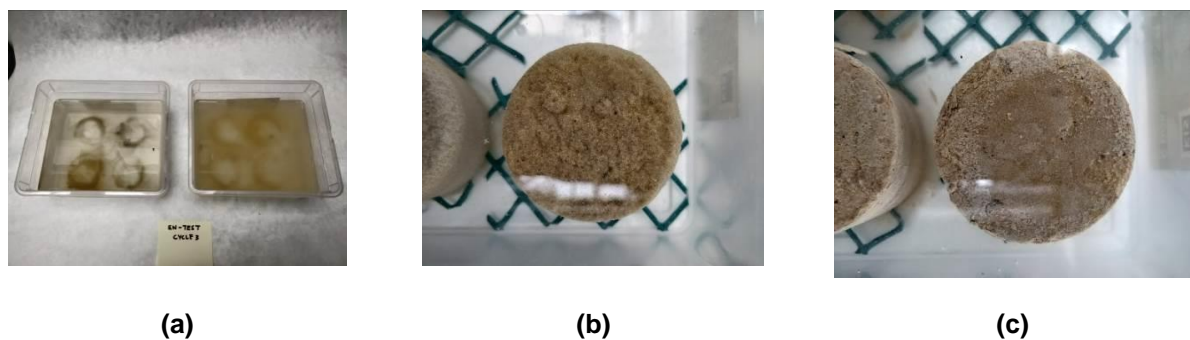
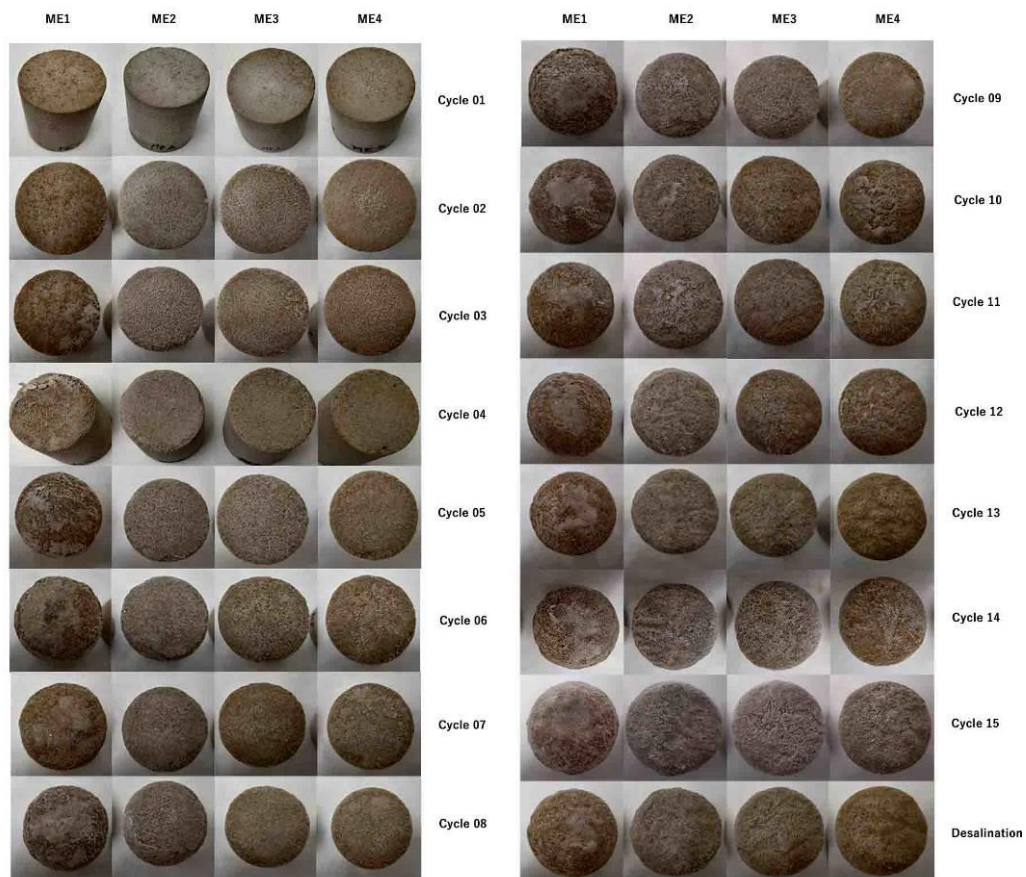
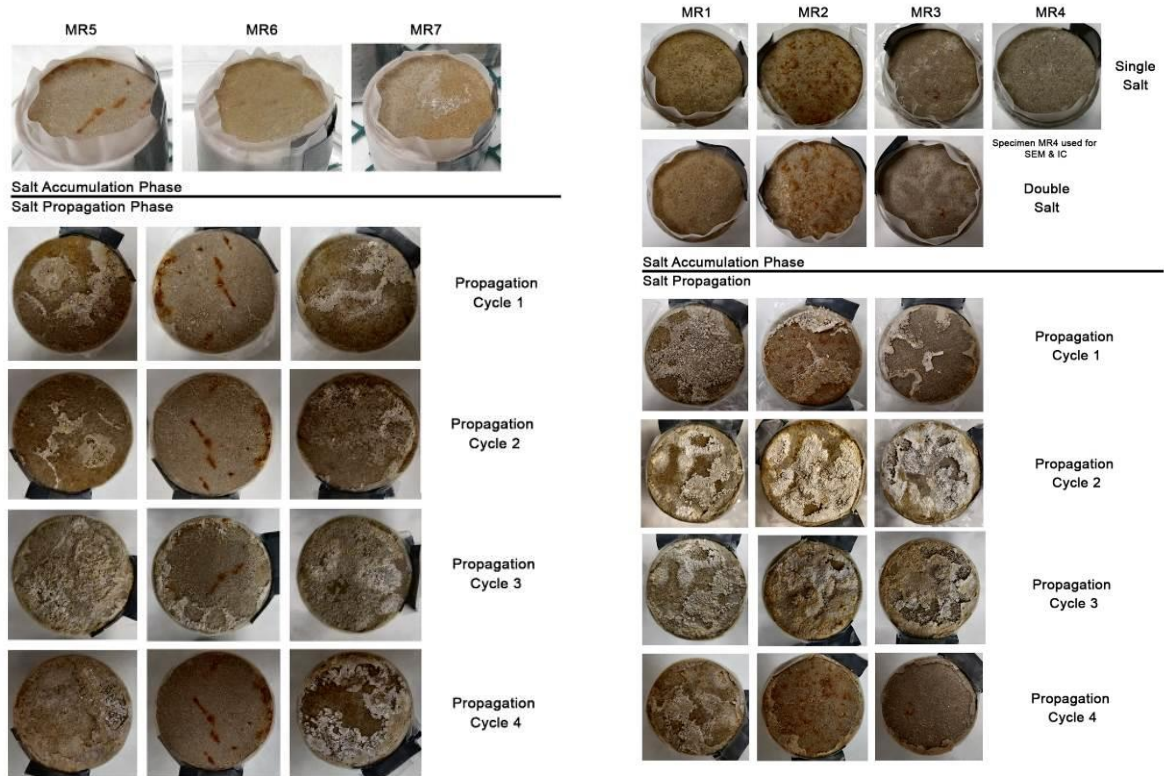


Figure 29: Example of material loss during EN12370 tests (a) Material Loss during wetting stage (b) Sand disintegration in Mšené specimens (ME1-ME4) (c) Scalping of sedimentation layers from sides of Opuka specimens (OPE1-OPE4)



**Figure 30: Example of chromatic alteration and material deterioration of EN Mšené specimens (ME1-ME4) tested with procedure P1 during 15 cycles**

Test procedure P2 and P3 were performed according to the RILEM standards showed different degradation pattern due to slow unidirectional drying and the deterioration was only concentrated towards the top evaporative surface of the specimens in comparison to EN test procedure P1 where the evaporation was through top, sides and partially bottom. All the Mšené specimens (MR1-MR4, MR5-MR7 and MRL1-MRL4) tested with RILEM standards showed no damage and no salt efflorescence during the salt accumulation phase (contamination with 5% sodium sulphate,  $\text{Na}_2\text{SO}_4$ ) but different deterioration patterns were observed during the propagation phase of the each test procedures (P2 and P3). At end of the each propagation cycle (with test procedure P2 and P3), surface salt efflorescence and visual deterioration was observed near the specimen's evaporative surface as the bottom and side surfaces were sealed during the drying allowing salt movement by capillarity only in one direction. Although the material loss was minimal, a pattern of sugaring or disintegration of sandy stone particles was observed when specimens were rewetted with distilled water by partial immersion in each cycle during the propagation phase. Salt efflorescence Figure 32 (a) and (b) and Figure 34 (a) developed during the propagation phase were mainly patchy (soft) and crusty (hard).



(a)

(b)

Figure 31: Summary of macroscopic visual observations during RILEM tests (a) 1-Salt contamination cycle, uncoated Mšené specimens (MR5-MR7) tested with procedure P2 (b) 2-Salt contamination cycles, uncoated Mšené specimens (MR1-MR3) tested with procedure P3



(a)

(b)

Figure 32: Example of debris (salt efflorescence and material loss) collected during RILEM tests (a) 1-Salt contamination cycle, uncoated Mšené specimens (MR5-MR7) tested with procedure P2 (b) 2-Salt contamination cycles, uncoated Mšené specimens (MR1-MR3) tested with procedure P3



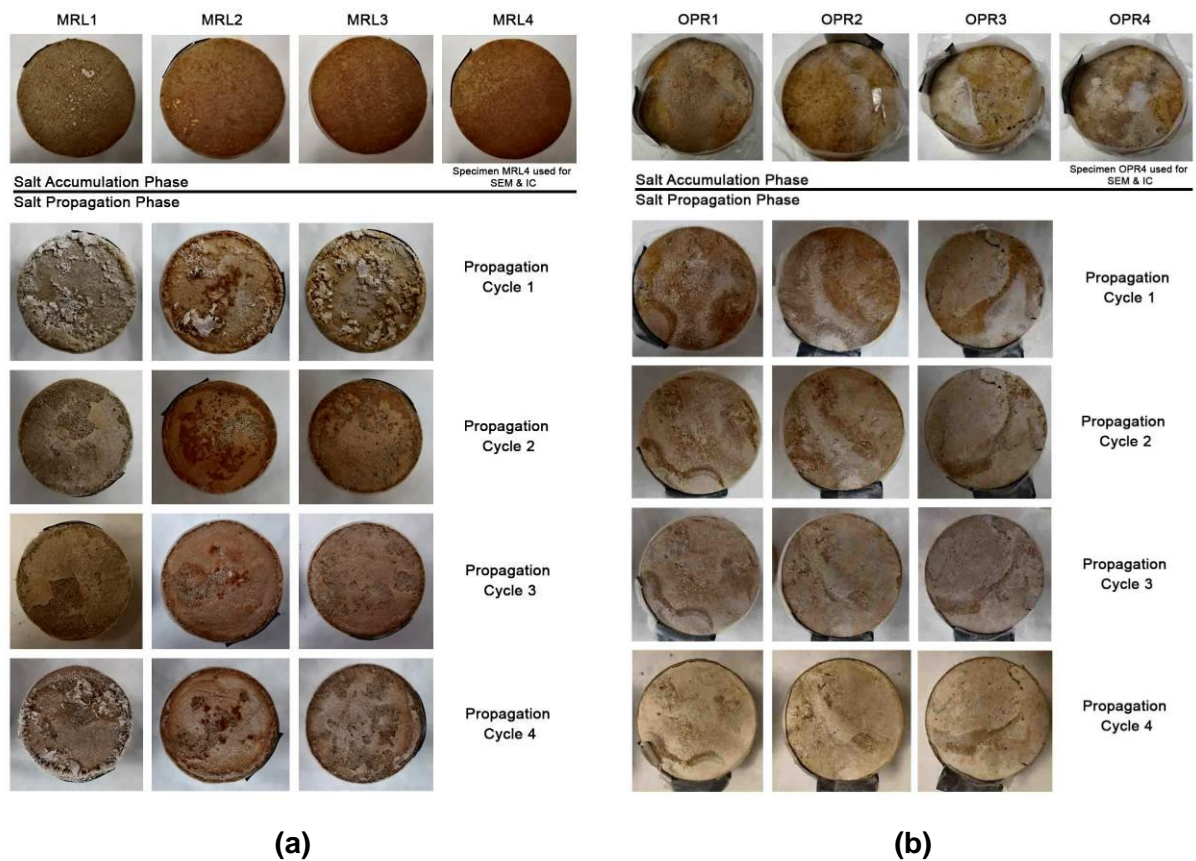


Figure 33: Summary of macroscopic visual observations during RILEM tests (a) 1-Salt contamination cycle, limewash coated Mšené specimens (MRL1-MRL4) tested with procedure P2 (b) 1-Salt contamination cycle, uncoated Opuka specimens (OPR1-OPR4) tested with procedure P2

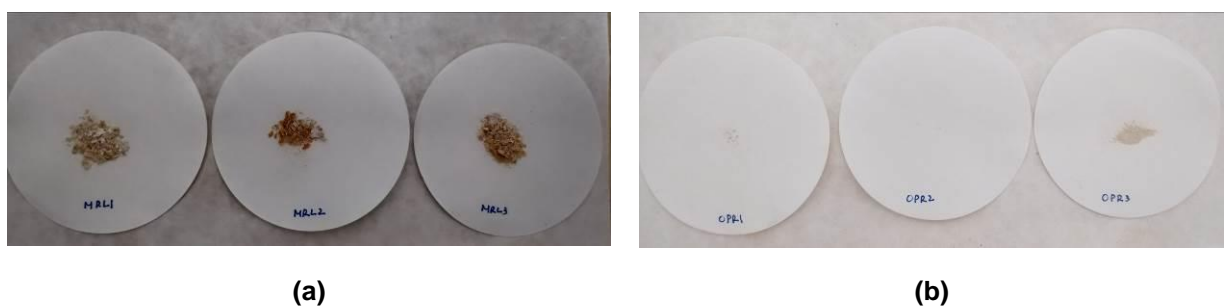
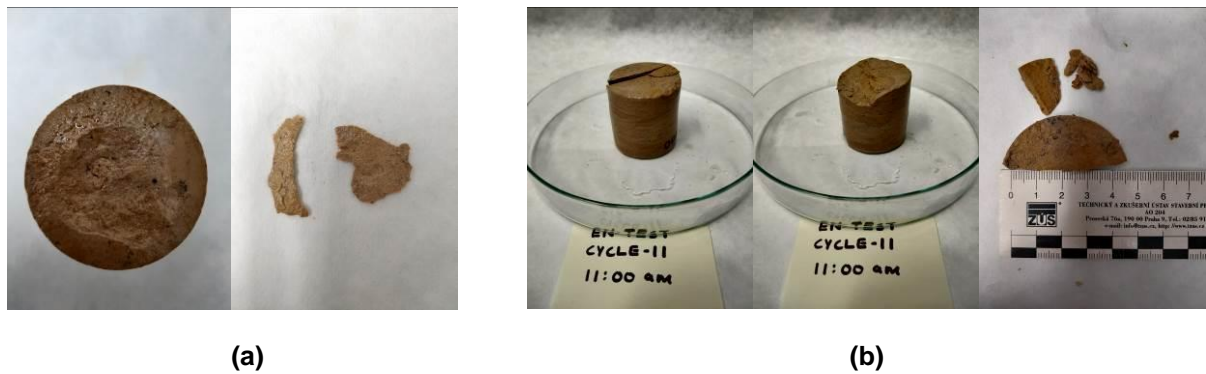


Figure 34: Example of debris (salt efflorescence and material loss) collected during RILEM tests (a) 1-Salt contamination cycle, lime-coated Mšené specimens (MRL1-MRL4) tested with procedure P2 (b) 1-Salt contamination cycle, uncoated Opuka specimens (OPR1-OPR4) tested with procedure P2



**Figure 35: Example of material loss from (a) bottom surface and (b) top surface (Right) of EN Opuka specimen during wetting stage tested procedure P1**

### Opuka

The Opuka specimens exhibited different degradation pattern as compared to the Mšené specimens tested with both EN and RILEM test procedures. Opuka EN specimens (OPE1-OPE4) showed more deterioration during the 15 aging cycle with test procedure P1 compared to RILEM uncoated specimens (OPR1-OPR4) tested with procedure P2 and a significant chromatic change in surface color (whitening) was observed after each drying stage during the EN test. As the EN specimens were contaminated for a very short duration (for 2h by complete immersion) with high concentration of sodium sulphate decahydrate salt solution (14wt.%  $\text{Na}_2\text{SO}_4 \cdot 10\text{H}_2\text{O}$ ), the change in color was mainly due to quick drying of salt accumulated on the surface of the specimens as there was very less surface salt efflorescence observed during the end each EN test cycle. Whitening of the surface was higher during the initial aging cycles when compared to the later half of the EN test test (Figure 37). Material loss in EN specimens was mainly in the form of fine powder (being a fine grained stone) [Figure 36 (a)] and scalping of small particles from sedimentary layers [Figure 29(c)] around the specimen's periphery was observed during the wetting stage making the salt solution murky. As the group of 4 EN opuka specimens were kept together in a single petri during the drying stage, specimens showed small dislodging of material layer from the bottom surface due to restricted drying from the specific surface [Figure 35(a)]. During the EN test material loss in 4 opuka specimens was of similar nature mainly concentrated around the peripheral sedimentary layers and one of the specimens (OPE1) showed significant material loss during the 10th cycle wetting stage of the test where a large part of material was detached from the top part of the specimen due to increased evaporative flux around the edge of the specimen as a result of salt crystallization [Figure 35(b)].

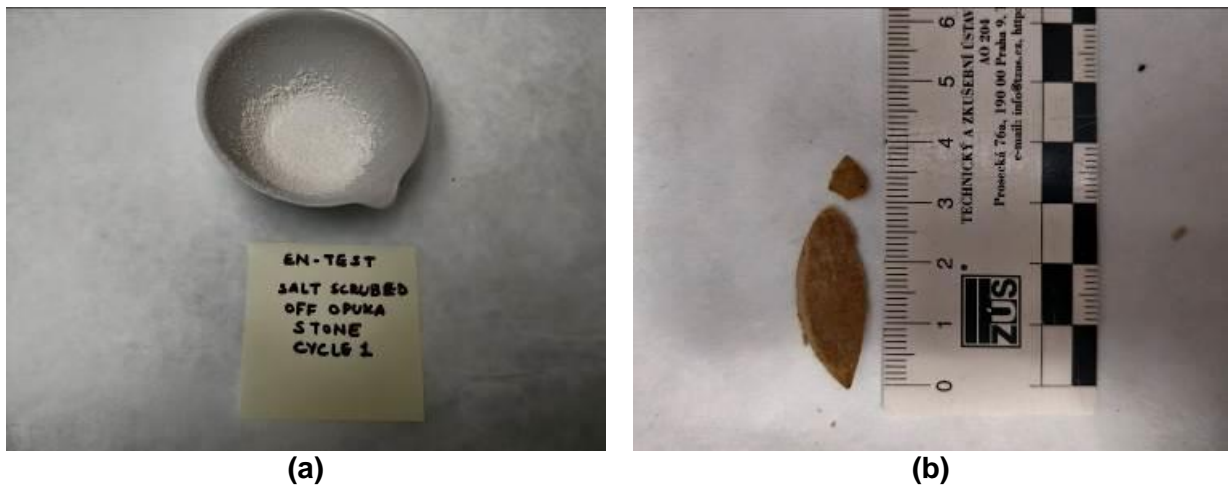


Figure 36: (a) Example of salt brushed off from Opuka specimens after drying stage (b) Example of stone material loss from top part of the specimen

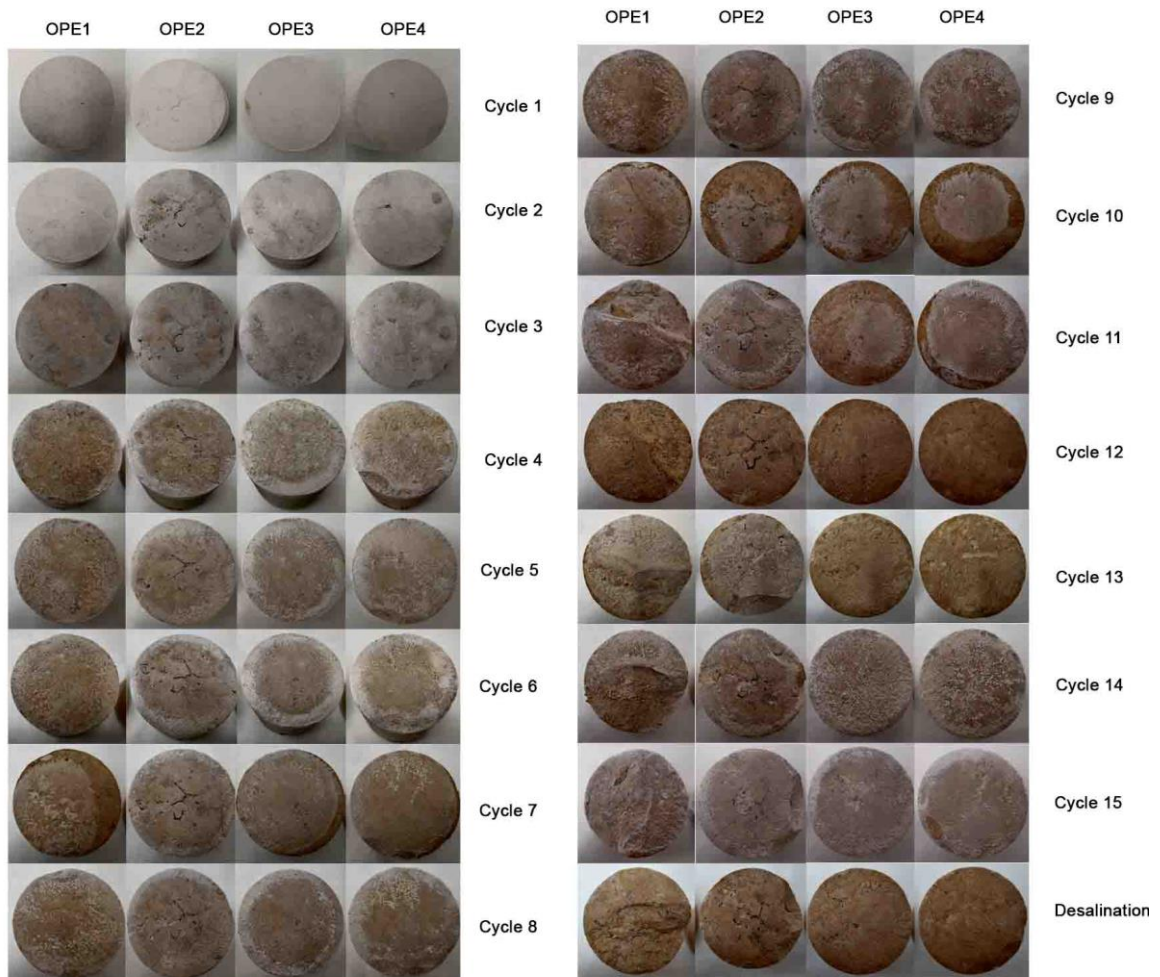
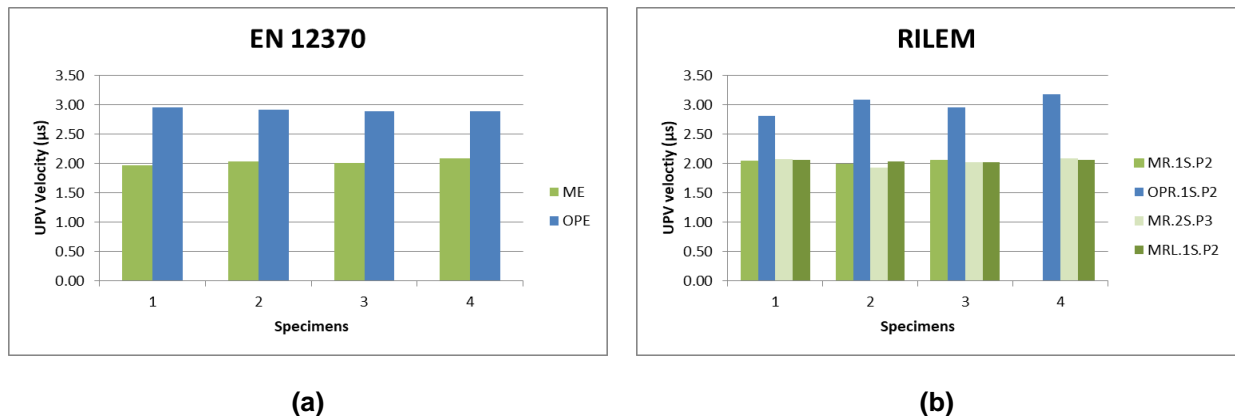


Figure 37: Example of chromatic alteration and material deterioration of EN Opuka specimens (OPE1-OPE4) tested with procedure P1 during 15 cycles

Opuka specimens contaminated with 5wt.% sodium sulfate salt solution ( $\text{Na}_2\text{SO}_4$ ) with RILEM test procedure P2 developed very less salt efflorescence near the evaporative surface which was mainly a yellowish white colored fine grained powder and there was no visible damage and very less chromatic alteration detected near the evaporative surface either during the salt accumulation or propagation cycles [Figure 33(b)]. At completion of 3rd propagation cycle dislodging of very minute sedimentary layers in microns was observed around the edges where evaporative flux is to be considered higher during drying.

#### 4.1.6 Ultrasonic pulse velocity (UPV)

Prior to the salt aging cycles with test procedure EN12370 and RILEM, the ultrasonic pulse velocity (UPV) test was performed on both Mšené and Opuka stone specimens in their sound state. In their sound state Opuka stone specimens exhibited higher velocity ( $\text{mm}/\mu\text{s}$ ) as compared to the Mšené stone specimens before starting the salt aging cycles Graph 15 (a)(b).

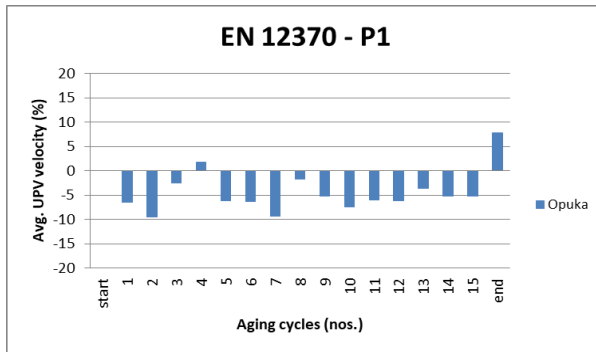


**Graph 15: UPV of specimens in sound state before starting (a) EN and (b) RILEM tests**

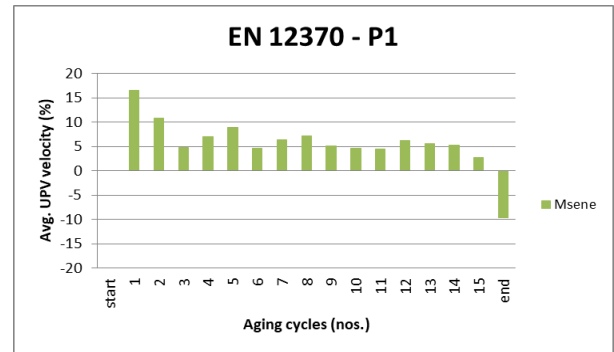
The group of four Opuka specimens (OPE1-OPE4) aged with procedure P1 showed decreasing trend in velocity after each contamination cycle throughout the EN test and only a small increase in plateau of ca.2% was observed during end of the 4<sup>th</sup> aging cycle bringing average velocity of four specimens close to their average initial sound state velocity (Graph 16A). Post desalination after completing 15 aging cycles, EN Opuka specimens showed an unexpected increased velocity of ca.8% which was unusual (could be attributed to experimental error). As EN Opuka specimens exhibited decrease in velocity after the end of each cycle during the test could be the result of damage propagation and alteration of porous network due to effect of salt crystallization hence altering the mechanical strength of the specimens. The values given correspond to the percentage change before and after contamination in each cycle.

On the contrary to Opuka, EN Mšené specimens (ME1-ME4) exhibited increased velocity at end of each cycle and drop in velocity of ca.10% was only observed at the end of EN test post desalination

[Graph 16(b)], which was due to salt removal from the pores. The increase in velocity of the EN Mšené specimens could be a result of positive pore filling with the salts during each contamination cycle making the porous structure more consolidating without developing subsurface micro cracks. Although the surface material loss in EN Mšené specimens was more compared to EN Opuka specimens, it still showed increasing velocity trend in each cycle.

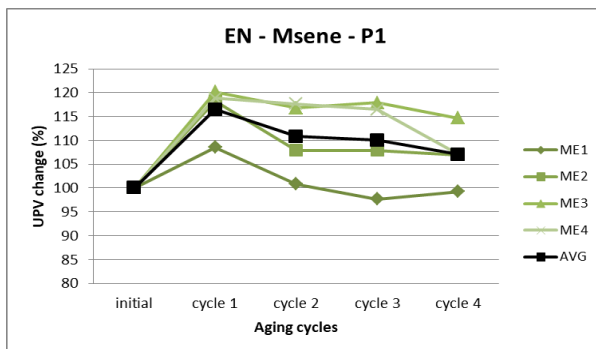


(a)

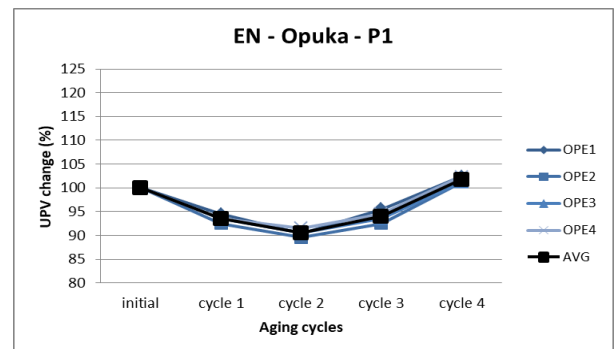


(b)

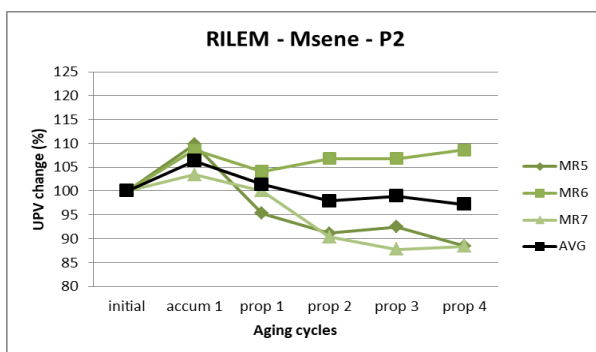
**Graph 16: Ultrasound Pulse Velocity (UPV) of (a) Opuka and (b) Mšené stone during 15 aging cycles of EN 12370 Test**



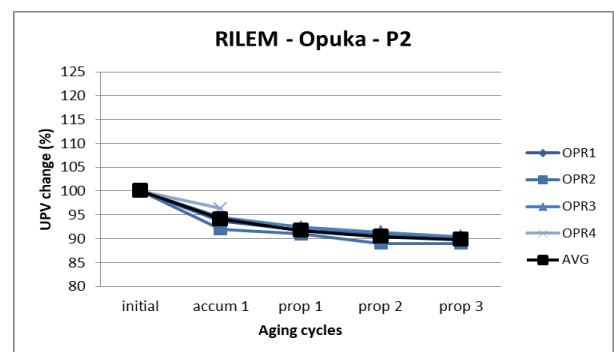
(a)



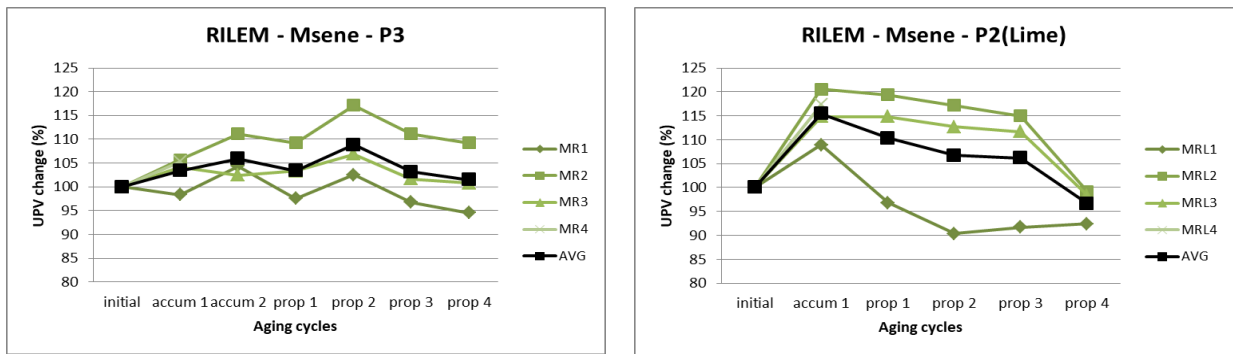
(b)



(c)



(d)



**Graph 17: Comparison of first 4 cycles ultrasound velocity (through height) for Opuka and Mšené samples with test procedure P1-P2-P3**

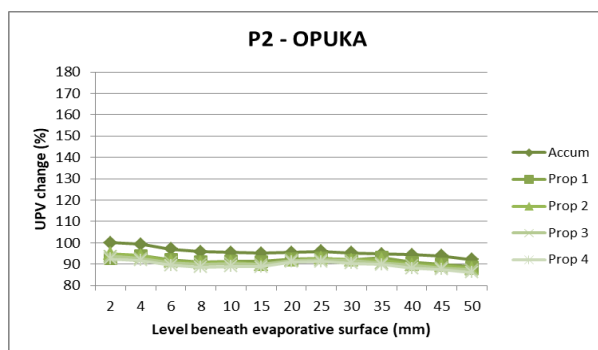
The ultrasonic pulse velocity results after the end of each aging cycle with RILEM procedure P2 are shown in Graph 17(c) and (d). At the end of salt accumulation phase with procedure P2 a significant increase of ca.6% in velocity was observed as a result of salt uptake in Mšené specimens (MR-MR7) due to pore filling. At the end of the final propagation cycle the velocity decreased to ca.3% from the initial sound velocity. An opposite trend was observed in the Opuka specimens (OPR1-OPR4) the velocity showed the decreasing trend after each cycle as a result of damage inside the subsurface although no damage or salt efflorescence was noticed during the four propagation cycles. After the completion of salt accumulation phase the average velocity change of ca.-6% was observed in RILEM Opuka specimens and the average velocity after the 4<sup>th</sup> propagation cycle was ca.10% less than the initial sound state velocity. As both the Mšené and Opuka specimens tested with procedure P2 showed decreased average velocity after the end of the final propagation cycle without any significant material loss from the evaporative showed the damage was mainly initiated in the subsurface of the two substrates and the salt crystallization pressure was still below the limit where the damage could not be propagated changing the mechanical properties of the substrates.

The comparison of first 5 aging cycles between Mšené and Opuka specimens tested with EN procedure P1 and RILEM procedure P2 shows that EN Mšené specimens showed increasing velocity upto ca.18% during the first salt contamination cycle and the velocity decreased as the contamination cycles continued further but at the end of the 5<sup>th</sup> cycle the average velocity was still ca.10% higher than the initial average sound velocity. This was the result of the continuous filling of pores and creating consolidating effect inside the pores after drying. As for EN Opuka specimens the decrease in average velocity of ca.6% was observed below the initial average sound velocity after the first salt contamination cycle which was similar to average velocity of the RILEM Opuka specimens after the end of the salt accumulation phase. At the end of 4<sup>th</sup> propagation cycle the average velocity in RILEM Opuka specimens was lower compared to the EN Opuka specimen but with both the procedures P1 and P2 the velocity observed was less than its initial sound state average velocity at the end of 5

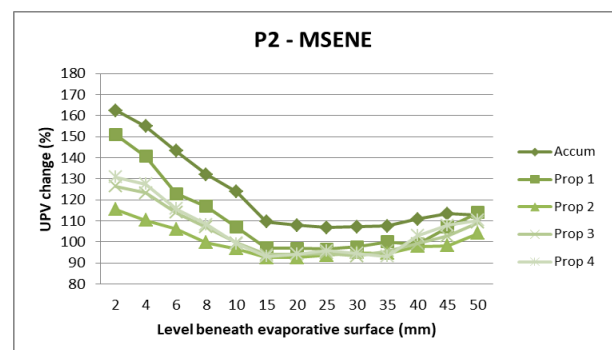
aging cycles. The decrease in the velocity of EN and RILEM Opuka specimens from their initial sound state average velocity was due to damage initiated inside the subsurface of the Opuka stone.

When the comparison is made for UPV between the two RILEM procedures P2 and P3 for Mšené specimens, it is seen the average velocity increased to ca.15% in limewash coated specimens tested with procedure P2 just after the salt accumulation phase [Graph 17(f)]. The average velocity of uncoated Mšené specimens (1-Salt) was found ca.6% higher than the average sound state velocity [Graph 17(c)] when compared to the uncoated Mšené (2-Salt) specimens which was ca.5% even after two repeated salt accumulation cycles but velocities observed were higher from their sound state velocity. The velocity of the uncoated Mšené specimens with procedure P2 and P3 was less than limewash coated Mšené specimens during the accumulation phase. At the end 5 test cycles the average velocity in uncoated and limewash coated Mšené specimens was in close range which decreased between ca.3-4% from their initial sound velocity. The decrease in UPV velocity in uncoated (MR5-MR7) and limewash coated Mšené(MRL1-MRL4) specimens with procedure P2 was a result of salt transport towards the evaporative surface as efflorescence inducing damage into subsurface during salt transport due to capillarity. The velocity of uncoated Mšené specimens(MR1-MR3) with 2-Salt accumulation cycle remained unchanged after the end of accumulation phase and at the end of final propagation cycle indicating salt clogged inside the pores of the Mšené substrate and continuing more rewetting could transport the salt towards the evaporative surface.

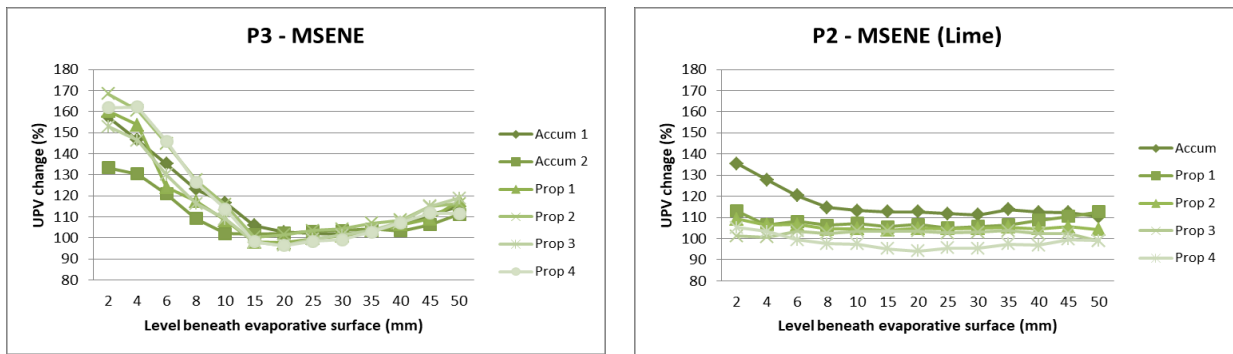
As the UPV test was performed along the height through the center of specimens, the anomalies could be considered in the results obtained because of the residual moisture content inside the specimens as the UPV tests were performed when the ca.80% moisture had evaporated during the drying, it could have altered the results due to varying moisture contents and heterogeneity of the substrates. UPV tests were also performed on RILEM specimens to track the damage propagation along the height (through diameter) and check the reliability of the UPV results with ion chromatography to check the salt concentration at different level beneath the evaporative surface.



(a)



(b)



(c)

(d)

**Graph 18: UPV changes in Opuka and Mšené stone measured at first 2-4-6-8-10 mm and after 5mm regular intervals from the evaporative surface in test procedure P2-P3**

The UPV test was also performed at a regular interval of 2mm for first 10 mm beneath the evaporative surface followed by performing it at a regular 5mm after the first 10mm till bottom of the RILEM specimens. With the RILEM test procedures P2 and P3, during drying stage the kinetics of evaporative drying draws the salt towards the evaporative surface which accumulates more salt near the evaporative layer, hence it is expected the UPV velocity will be higher in first 5-6mm layer beneath the evaporative surface. The reliability of the results was confirmed with ion chromatography results. As seen from the Graph 18 (a,b,c,d) the average velocity is higher in the first 2mm close evaporative surface. It is seen from the Graph 18 the average velocity near the evaporative surface is higher during the accumulation stage in the RILEM specimens for both coated and uncoated specimens and the velocity decreases after each propagation cycle as the salt migrates towards the evaporative surface but the trend is similar that near the evaporative surface the velocity is higher than the rest of the layers beneath evaporative surface.



## **5. CONCLUSIONS AND RECOMMENDATIONS**

The objective of this thesis research was to check the reliability of the newly developed test procedure by RILEM Technical Committee 271-ASC and compare it with the existing test standard EN12370 to assess the resistance of porous materials to salt crystallization. Under the scope of this thesis effectiveness of limewash application was also assessed on one of the natural stone (Mšené Sandstone) tested with the newly developed RILEM test standards. The overall thesis is more focused on using only single salt (sodium sulphate) for aging the substrates with the two accelerated test standards. The damage due to salt crystallization was assessed with both destructive and non-destructive tests which were effective in understanding the salt crystallization in a broader way. Results and observations discussed in the previous chapter relates several factors required to assess the durability of the porous materials and how change in the testing conditions can highly influence the damage and soundness of the material.

### **5.1 Durability of the Porous Material**

The two substrates used during the test were selected due to their distinctive nature. Mšené and Opuka have a different pore network which makes them unique when a comparison needs to be made in terms of how susceptible they could become towards salt crystallization. The degree of damage was different in both the stones tested with similar conditions with two different test standards. Mšené has a large pore size as compared to Opuka stone but more damage and material loss was observed with the EN test in Mšené stone compared to Opuka. Both the stones have different capillary transport mechanism due to the difference in the porosity which means their absorption rate significantly varies and water or salt movement will be impacted during the weathering. Mšené EN specimens showed more material deterioration compared to specimens tested with RILEM standards. During the aging cycles Mšené became saturated easily and dried faster with both the test standards compared to Opuka stone. Opuka stone has small pores which makes it more susceptible to damage as movement of water or salts inside the small pores take more time during drying and movement of salt towards the evaporative surface is very slow which develops more crystallization pressure inside the pores of Opuka stone. As with RILEM tests the stones were wetted (with salt and water) till the top of the surface was wet and they were dried till 80% of the moisture was removed proved to be more effective way for salt transport within pores. The same could be tested for various materials and a reliable conclusion could be developed by performing the tests on various substrates with different porosity. Also the application of lime was efficient and effective in reducing the surface damage for Mšené RILEM specimens as lime penetrated the subsurface easily compared to Opuka stone and even accelerated the movement of salt towards evaporative surface without damaging the surface.

### **5.2 Aging tests**

The two aging tests varied with each other in many aspects. Both EN and RILEM test used the same substrates (Mšené and Opuka) for the test but the durability of the material was affected mainly

because of the testing conditions like salt concentration, contamination method, drying conditions adopted during the test.

EN test being more aggressive because of its testing methods induced more damage in the material compared to RILEM standard. One of the reason was the use of higher salt concentration (14% mirabilite) used in the EN test that showed faster and more decay in the two stones. As the cycles continued, more and more damage was observed in specimens during the EN test due to continuous repeated contamination of stones which is not observed in the real conditions. With RILEM test procedure the damage was negligible in the stones with the low salt concentration (5% thenardite) and mainly because of the method of contamination. EN samples had the higher salt concentration near the evaporative surface due the complete immersion of the samples in the salt solution in each cycle solution whereas with RILEM the durability was assessed with partial immersion with two phase test procedure (accumulation and propagation).

The immersion method used in the two tests highly impacted the soundness of the two stones. RILEM's partial immersion method was more realistic when compared to the in-situ conditions as most of the salt was slowly transported towards the evaporative surface through capillarity which was not the case with the EN test. With RILEM test both Mšené and Opuka stones were saturated with salt solution until the top of the evaporative surface was wet, which uniformly transported the salt within the pores of the stones. But with EN test the two stones were soaked in salt solution (with complete immersion) for only 2h which limited the salt impregnation especially in Opuka stone. It was also observed during EN test, Opuka stone lost less material compared to Mšené stone because of the limited time (2h) available for salt to get absorbed into its small pores and reach saturation and create crystallization pressure to induce damage. On the contrary more material loss was observed in Mšené stone (with EN test) mainly due to its larger pore size and ability to reach saturation within 2h compared to Opuka. When EN and RILEM results were compared for material loss amongst each other one of the reasons for less material loss and damage within RILEM specimen could be because of the repeated rewetting of stones with water during propagation phase after the completion of salt accumulation phase. Rewetting during RILEM propagation cycles allowed movement of salt towards evaporative surface and concentrating damage mainly near the evaporative surface. With application of limewash the damage observed (visually) near the evaporative surface was significantly less when compared with uncoated Mšené specimen as it was seen during drying more salt efflorescence was formed and less material loss was seen between the RILEM Mšené stone specimens coated with limewash.

When comparing the drying conditions of the two test procedures drying with EN standards was although accelerated but was more damaging compared to drying following the RILEM standards. Drying stones at higher temperature with EN standard removed more than 80% of moisture in less than 16h time which is again an unrealistic parameter compared to existing environmental conditions around historical buildings. As compared to EN standards RILEM test procedure allowed slower

unidirectional drying in the stone specimens, which caused salt to move towards the evaporative surface causing damage and salt efflorescence in the exterior of the stones. It was seen during the accumulation phase the drying was slow compared to propagation phase as most of the salt had already migrated towards the exterior side of the stones. It was observed with application of limewash drying was further accelerated compared to uncoated Mšené specimens with RILEM test procedure without damaging the stone fabric.

As the above factors highly influenced the durability of two stone tested with two test standards there are still some error which could have developed while performing the experimental tests. Further comparison could be made more reliable by performing the similar number of aging cycles with variation in testing conditions on different substrates and leave less room for the error.

### **5.3 Assessment methods**

Mapping damage propagation in the porous substrates is a challenging and time consuming task but with the use of destructive and non-destructive techniques lot of information about the distribution of salt inside the pores and how damage is propagated during several aging cycles could be understood. As the assessment methods could have their own limitations and strength basic idea could be made even by performing few selected assessment tests.

In the following thesis the initial damage assessment was made with the help of the photographic documentation which was effective in understanding the physical change in the appearance due to salt crystallization over the period of time. The material loss, salt uptake and salt efflorescence were easily monitored by calculating the mass variation during each cycle. Monitoring salt absorbed by the stones and transported as a salt efflorescence proved an effective way to track the residual salt content remaining inside the stones especially for the RILEM samples. Debris those were collected and filtered from the specimens during each aging cycles could gave broader idea about the material loss in each cycle and how much salt was removed from the pores of the stones.

The non-destructive UPV test was effective in understanding the damage propagation after the end of each aging cycles. As it was seen the specimens tested with EN standard lost almost all the moisture present inside the stones in less than 24h compared to RILEM standard. The UPV test was carried out on RILEM specimens after 80% of moisture was evaporated some anomalies could have been in the results while performing UPV study as the specimens still had some moisture content inside. Testing specimens with different moisture content could help to assess reliability of UPV results. As UPV test was effective in mapping damage propagation and was performed without damaging the specimens in lab during the experiment, the samples tested with UPV could also be used to correlate the results between the destructive and non-destructive damage assessment methods for salt crystallization.

Ion chromatography was able to give the precise content of salts near the evaporative surface which helped in understanding the salt efflorescence and damage developed during the different propagation cycles. Although this assessment method gives precise results about the salt concentration through

destructive testing, one of the disadvantage is being expensive compared to the other salt assessment methods and could be a challenge when testing large number of samples. Also samples preparation for the ion chromatography needs to be precise as it might change the fabric of salt laden specimens while preparing samples.

SEM was more effective for polished samples compared to freshly broken samples. Due to the unevenness of the surface of freshly broken samples it was hard to analyze the SEM specimens for salt crystals. The results obtained from SEM analysis are accurate in understanding how salt crystallizes inside the samples and with higher magnification and elemental mapping the salt crystals could be located easily. One of the disadvantages of analysis with SEM technique is only small size sample could be used for analysis and there is a risk of tempering with the salt distribution while preparing the samples.

#### **5.4 Future work**

RILEM test was more effective in understanding the salt crystallization mechanism and creating more realistic site conditions during the test. As salt crystallization is a complex and an interesting phenomenon more work is needed to understand it much better. In continuation to the present research thesis following parameters could be considered for future studies:

- Testing the two substrates (Mšené and Opuka) used in the present research with different types of salts as in real conditions mixture of salts is generally found.
- As EN12370 test was performed for 15 aging cycles, it is recommended with RILEM standards similar number of cycles should be performed to quantify the damage and check the reliability of the two test procedures.
- Testing different substrates with varying properties will be able to give more reliable information about the salt (sodium sulphate) behavior used in the present research thesis.
- Combination of substrates and mortars could be one parameter which could replicate the in-situ behavior of the substrates which could make the results more reliable.
- More advanced methods for making damage assessment could be an effective way to give precise idea about the salt accumulation inside the substrates and quantify the deterioration.
- As limewash was more effective on Mšené specimens to decrease the damage near the evaporative surface, further research works is suggested for different substrates with different porosity and suggest alternative methods desalinating the substrates which are more susceptible to damage.

## REFERENCES

- [1] Barbara Lubelli, Rob P.J. van Hees, Effectiveness of crystallization inhibitors in preventing salt damage in building materials, *Journal of Cultural Heritage*, Volume 8, Issue 3, 2007, Pages 223-234
- [2] Flatt, R.; Aly Mohamed, N.; Caruso, F.; Derluyn, H.; Desarnaud, J.; Lubelli, B.; Espinosa Marzal, R. M.; Pel, L.; Rodriguez-Navarro, C.; Scherer, G. W.; Shahidzadeh, N.; Steiger, M. Predicting Salt Damage in Practice: A Theoretical Insight into Laboratory Tests. *RILEM Tech Lett* 2017, 2, 108-118
- [3] E Molina, G Cultrone, E Sebastián, F J Alonso, Evaluation of stone durability using a combination of ultrasound, mechanical and accelerated aging tests, *Journal of Geophysics and Engineering*, Volume 10, Issue 3, June 2013, 035003, <https://doi.org/10.1088/1742-2132/10/3/035003>
- [4] D'Altri, Antonio and Miranda, Stefano and Beck, Kevin and De Kock, Tim and Derluyn, Hannelore. (2021). Towards a more effective and reliable salt crystallisation test for porous building materials: Predictive modelling of sodium chloride salt distribution. *Construction and Building Materials*. 304. 124436. 10.1016/j.conbuildmat.2021.124436
- [5] S. Ordóñez, R. Fort, M. A. Garcia del Cura; Pore size distribution and the durability of a porous limestone. *Quarterly Journal of Engineering Geology and Hydrogeology* 1997;; 30 (3): 221–230. doi: <https://doi.org/10.1144/GSL.QJEG.1997.030.P3.04>
- [6] Property Care Association, Paper 3 – Salts Analysis: Diagnosis, Assessment and Treatments, 'Paula's Papers': Salts in Porous Construction and Building Materials, April 2020,
- [7] Charola, A. E., Rörig-Dalgaard, I., Chwast, J., and Elsen, J. (2017). Salt crystallization tests: Focus on their objective. Paper presented at 4th International Conference on Salt Weathering of Buildings and Stone Sculptures, Potsdam, Germany
- [8] Cristiana Nunes, Asel Maria Aguilar Sanchez, Sebastiaan Godts, Davide Gulotta, Ioannis Ioannou, Barbara Lubelli, Beatriz Menendez, Noushine Shahidzadeh, Zuzana Slížková, Magdalini Theodoridou, Experimental research on salt contamination procedures and methods for assessment of the salt distribution, *Construction and Building Materials*, Volume 298, 2021, 123862
- [9] D. Benavente, M.A.García del Cura, J. García-Guinea, S. Sánchez-Moral, S. Ordóñez, Role of pore structure in salt crystallisation in unsaturated porous stone, *Journal of Crystal Growth*, Volume 260, Issues 3–4, 2004, Pages 532-544
- [10] Swe Yu, Chiaki T. Oguchi, Role of pore size distribution in salt uptake, damage, and predicting salt susceptibility of eight types of Japanese building stones, *Engineering Geology*, Volume 115, Issues 3–4, 2010, Pages 226-236
- [11] Lubelli, B., Cnudde, V., Diaz-Goncalves, T. et al. Towards a more effective and reliable salt crystallization test for porous building materials: state of the art. *Mater Struct* 51, 55 (2018). <https://doi.org/10.1617/s11527-018-1180-5>
- [12] CEN (1999) EN 12370 Natural stone test methods. Determination of resistance to salt crystallization
- [13] RILEM TC 127-MS (1998) MS-A.1—determination of the resistance of wallettes against sulphates and chlorides. *Mater Struct* 31:2–9

- [14] ASTM Subcommittee D18.17 (2013) ASTM 5240 standard test method for evaluation of durability of rock for erosion control using sodium sulphate or magnesium sulphate
- [15] Steiger M, Asmussen S (2008) Crystallization of sodium sulfate phases in porous materials: the phase diagram Na<sub>2</sub>SO<sub>4</sub>–H<sub>2</sub>O and the generation of stress. *Geochim Cosmochim Acta* 72(17):4291–4306. <https://doi.org/10.1016/j.gca.2008.05.053>
- [16] Henriques FMA, Charola AE (2000) Development of lime mortars with improved resistance to sodium chloride crystallization. In: Fassina V (ed) *Proceedings of the 9th international conference on deterioration and conservation of stone*, vol 2. Elsevier, Venice, pp 335–342
- [17] Flatt R et al (2017) Predicting salt damage in practice: a theoretical insight into laboratory tests. *RILEM Tech Lett* 2:108–118
- [18] Arizzi A, Viles H, Cultrone G (2012) Experimental testing of the durability of lime-based mortars used for rendering historic buildings. *Constr Build Mater* 28(1):807–818. <https://doi.org/10.1016/j.conbuildmat.2011.10.059>
- [19] Diaz Gonçalves T, Brito V (2014) Alteration kinetics of natural stones due to sodium sulfate crystallization: can reality match experimental simulations? *Environ Earth Sci* 72(6):1789–1799. <https://doi.org/10.1007/s12665-014-3085-0>
- [20] Gomez-Heras M, Fort R (2007) Patterns of halite (NaCl) crystallisation in building stone conditioned by laboratory heating regimes. *Environ Geol* 52(2):239–247. <https://doi.org/10.1007/s00254-006-0538-0>
- [21] RILEM (1980) Recommended tests to measure the deterioration of stone and to assess the effectiveness of treatment methods, Test V.1a—crystallization test by total immersion (for untreated stone); Test V.1b—crystallization test by total immersion (for treated stone); Test V.2—crystallization test by partial immersion. *Mater Struct* 13(75):175–253
- [22] RILEM TC 127-MS (1998) MS-A.1—determination of the resistance of wallettes against sulphates and chlorides. *Mater Struct* 31:2–19
- [23] Vázquez P, Menéndez B, Denecker MFC, Thomachot-Schneider C (2015) Comparison between petrophysical properties, durability and use of two limestones of the Paris region. *Geol Soc Lond Spec Publ*. <https://doi.org/10.1144/SP416.15>
- [24] Binda L, Baronio G, Ferrieri ED (1997) Durability of brick masonry surface treatments to salt crystallization. In: *Proceedings of the 11th international brick/block masonry conference*, Tongji University, Shanghai, pp 732–741
- [25] Gomez-Heras M, Smith BJ, Viles HA, Meneely J, McCabe S (2008) High definition laser scanning for the evaluation of salt decay laboratory simulations of building limestone. In *Proceedings of the salt weathering on buildings and stone sculptures (SWBSS 2008)*, Technical University of Denmark, Copenhagen, pp 149–158
- [26] Diaz Gonçalves T, Brito V (2014) Alteration kinetics of natural stones due to sodium sulfate crystallization: can reality match experimental simulations? *Environ Earth Sci* 72(6):1789–1799. <https://doi.org/10.1007/s12665-014-3085-0>
- [27] Derluyn H (2012) Salt transport and crystallization in porous limestone: neutron—X-ray imaging and poromechanical modeling, Dissertation ETH No. 20673, ETH Zurich, Switzerland. <https://doi.org/10.3929/ethz-a-007578301>

- [28] Ioannou I, Hall C, Hoff WD, Pugsley VA, Jacques SDM (2005) Synchrotron radiation energy-dispersive X-ray diffraction analysis of salt distribution in Lépine limestone. *Analyst* 130(7):1006–1008. <https://doi.org/10.1039/b504274g>
- [29] Nunes C, Slížková Z, Křivanková D (2013) Lime-based mortars with linseed oil: sodium chloride resistance assessment and characterization of the degraded material. *Period Mineral* 82(3):411–427. <https://doi.org/10.2451/2013pm0024>
- [30] Charola A.E., Weber J., The hydration-dehydration mechanism of sodium sulphate. In: 7th International Congress on Stone Deterioration and Conservation, eds. Delgado Rodrigues J., Henriques F., F.Telmo Jeremias F., Laboratório Nacional de Engenharia Civil, Lisbon, 1992, 581-590.
- [31] Rodriguez-Navarro C., Doehne E., Sebastian E., How does sodium sulfate crystallize? Implications for the decay and testing of building materials. *Cement and Concrete Research*, (30), (2000), 1527-1534.
- [32] Cultrone G., Sebastián E., Laboratory simulation showing the influence of salt efflorescence on the weathering of composite building materials. *Environmental Geology*, (56), (2008), 729-740.
- [33] Benavente D, Cueto N., Martínez-Martínez J., García del Cura M.A, J.C. Cañaveras J.C., The influence of petrophysical properties on the salt weathering of porous building rocks. *Environmental Geology*, (52), (2007), 215–224.
- [34] Somsiri S., Zsembery S., Ferguson J.A., A study of pore size distributions in fired clay bricks in relation to salt attack resistance. In Proc.7th International Brick Masonry Conference, eds. McNeilly T., Scrivener J.C., eds. University of Melbourne, Melbourne,1985, 253- 260
- [35] Alyami, Mohammed and Alrashidi, Raid and Mosavi, Hossein and Almarshoud, Mohammed and Riding, Kyle. (2019). Potential accelerated test methods for physical sulfate attack on concrete. *Construction and Building Materials*. 229. 10.1016/j.conbuildmat.2019.116920.
- [36] H. Derluyn1 , A.S. Poupeleer , D. Van Gemert and J. Carmeliet, Salt Crystallization in Hydrophobic Porous Materials Department of Civil Engineering, Katholieke Universiteit Leuven, Heverlee, Belgium Faculty of Building and Architecture, Building Physics and Systems, T.U. Eindhoven, The Netherlands, Hydrophobe V 5th International Conference on Water Repellent Treatment of Building Materials Aedificatio Publishers, 97-106 (2008)
- [37] Krista MacWilliam, Aging tests to assess the durability of building materials to salt crystallization - towards a more realistic and effective use of sodium sulphate, SAHC masters thesis, 2017
- [38] Heather Viles, Salt Crystallisation in Masonry, <https://www.buildingconservation.com/articles/salt-crystallisation/salt-crystallisation.htm>
- [39] Mold, P.; Godbey, R. Limewash: Compatible coverings for masonry and stucco. In Proceedings of the International Building Lime Symposium, Orlando, FL, USA, 9–11 March 2005.
- [40] Nunes, C.L.; Mlsnová, K.; Slížková, Z. Limewashes with Linseed Oil and Its Effect on Water and Salt Transport. *Buildings* 2022, 12, 402. <https://doi.org/10.3390/buildings12040402>
- [41] Nunes unpublished reference paper. Assessment of new RILEM salt crystallization procedure via a round robin test
- [42] EN 459-1(2015) Building Lime. Part-1: Definitions, Specifications and Conformity Criteria

- [43] ICOMOS-ISCS (2008) Illustrated glossary on stone deterioration patterns. Ateliers 30 Impression, Champigny/Marne
- [44] Monument Diagnosis and Conservation System. <https://mdcs.monumentenkenis.nl/> (accessed May 2020)
- [45] E Molina, G Cultrone, E Sebastián, F J Alonso, Evaluation of stone durability using a combination of ultrasound, mechanical and accelerated aging tests, Journal of Geophysics and Engineering, Volume 10, Issue 3, June 2013, 035003, <https://doi.org/10.1088/1742-2132/10/3/035003>



## APPENDIX